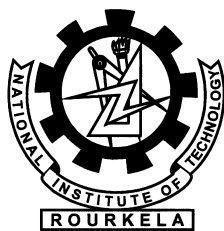


# Development and Evaluation of Clinker Stabilized Fly Ash Based Composite Material for Haul Road Application

Soumya Ranjan Mallick



Department of Mining Engineering  
National Institute of Technology, Rourkela  
Rourkela-769 008

**Development and Evaluation of Clinker Stabilized  
Fly Ash Based Composite Material  
For Haul Road Application**

*Thesis submitted in partial fulfillment  
of the requirements for the degree of*

**Master of Technology**  
(Research)

*in*

**Mining Engineering**

*by*

**Soumya Ranjan Mallick**  
(Roll No. 609MN602)

*under the guidance of*

**Prof. Manoj Kumar Mishra**  
Associate Professor



Department of Mining Engineering  
National Institute of Technology, Rourkela  
Rourkela-769 008  
December-2012



Department of Mining Engineering  
**National Institute of Technology, Rourkela**  
Rourkela-769 008

December 13, 2012

## Certificate

This is to certify that the thesis entitled *Development and Evaluation Of Clinker Stabilized Fly Ash Based Composite Material for Haul Road Application* submitted by *Soumya Ranjan Mallick* to National Institute of Technology, Rourkela for the award of the degree of Master of Technology (Research) is a record of bonafide research work under my supervision. The research scholar has fulfilled all prescribed requirements for the thesis, which is based on his own work and the thesis in my opinion, is worthy of consideration for the award of the degree of Master of Technology (Research) of the Institute.

The results reported in this thesis have not been submitted to any other University/Institute for the award of any other degree or diploma.

**Prof. Manoj Kumar Mishra**

Associate Professor

Department of Mining Engineering

National Institute of Technology, Rourkela

## Acknowledgement

I would first like to express my deep sense of respect and gratitude towards my supervisor Prof. Manoj Kumar Mishra for his inspiration, motivation, guidance and moral support throughout my research work. I am highly obliged to him for his regular supervision at every phase of my Masters programme. The research work would not have been possible without his guidance and support.

I would like to express my sincere gratitude to the members of my Masters Scrutiny committee Prof. Manoranjan Barik, Department of Civil Engineering, Prof. Swadesh Kumar Pratihar, Department of Ceramic Engineering, Prof. Himansu Bhusan Sahu, Department of Mining Engineering for their comments and suggestions throughout my research work.

I would like to express my respect to Prof. (Ms.) Susmita Mishra, Department of Chemical Engineering, Prof. Nagendra Roy, Department of Civil Engineering, Prof. Singam Jayanthu, Department of Mining Engineering, Prof. Shishir Kumar Sahu, Department of Civil Engineering and Prof. Bibhuti Bhusan Nayak, Department of Ceramic Engineering for teaching me my research related subjects. They have been great sources of inspiration to me and I really thank them from the bottom of my heart.

I would like to express my special thanks to Er. K.C. Khuntia, Deputy General Manager and other staff members of BOCM for their assistance in collection of necessary data and overburden materials used for my research work. I also express my thanks to HOD, CPP-II as well as Er. J. Delai, Senior Manager, CPP-II, NSPCL, Rourkela for facilitating fly ash for research work.

I express my gratitude to the HRDG, CSIR, New Delhi to select me as Senior Research Fellow and to provide the financial assistance to carry this investigation.

I express my thanks to Prof. D.P. Tripathy, Head of Mining Engineering Department, all faculty members Prof. B.K. Pal, Prof. S. Jayanthu, Prof. H.K. Naik, Prof. H.B. Sahu, Prof. D.S. Nimaje, Prof. Sk. Md. Equeenuddin, Prof. S. Chatterjee, staff members of the department for their genuine advice and help in completion of

my Masters programme.

I also express my thanks to HODs and staff members of Civil Engineering, Chemical Engineering, Metallurgical and Materials Engineering and Ceramic Engineering for their help in sample testing in their departments.

I am thankful to my friends and co-research scholars B. Behera, N.P. Nayak, M.M. Mohanty, R. Srinivas, S.K. Singh, R. Sarkar and B. Patro whose company have made the time enjoyable.

I am very much grateful to Mr. Simanchala Sahu, Project assistant for his assistance throughout my experimental work.

Finally, I would like to express my deepest gratitude to my beloved parents, my elder sister who made all of this possible by their endless encouragement and support.

*Soumya Ranjan Mallick*

## Abstract

India is expected to generate more than 2,50,000MW during 12<sup>th</sup> five year plan period. The coal production would be 1000MT per year. Opencast mining plays a major role in meeting the demand of fossil fuel for thermal power generation. Mine activities have to be expanded to meet this demand. It would lead to use of large capacity haul trucks. Carrying capacity of trucks/dumpers used in opencast mines has grown from 10 T to 200 T in recent years, with higher capacity being considered at places. Introduction of large capacity haul trucks demands well-designed haul roads. At present design of new haul roads is based on past experience and empirical methods. Opencast mines displace large amount of overburden as waste material. The sub-grade, sub-base and/or base of haul road typically uses those overburden materials. This investigation wants to focus on replacing a part of overburden material with another suitable and better material. There are about 170 opencast coal mines and many are near to thermal power stations. Problems associated with vehicular breakdown and poor performances as well as low morale work force of manpower have been attributed to the poor condition of haul road. The current fly ash production is about 180 MT that will rise to about 600 MT by 2030. The usage percentage of fly ash is about 50% leaving the rest as plant waste occupying huge land area and creating environmental problems. Dumped fly ash adversely affects land, air and water resources. So its gainful bulk utilization is a major challenge to India's growing power sectors.

The investigation has characterised fly ash, mine overburden material as well as clinker. Data pertaining to existing practice and layout of haul road were reported. Geotechnical properties of untreated fly ash, mine overburden, fly ash-mine overburden mixes and clinker treated fly ash-mine overburden mixes were determined. Numerical analyses were carried out to determine stress and strain of haul road for both conventional material and developed FCMs. Clinker percentage, curing period as well as fly ash percentage were observed to have strong bearing on the strength parameters of the developed FCMs. The best material obtained was 62% FA+30%

O/B+8% CL with highest CBR and UCS values. Existing dimension was evaluated and found to be inadequate. A few different dimensions for haul road pavement have been proposed. Model equations have been developed to correlate between different variables. Microstructural analyses as well as ultrasonic pulse velocity measurement were carried out to confirm the values. Maximum Dry Density, Optimum Moisture Content, CBR, UCS, BTS and P-wave velocity of best developed material is 1559 kg/m<sup>3</sup>, 16.9%, 140%, 1.4 MPa, 150 kPa and 1785 m/s respectively.

Keywords: Fly ash, Mine overburden, Haul road, Brazilian tensile strength, California bearing ratio, Unconfined compressive strength, P wave velocity.

# Contents

<b>Certificate</b>	<b>ii</b>
<b>Acknowledgement</b>	<b>iii</b>
<b>Abstract</b>	<b>v</b>
<b>List of Figures</b>	<b>xi</b>
<b>List of Tables</b>	<b>xvi</b>
<b>List of Abbreviations</b>	<b>xviii</b>
<b>1 Introduction</b>	<b>1</b>
1.1 Background . . . . .	1
1.2 Statement of the Problem . . . . .	2
1.3 Aim and Objectives . . . . .	4
1.4 Scope and Methodology . . . . .	4
1.5 Parametric Variations . . . . .	7
1.6 Organization of Thesis . . . . .	7
<b>2 Literature Review</b>	<b>9</b>
2.1 Introduction . . . . .	9
2.2 Mine Haul Roads and Haul Trucks . . . . .	11
2.2.1 Classification of haul roads . . . . .	11
2.2.2 Design of haul road pavement . . . . .	12
2.2.3 Critical strain limit . . . . .	22



2.3	Symptoms and Causes of Haul Road Deterioration . . . . .	23
2.3.1	Demerits of base/ sub-base course materials of the haul road . . . . .	23
2.3.2	Haul Trucks . . . . .	24
2.4	Fly ash Generation and Collection . . . . .	30
2.4.1	Problems associated with Fly ash Generation . . . . .	31
2.4.2	Status of Fly ash Utilization . . . . .	32
2.5	Properties of Fly ash . . . . .	33
2.5.1	Physical Properties . . . . .	33
2.5.2	Chemical Properties . . . . .	35
2.5.3	Engineering Properties . . . . .	38
2.5.4	Compaction Characteristics . . . . .	39
2.5.5	Unconfined Compressive Strength . . . . .	40
2.5.6	California Bearing Ratio . . . . .	41
2.5.7	Ultrasonic Velocity . . . . .	42
2.6	Uses and Strength Behaviour of Fly ash . . . . .	44
2.7	Inference . . . . .	48
<b>3</b>	<b>Methodology</b>	<b>49</b>
3.1	General . . . . .	49
3.2	Materials and Methods . . . . .	49
3.2.1	Materials . . . . .	49
3.2.2	Methods . . . . .	52
3.2.3	Experimental methods . . . . .	55
3.2.4	Experimental Size . . . . .	62
<b>4</b>	<b>Results and Discussion</b>	<b>64</b>
4.1	Introduction . . . . .	64
4.2	Mine Site Observations . . . . .	65
4.3	Characterization of Ingredients . . . . .	66
4.3.1	Physical Properties . . . . .	66
4.3.2	Chemical Properties . . . . .	68

4.3.3	Engineering Properties . . . . .	71
4.4	Geotechnical Properties of Developed FCMs . . . . .	73
4.4.1	Compaction Characteristics . . . . .	73
4.4.2	California Bearing Ratio Behaviour . . . . .	76
4.4.3	Unconfined Compressive Strength . . . . .	81
4.4.4	Brazilian Tensile Strength Characteristics . . . . .	88
4.4.5	Ultrasonic Pulse Velocity . . . . .	90
4.5	Microstructural Analysis . . . . .	93
4.5.1	Energy Dispersive X-ray Analysis . . . . .	96
4.5.2	X-ray Diffraction Analysis . . . . .	97
4.6	Development of Empirical Models . . . . .	99
4.6.1	Relationship between CBR, UCS, BTS and P-wave velocity . . . . .	99
4.6.2	Effect of Chemical composition on CBR, UCS, BTS and P-wave Velocity Values . . . . .	102
<b>5</b>	<b>Numerical Investigation</b>	<b>107</b>
5.1	General . . . . .	107
5.2	Axisymmetric solutions . . . . .	108
5.2.1	Elastic Equations . . . . .	109
5.2.2	Axisymmetric elements . . . . .	110
5.2.3	Axisymmetric formulation . . . . .	111
5.3	Tire Pressure Calculation . . . . .	112
5.4	Modelling . . . . .	112
<b>6</b>	<b>Summary and Conclusion</b>	<b>126</b>
6.1	Untreated Materials . . . . .	127
6.2	Treated Materials . . . . .	128
6.3	Numerical Analysis . . . . .	129
6.4	Recommendation for future work . . . . .	130
	<b>Bibliography</b>	<b>131</b>

**Publications**

**147**

**Biodata**

**148**

# List of Figures

1.1	Flow chart of the methodology . . . . .	6
2.1	A typical mine with permanent and temporary haul roads . . . . .	11
2.2	Typical haul road cross-section . . . . .	13
2.3	CBR curves [8] . . . . .	15
2.4	Stresses due to vertical line load in rectangular coordinates [130] . . .	20
2.5	Variation of vertical stresses at different depths Z [110] . . . . .	21
2.6	Response of pavement layers to load [135] . . . . .	22
2.7	Deflection factors for ESWL determination [51] . . . . .	28
2.8	Influence of multiple wheels on sub-grade stress for dual and front and rear axles [195] . . . . .	29
2.9	Horizontal positions for critical points A, B, C, D for R170 truck (fully laden) [195] . . . . .	29
2.10	A schematic layout of generation and collection of fly ash . . . . .	31
2.11	Typical arrangement of Ultrasonic velocity measurement [108] . . . .	43
3.1	Map of IB Valley coal field showing Basundhara Coal Mine . . . . .	51
3.2	Collection of mine overburden samples . . . . .	52
3.3	California Bearing Ratio Test . . . . .	59
3.4	Unconfined Compressive Strength Test . . . . .	60
3.5	Brazilian Tensile Strength Test . . . . .	61
3.6	Ultrasonic Pulse Velocity Test Instrument and view of Test in Progress	62
4.1	Uneven surfaces and potholes observed in the haul roads . . . . .	65
4.2	Grain size distribution curves of fly ash and mine overburden . . . . .	68

4.3	SEM Image of (a) fly ash; (b) mine overburden . . . . .	69
4.4	XRD of (a) fly ash; (b) mine overburden . . . . .	70
4.5	Compaction curves of fly ash and mine overburden . . . . .	73
4.6	Compaction curves of untreated composites . . . . .	74
4.7	Compaction curves of the composites containing 10% and 20% O/B .	75
4.8	Compaction curves of the composites containing 30% and 40% O/B .	75
4.9	CBR values of fly ash-mine overburden mixes . . . . .	77
4.10	CBR values of fly ash-mine overburden mixes . . . . .	77
4.11	CBR values of developed composites in soaked condition . . . . .	78
4.12	CBR values of developed composites at 7 days curing . . . . .	79
4.13	CBR values of developed composites at 28 days curing . . . . .	79
4.14	Effect of curing period on CBR . . . . .	80
4.15	UCS values of fly ash-mine overburden mixes . . . . .	82
4.16	UCS values of developed composites at 7 days curing . . . . .	83
4.17	UCS values of developed composites at 14 days curing . . . . .	83
4.18	UCS values of developed composites at 28 days curing . . . . .	84
4.19	Young's modulus values of developed composites at 7 days curing . .	85
4.20	Young's modulus values of developed composites at 14 days curing . .	85
4.21	Young's modulus values of developed composites at 28 days curing . .	86
4.22	Post failure profiles of few UCS samples . . . . .	86
4.23	Effect of curing period on UCS . . . . .	87
4.24	Post failure profiles of few Brazilian tensile test samples . . . . .	89
4.25	Tensile Strength values of developed composites at 28 days curing . .	90
4.26	P wave velocity values of developed composites at 7 days curing . . .	91
4.27	P wave velocity values of developed composites at 14 days curing . .	91
4.28	P wave velocity values of developed composites at 28 days curing . .	92
4.29	SEM image of 68%FA+30%O/B+2%CL . . . . .	94
4.30	SEM image of 66%FA+30%O/B+4%CL . . . . .	95
4.31	SEM image of 64%FA+30%O/B+6%CL . . . . .	95
4.32	SEM image of 62%FA+30%O/B+8%CL . . . . .	96

4.33	XRD of (70FA+30O/B) stabilized with 2, 4, 6, 8% clinker at 28 days curing . . . . .	99
4.34	Relationship between unconfined compressive strength and P wave velocity . . . . .	100
4.35	Relationship between CBR and unconfined compressive strength . . .	101
4.36	Relationship between CBR and P wave velocity . . . . .	101
4.37	Relationship between CBR and BTS . . . . .	102
4.38	Relationship between BTS and P wave velocity . . . . .	102
4.39	Effect of CaO content on CBR . . . . .	103
4.40	Effect of CaO content on UCS . . . . .	103
4.41	Effect of CaO content on BTS . . . . .	104
4.42	Effect of CaO/SiO <sub>2</sub> on CBR . . . . .	104
4.43	Effect of CaO/SiO <sub>2</sub> on UCS . . . . .	105
4.44	Effect of CaO/SiO <sub>2</sub> on BTS . . . . .	105
5.1	Haul road cross-section under axisymmetry loading [43] . . . . .	109
5.2	A schematic layout of existing haul road pavement . . . . .	113
5.3	Maximum strain of haul road pavement with conventional material .	114
5.4	Strain behaviour vs. dumper capacity . . . . .	115
5.5	Stress behaviour vs. dumper capacity . . . . .	115
5.6	Maximum strain and strss values for different pavement thickness for 80T dumper . . . . .	117
5.7	Maximum strain and strss values for different pavement thickness for 200T dumper . . . . .	119
5.8	Maximum strain and strss values for different pavement thickness for 300T dumper . . . . .	119
5.9	Strain values with (62%FA+30%OB+8%CL) composite . . . . .	121
5.10	Strain values with (62%FA+30%OB+8%CL) composite . . . . .	121
5.11	Strain values with composites containing 10% mine overburden as sub-base material . . . . .	122

5.12	Stress values with composites containing 10% mine overburden as sub-base material . . . . .	122
5.13	Strain values with composites containing 20% mine overburden as sub-base material . . . . .	123
5.14	Stress values with composites containing 20% mine overburden as sub-base material . . . . .	123
5.15	Strain values with composites containing 30% mine overburden as sub-base material . . . . .	124
5.16	Stress values with composites containing 30% mine overburden as sub-base material . . . . .	124
5.17	Strain values with composites containing 40% mine overburden as sub-base material . . . . .	125
5.18	Stress values with composites containing 40% mine overburden as sub-base material . . . . .	125
1	Variation of Maximum dry density with clinker content . . . . .	149
2	Effect of curing period on P-wave velocity of developed composites . .	149
3	Strain at various layers of haul road pavement with (82FA+10O/B+8CL) composite . . . . .	150
4	Stress at various layers of haul road pavement with (82FA+10O/B+8CL) composite . . . . .	150
5	Strain at various layers of haul road pavement with (72FA+20O/B+8CL) composite . . . . .	151
6	Stress at various layers of haul road pavement with (72FA+20O/B+8CL) composite . . . . .	151
7	Strain at various layers of haul road pavement with (62FA+30O/B+8CL) composite . . . . .	152
8	Stress at various layers of haul road pavement with (62FA+30O/B+8CL) composite . . . . .	152
9	Strain at various layers of haul road pavement with (52FA+40O/B+8CL) composite . . . . .	153

10	Stress at various layers of haul road pavement with (52FA+40O/B+8CL) composite . . . . .	153
----	---	-----



# List of Tables

1.1	Parametric variations considered for the study . . . . .	7
2.1	Haul road cross-section based on the CBR chart for a wheel load of 80T [191] . . . . .	16
2.2	Diseases due to the presence of heavy metals in fly ash [164] . . . . .	32
2.3	Utilization of fly ash in Various Sectors . . . . .	33
2.4	Range of chemical composition of fly ash from different types of coal .	36
2.5	Range of chemical composition of Indian coal ashes and soils [138] . .	37
2.6	Relationship between UCS and quality of sub-grade soil [37] . . . . .	41
2.7	Relationship between CBR and quality of sub-grade soil [16] . . . . .	42
3.1	Various proportions of flyash, mine overburden and clinker . . . . .	53
3.2	Experimental Design Chart . . . . .	63
4.1	Physical properties of fly ash and mine overburden . . . . .	67
4.2	Chemical Compositions of Fly ash, Mine overburden and Clinker . . .	70
4.3	Engineering Properties of Overburden and Fly ash . . . . .	72
4.4	CBR Gain of Fly ash-Mine overburden-Clinker Composites . . . . .	81
4.5	UCS Gain of Fly ash-Mine overburden-Clinker Composites . . . . .	88
4.6	Poisson's Ratio Values of Developed Composite Materials . . . . .	93
4.7	Chemical Compositions of the Composites, cured for 28 days . . . . .	98
4.8	The developed correlation among various parameters of fly ash-mine overburden-clinker mixes . . . . .	106

5.1	Young's modulus, E (MPa) and Thickness, t (m) of the pavement layers for Conventional material and sub-base replaced with FCM . . . . .	114
5.2	Young's modulus, E (MPa) and Thickness, t (m) of the pavement layers for proposed dimensions . . . . .	116
5.3	Maximum stress and strain values for different dumper capacity and pavement thickness . . . . .	118
5.4	Young's modulus, E (MPa) and Poisson's ratio of different developed composites . . . . .	120

## List of Abbreviations

BTS	Brazilian Tensile Strength
CACS	Coal Ash Classification System
CBR	California Bearing Ratio
EDX	Energy Dispersive X-Ray Spectroscopy
ESWL	Equivalent Single Wheel Load
FCM	Fly ash Composite Material
FSW	Free Swell Index
HEMM	Heavy Earth Moving Machinery
LL	Liquid Limit
PI	Plasticity Index
PL	Plastic Limit
SEM	Scanning Electron Microscopy
SL	Shrinkage Limit
UCS	Unconfined Compressive Strength
XRD	X-Ray Diffraction

# Chapter 1

## Introduction

### 1.1 Background

The overall development of a nation primarily depends on the power or energy available as it is directly related to the growth of the nation. India needs huge power resources to meet the expectation of its denizen. Fossil fuel continues to be the dominant source in meeting the demand for power generation and the trend is expected to continue for next two to three decades. Coal is world's most abundant and widely distributed fossil fuel. An estimate reflects that 75% of India's total installed power is thermal out of which the share of coal is about 90%. Mining of the coal will remain a major activity. With the recent advances in mining technology, majority of the coal demand is met from surface mining due to its speed and ease of operations. The current coal production from surface mines in India is about 400 MT (85%) that will have to be increased substantially to meet the demand for power. Haul roads are the life line of any surface mine. Opencast mine economy depends on the cost of haul road design, construction as well as its maintenance in addition to other factors. These roads are used by heavy earth moving equipments and machineries. Production suffers, accident and breakdowns occur if they are not properly laid, constructed and maintained. Traditionally least attention is extended to its design, construction and maintenance. It adversely affects mine economics in terms of loss of production, breakdown of dumpers, poor working conditions etc. The surface of the haul

road depends on the behaviour of material beneath it. Strengthening of the base and sub-base layers beneath the surface of the surface coal mine haul road are of vital importance to improve upon mine economics. India produce huge quantity of fly ash due to high ash content in the coal resources and its disposal is a major challenge to power plant operators. Though due to technological advances fly ash has found multiple gainful usages in many applications, yet those approaches do not address the huge generation completely.

## 1.2 Statement of the Problem

A stable road base is one of the most important components of road design. Haul road is a multi-layered structure which consists of four layers as surface, base, sub-base and sub-grade. A typical surface coal mine has about 3 to 5 kms of permanent haul road, larger ones having longer lengths and various other branch roads that are constructed either with overburden material or with locally available material found near to the mine property. Common surface coal mine haul road construction material consists of alluvial soil, crushed rock, sand, gravel, broken shale, sandstone, morrum, clay etc. result only in filling the spaces instead of offering total solution to ground stability [204]. The behaviour of the surface course of haul road depends on the bearing capacity of the materials that are lying beneath it. It has been observed that surface course exhibits excessive rutting, potholes, settlement, sinking and overall deterioration. There has been exponential rise in carrying capacity of dumpers. But the construction of haul road has not been appropriately addressed to accommodate these changes. Typically truck haulage cost is nearly 50% of the total operating cost incurred by a surface mine [194]. The cost increases as the tonnage increases with large capacity dumpers. Poor construction materials result in haul road accidents, high maintenance cost of road as well as that of resulting in the machines reduce profit. Surface mine operators spend a significant amount of money on haul road construction and its maintenance. In the past 30 years the carrying capacity of hauling equipments e.g. dumpers/trucks in India has grown from 12 T to 170 T, 220 T to 300 T being

envisioned at places, requiring better haul roads to carry heavy loads. However, there is a need to reduce vehicle operating cost and maintenance cost by well constructed haul roads. Strengthening of the base and sub-base of the surface coal mine haul road is of vital importance to improve upon mine economics. It is desired that the base and sub-base of the haul road should exhibit reduced strain so as to achieve a strong and smooth road surface course.

Solid wastes from the combustion of coal pose serious environmental problems of vital concern to the producers and users of coal as well as the general public. Opencast mining involves displacement of large amount of overburden material as mine waste to excavate coal from the earth. Overburden is the waste material which lies above the coal seams. With the rising demand for coal, often surface mine operations go deeper and deeper. It creates dump site with huge excavated wastes. The overburden dumps formed outside or adjacent to the open pits occupy land, alter the surface topography and contribute to the environmental degradation.

Fly ash is a waste by-product from thermal power plants, which use coal as fuel. Typically thermal plants are located near to surface coal mines. The current annual production of coal ash is estimated around 600 million tons worldwide, with fly ash constituting about 500 million tons at 75-80% of the total ash produced [3]. Thus the disposal of the large amount of fly ash is a serious environmental problem. The problem with safe disposal of fly ash is a major issue as India is poised to burn 1800 million tones generating about 600 million tones of fly ash by 2031-32 due to the high ash (30% to 40%) content of the coal. Present generation of fly ash in India is 160 MT/year and it is expected to increase upto 300 MT/year by 2016-17 [152]. Currently there exist about 170 opencast coal mines in India of various capacities. In most of the mines, the material used in the haul road is not adequate for supporting the wheel loads. Fly ash has potential to meet this criterion. The prospects of utilizing fly ash that would have been dumped as waste needs to be investigated experimented and documented. The research undertaken focused on development of fly ash based composite materials using mine overburden and evaluated its performance to support heavy truck loads or dumpers in both dry as well as wet climatic conditions in the

haul road.

### 1.3 Aim and Objectives

The aim of the investigation was to reduce the stress and strain experienced at the surface course of the haul road by replacing the sub-base with an improved material as well as to increase the fly ash utilization prospects. The specific objectives to meet the goal were the following.

1. Characterization of fly ash, mine overburden and clinker.
2. Determination of geotechnical properties of fly ash and mine overburden material.
3. Development of composite materials with fly ash, mine overburden and clinker at their respective OMC-MDD.
4. Determination of geotechnical properties such as California Bearing Ratio (CBR), Unconfined Compressive Strength (UCS), Brazilian Tensile Strength (BTS) and Ultrasonic P wave velocity.
5. Micro-structural analysis of the developed composites.
6. Determination of stress and strain values of haul road using both conventional material and developed composite material through simulation and modeling.
7. Development of model equations to correlate different parameters.

### 1.4 Scope and Methodology

Coal extraction through opencast coal mines will continue to be a major source of power. Opencast mine economy depends on the cost of haul road design, construction and its maintenance besides other factors. Surface mine operators bear significant amount of expense on haul road construction and its maintenance. The sub-base material for the haul road is sourced either from far off places, from the local clay or from

the overburden material. Typically thermal power plants are located near to surface coal mines that produce huge amount of fly ashes. Its disposal is a major problem. Fly ash has many attributes for geotechnical applications. But its effectiveness in the use of haul road has not yet been completely explored and established. The present research focuses on the use of the fly ash based composite materials for haul road construction and evaluate its performance to support heavy truck loads in both dry as well as wet climatic conditions in the haul road. The outcome of the research would be useful in improving the performance of haul road as well as increasing the prospects of utilization of fly ash by the industry. In addition to improve in mine economics, saving due to gainful utilization of fly ash disposal would be substantial.

This investigation was an attempt to utilize coal mine overburden material and fly ash in different compositions along with clinker, a popular strength enhancing media to improve the behaviour of haul road. The overall approach adopted to achieve the various objectives to reach the goal is outlined (Figure 1.1 ).

1. Review of available literature including both published and unpublished to critically obtain information on haul road construction, on dumpers, on geotechnical properties of fly ash, on strength enhancing materials etc.
2. Development of experimental setup and characterization of ingredients.
3. Development of composite material with fly ash in major and mine overburden material stabilized with additive and optimization of parametric variations.
4. Determination of geotechnical properties of the developed composites by performing the tests and analyses as moisture density relationship, unconfined compressive strength, California bearing ratio, Brazilian tensile strength, Ultrasonic pulse velocity, morphological behaviour, X-ray diffraction analysis, energy dispersive X-ray analysis etc.
5. Simulation of stress-strain behaviour to predict the thickness of the sub-base layer as well as project the amount of fly ash usage.



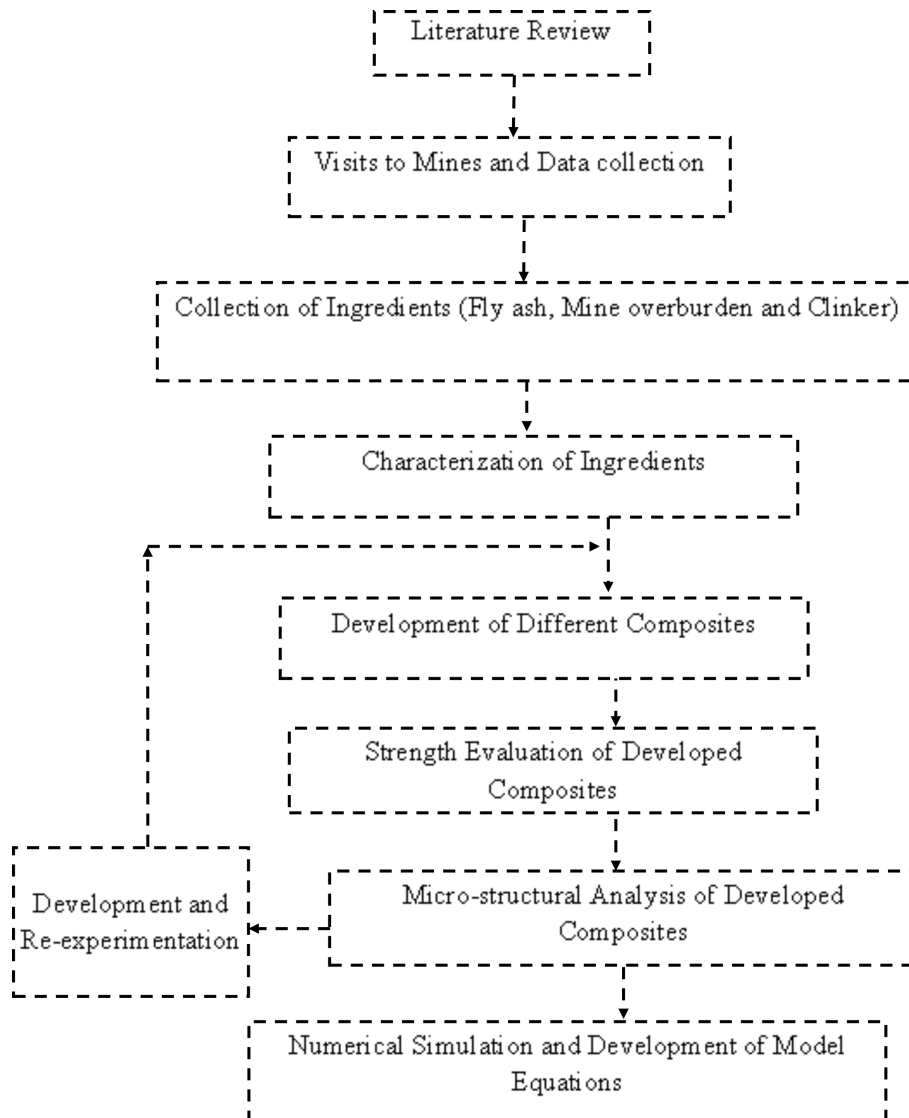


Figure 1.1: Flow chart of the methodology

## 1.5 Parametric Variations

The objectives have been achieved by following a well designed methodology as well as considering the following parametric variations (Table 1.1).

Table 1.1: Parametric variations considered for the study

A. Laboratory Investigation	Parameters	Variations
1.Characterization of ingredients	Fly ash and mine overburden	Physical properties: specific gravity, particle size distribution, Atterberg limits, free swell index Chemical properties: chemical composition, pH Engineering properties: compaction characteristics, cohesion, angle of internal friction, angle of repose, California Bearing Ratio, Unconfined Compressive Strength
	Clinker	Chemical composition
2.Development of composite material	Fly ash (%)	50 to 90
	Mine overburden (%)	10 to 40
	Clinker (%)	2 to 8
	Curing period (days)	7, 14 and 28
3. Geotechnical characterization		Compaction characteristics, California Bearing Ratio (CBR), Unconfined Compressive Strength (UCS), Brazilian Tensile Strength, P-wave velocity, Young's modulus, Poisson's ratio
B. Numerical modeling		.
1. Finite element analysis software		ANSYS
2. Modeling		2D (Axisymmetric), Quadrilateral 4-noded
3. Model haul road pavement		4 layers: Surface, Base, Sub-base and Sub-grade
4. Layer thickness (s)		Surface (m): 0.15 to 0.5 Base (m): 0.2 to 1.0 Sub-base (m): 0.35 to 1.5 Sub-grade (m): 0.5 to 2.0
5. Tire pressure (kPa)		520, 555, 700 [for 80T, 200T and 300T Dumper]

## 1.6 Organization of Thesis

The thesis is covered in six chapters. The first chapter gives an introduction which includes background of the research, statement of problem, objectives, scope and

methodology of research work as well as parametric variations. Second chapter includes a detailed review of literature on mine haul road, haul trucks and geotechnical properties as well as applications of fly ash. Besides it also covers environmental aspects of fly ash utilization. The materials used and methods adopted for the investigation including collection of ingredients, sample preparation and testing techniques used for characterization of ingredients as well as developed of composite materials are described in chapter three. Chapter four deals with results, discussion and analysis which include the results of geotechnical properties of ingredients and developed composite materials, results of micro-structural analyses and finally development of model relationship between geotechnical parameters. Numerical investigation to study the effectiveness of the developed composite materials on the stress-strain behavior of haul road pavement is described in Chapter five. Chapter six includes summary and conclusion of the investigation. At the end the reference and the detail experimental and numerical results are included in appendix.

# Chapter 2

## Literature Review

### 2.1 Introduction

Mining is the extraction of minerals from the earth crust. The total numbers of working mines at present are 2628 out of which 574 mines deal in coal and lignite, 608 mines deal in metallic minerals and rest deals in non-metallic minerals. Presently, India produces around 90 minerals out of which 4 are fuel minerals, 10 are metallic minerals, 50 are non-metallic minerals, 3 are atomic minerals and 23 are minor minerals [77].

Coal is world's most abundant and widely distributed fossil fuel. India is 3<sup>rd</sup> largest producer of coal in the world and has 4th largest reserves of coal in the world [152]. India is expected to generate more than 2, 50,000 MW during 12<sup>th</sup> five year plan period. The coal production would be 1000 MT per year to meet the energy demand of the country. Opencast mining plays a major role in meeting the demand of fossil fuel for thermal power generation. The surface mining activities have to be expanded to meet this demand.

In surface coal mines, explosives are used to break the surface or overburden. The overburden is then removed. Once the coal seam is exposed, it is drilled, fractured and thoroughly mined in strips. The coal is then loaded on to large trucks or conveyors for transport to either the coal washing plant or directly to where it will be used. The average stripping ratio in surface coal mines in India is about 1:2.5[129]. The

bulk density of overburden dump is less than that of the bank density. As a result a substantial overburden material remains un-reclaimed even after filling voids created during excavation.

One of the major environmental challenges is to manage the huge volume of overburden generated in these opencast mines which is associated with the problems as aesthetics, visual impacts and landslides, loss of topsoil, soil erosion, water and air pollution, ecological disruption, social problems, safety, risk and health etc. The overburden is highly heterogeneous. These consists of alluvium, laterite, sandstone, carbonaceous shale, coal bands, clays, between coarse to medium grained highly feruginous sandstone etc. [166]. Though the material sizes vary over a wide range, yet there are reports that suggest that fines and coarse grains are approximately equally represented [204].

A typical surface coal mine has about 3 to 5 km of permanent haul road and various other lumpy roads that are constructed either with overburden material or from locally available material found near to the mine boundary. Some of those materials typically are asphaltic concrete, mudstone, sandstone, gravel, clay etc. Asphaltic concrete is very costly. Further it becomes slicky in excessive rain. Its effectiveness is also sensitive to temperature and compaction. Sand, gravel, clay etc. are used only as filling material. These materials don't offer any ground stability. Often it is observed that the operating and maintenance cost of dumpers are significantly high in addition to haul road maintenance cost. It results in reduced production, frequent breakdown, accidents, death hazards, low worker motivation etc. These days' opencast mines are planned to significant depths, often beyond industry's current experience, expertise and knowledge. In the past 30 years the carrying capacity of hauling equipments e.g. dumpers/trucks has grown from a tiny 10 T to 170 T, 350 T being envisioned at places, requiring better haul roads to carry heavy loads.

Surface coal mine haul road undergoes more strain due to multiple reasons such as poor surface course, inadequate construction process, poor construction materials, varying load on the surface, improper drainage system, etc. Literature related to surface coal mine haul road construction and fly ash as construction material is reviewed

in this chapter.

## 2.2 Mine Haul Roads and Haul Trucks

In an open cast coal mine, haul roads are basically required for the transportation of coal from the various coal faces to the coal stockyard, overburden material to the dump yard and also for the movement of vehicles to the workshop (Figure 2.1 ).



Figure 2.1: A typical mine with permanent and temporary haul roads

### 2.2.1 Classification of haul roads

Haul roads are classified into following categories depending upon the traffic and the nature of operations on the various haul roads.

- Permanent haul roads: Life span of such road is equal to the life of mine. These roads are made up of highly durable materials. These roads are generally made outside the quarry area.
- Temporary haul roads: These roads are used mainly for shovel or dumping yard access. They change considerably with the advancement of the quarry face. Such roads are generally made up of lower quality materials. Life of such

road is very short, often varying from few weeks to few months depending on production.

### 2.2.2 Design of haul road pavement

A typical haul road pavement is a structure of superimposed layers of chosen material that is placed on the native soil or sub-grade. The main function of the haul road pavement is to support the wheel loads of the dumpers and distribute them to the underlying sub-grade. Pavements are of two broad types i.e. flexible and rigid. The flexible type is popular. Haul road design concerns the ability of the road to carry the imposed loads without need for excessive maintenance. Haul roads deteriorate with time due to interactive effect of traffic load, in-situ material strength, structural thickness and specific sub-grade. Road surface should not only be stable, non-yielding but also even along the longitudinal profile to enable the vehicles move faster safely and comfortably. The pavement carries the wheel load and transfers the stresses through a wide area on the soil sub-grade below. It results in the stress being transferred to the sub-grade soil through pavement layers considerably lower than the contact pressure under the wheel load on the surface. This reduction in wheel stresses depends on factors as thickness of layer as well as characteristics of the pavement layers. So though an effective pavement construction ensures distribution of wheel load stress to a larger area per unit depth of the layer, yet a small amount of temporary deformation is always associated.

Design and construction should ensure to keep this elastic deformation of pavement within limits. Flexible pavement structure is typically composed of several layers of materials. Each layer receives loads from the above layer, spreads them out and passes on these loads to the next layer below. Thus the stresses are reduced from top layer to the bottom layer. The layers are usually arranged in the order of descending load bearing capacity with the highest load bearing capacity material (most expensive) on the top and the lowest load bearing capacity material (least expensive) on the bottom. It transmits the vertical or compressive stresses to the lower layer by grain to grain transfer through the points of contact in the granular structure. It needs

a well compacted granular structures consisting of strong materials to transfer the compressive stresses. The stress or compressive loading is maximum on the pavement surface directly under the wheel load and is equal to the contact pressure under the wheel. These stresses get distributed to a larger area in the shape of truncated cone and hence decrease at lower layers. Hence multilayer construction of road is desirable. Haul road pavement consists of four distinct layers namely, surface course, base course, sub-base and sub-grade (Figure 2.2 ).

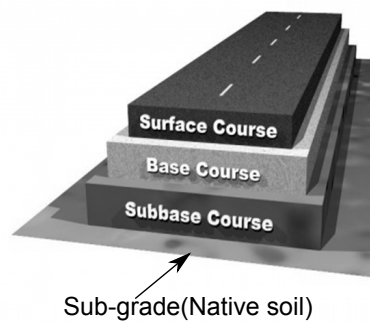


Figure 2.2: Typical haul road cross-section

- The surface course is the layer of a haul road with which the wheels of vehicles are in actual contact. The characteristics of the surface course should be of high adhesion, low rolling resistance coefficient, no penetration under load. It is generally made of bitumen, asphalt or compacted gravel to provide a smooth riding surface and will resist pressure exerted by the tires.
- The base course is the layer of material which lies immediately below the surface course. It consists of granular material like stone fragments or slag that can be stabilized with binding materials like cement, natural pozzolans etc. The base course is the main source of the structural strength of the road.
- Sub-base is the layer of a haul road pavement, which lies between base course and sub-grade. The base course and sub- base courses are primarily used to improve load supporting capacity by distributing the load. It usually consists of same type of materials used in base course like laterite, crushed stone, gravel,



Moorum, natural sand either cemented or untreated. Apart from providing structural strength to the road, it serves many other purposes such as preventing intrusion of sub-grade soil into the base course, accumulation of water in the road structure, and providing working platform for the construction equipment.

- The sub-grade is the naturally occurring surface on which the haul road pavement is constructed. It may be leveled by excavation or back-filled to provide a suitable surface. The performance of the haul road is affected by the characteristics of the sub-grade. The loads on the pavement are ultimately received by the sub-grade to be transferred to the earth mass. It should not be overstressed at anytime i.e. Pressure on top of it should be within permissible limit.

Appropriate thickness of each layer in the haul road is calculated by two methods i.e. California Bearing Ratio (CBR) and resilient modulus approach. Resilient modulus is a non-linear approach to measure the pavement road bed soil strength under dynamic loading. It considers the strain experienced at each layer as those varies widely, because of different properties. Failure occurs when maximum strain at each layer exceeds the critical strain limit of that layer. The CBR is one of the most popular and widely practiced empirical methods around the world. Indian coal mines also follow this mechanism [33].

### **Haul Road Pavement design based on CBR**

CBR is a load penetration test of a soaked sample of pavement construction materials as an inference of its shear strength. CBR value is a relationship between the force necessary to drive a piston into the material and corresponding value to likewise drive the piston into a standard gravel sample up to a known depth and the results are reported as a percentage of standard (gravel) tests. It is observed that failure or poor pavement performance of road occur due to inadequate compaction of materials forming the road layers and insufficient cover thickness over weak in situ material. Porter (1949) developed the cover thickness requirements over in situ materials of specific CBR (%) values that were applicable for airfield pavement design. The use

of CBR method for the design of haul roads in surface mines was first recommended by Kaufman and Ault (1977). CBR value for a specific material is developed from a laboratory penetration test of a soaked samples of pavement material from which its shear strength is inferred.

### Design procedure

The CBR method estimates the bearing capacity of a construction material by measuring the resistance offered by it to the penetration of a standard cylindrical plunger. The detail procedure for conducting the test is described elsewhere (IS: 2720 Part 16). Design charts have been developed that relate pavement, base and sub base thickness to vehicle wheel load and CBR values (Figure 2.3 ). Cover thickness requirements for various wheel loads corresponding to a wide range of CBR values of the construction materials are also illustrated. The CBR method assumes that failure will occur when the cover thickness above a certain material is less than that is required. The maximum wheel load is determined by dividing the loaded vehicle weight over each axle by the number of tires on that axle. The highest wheel load of a loaded vehicle is used in the CBR design chart.

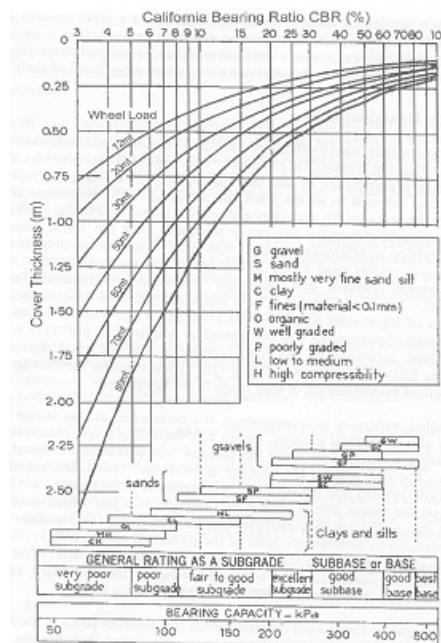


Figure 2.3: CBR curves [8]

A relation between CBR, layer thickness, layer type and total fill cover has been suggested (Table 2.1). The layer thickness can be determined from the cover thickness required by one possible layer from the cover thickness required for the immediate lower layer. The CBR method of haul road design has been very popular and is being followed [85, 8, 195, 33]. The method is simple, well understood and gives good design guidelines for haul roads. In India, CBR method is used for haul road construction in surface mines [33].

Table 2.1: Haul road cross-section based on the CBR chart for a wheel load of 80T [191]

Layer	Typical material	CBR (%)	Total fill cover (m)	Layer thickness (m)
Surface	Crushed rock	95	.....	0.30
Base	Pitrun sand & gravel	60	0.30	0.30
Sub-base	Till, mine spoil	25	0.60	1.60
Sub-grade	Firm clay	4	2.20	.....

### Development of CBR Equation

There exists a constant relation between pavement thickness to the radius of the loaded area as below [12].

$$t = k.r = k.\sqrt{\frac{P}{\pi.p}} = \frac{k}{\sqrt{\pi.p}}\sqrt{P} = K.\sqrt{P} \quad (2.1)$$

Where

t = thickness of required pavement

r = radius of loaded area

k = constant ratio of thickness over radius

P = Total wheel load

p = Contact pressure

K = A constant for a constant contact pressure

The adjustment from low tire pressure to high tire pressure is made by increasing required thickness of base and pavement, so that theoretical deflections produced by

the tire with higher pressure would be equal to theoretical deflections produced by the tire with lower pressure. The theoretical deflections are determined from the relation applicable to elastic solid with Poisson's ratio of 0.5.

$$w_1 = \frac{3 \times P}{2 \times E \times (r_1^2 + t_1^2)^{\frac{1}{2}}} = w_2 = \frac{3 \times P}{2 \times (r_2^2 + t_2^2)^{\frac{1}{2}}} \quad (2.2)$$

Where

w = Deflection under the center of loaded area

E = Elasticity Modulus It is inferred from the above equation that sum of the square of radius and square of pavement thickness has to be a constant (Equation 2.3 ).

$$r_1^2 + t_1^2 = r_2^2 + t_2^2 = Constant \quad (2.3)$$

$$\frac{t^2}{P} + \frac{1}{p \times \pi} = D \quad (2.4)$$

$$D = K^2 + \frac{1}{p \times \pi} \quad (2.5)$$

$$D = \frac{1}{8.1 \times CBR} \frac{in^2}{lb} \quad (2.6)$$

$$t = \sqrt{P \left[ \frac{1}{8.1 \times CBR} - \frac{1}{p \times \pi} \right]} \quad (2.7)$$

$$t = \sqrt{\frac{P}{8.1 \times CBR} - \frac{A}{\pi}} \quad (2.8)$$

Stress distribution in a homogeneous half-space is described by use of stress concentration factor that consider the variable vertical load [12]. The general formula is

$$\sigma_t = \frac{n \times P}{2 \times \pi \times R^2} \times \cos^n \phi \quad (2.9)$$

Where P = Applied point load at surface

$\sigma_t$  = Stress at arbitrary point in vertical direction

R = Distance from point load to the location of  $\sigma_t$

$n$  = Frohlich's concentration factor = 3 (depends on site parameter)

The vertical stress at any arbitrary location in a semi-infinite medium due to a loaded area (as in haul road pavement) is evaluated with depth along the central line of a uniformly distributed circular load from equation

$$\sigma_t = \sigma_0 \times \left[ 1 - \frac{1}{\left\{ \sqrt{1 + \left(\frac{r}{t}\right)^2} \right\}^n} \right] \quad (2.10)$$

Where  $r$  = Radius of load area

$t$  = Depth to location of computed stress

$\sigma_0$  = Applied stress over loaded area

At a stress concentration factor 3, the (Equation 2.10) is similar to the Boussinesq's (Equation 2.16). At a stress concentration factor 2, the equation takes the form

$$\sigma_t = \sigma_0 \times \left[ 1 - \frac{1}{1 + \left(\frac{r}{t}\right)^2} \right] \quad (2.11)$$

$$\sigma_t = \sigma_0 \times \left[ \frac{1}{1 + \left(\frac{t}{r}\right)^2} \right] \quad (2.12)$$

Where  $t = K\sqrt{P}$

$P$  = wheel load

$k$  = constant (a function of sub-grade CBR and tire contact pressure).

If the load,  $P$  is a uniform pressure, over a circular area with a radius,  $r$ , then  $t = K \cdot \sqrt{p \cdot \pi \cdot r^2}$  which can be written as  $\left(\frac{t}{r}\right)^2 = K^2 \cdot p \cdot \pi$ .

$$\sigma_t = \left[ \frac{1}{1 + K^2 \times p \times \pi} \right] \quad (2.13)$$

$$\sigma_t = \left[ \frac{1}{\pi \times \left( K^2 + \frac{1}{p \times \pi} \right)} \right] \quad (2.14)$$

$$\frac{\pi \times \sigma_t}{CBR} = \frac{1}{CBR \times \left[ K^2 + \frac{1}{\pi \times p} \right]} \quad (2.15)$$

The term  $[K^2 + \frac{1}{\pi \cdot p}]$  is termed as D. The product CBR\*D is a constant. It is evaluated from design curve. Vertical stress at top of sub-grade ( $\sigma_t$ ) as computed in (Equation 2.11 ) must represent a limiting vertical stress, may be referred as a design stress ( $\sigma_{design}$ ). The term  $[\frac{\sigma_{design} \cdot \pi}{CBR}]$  is a constant and is a design criterion for classical CBR equation. The derivation of equations is given in appendix (page-156).

### **Stress distribution in pavement**

Estimation of vertical stresses at any point in a soil mass due to external vertical loadings are important in evaluating stress-strain behaviour of structural elements. The theory of elasticity is used to compute stresses at any point in the soil mass. With vertical loading, new stresses are created within the mass. Load transferred to the soil mass spreads laterally with increasing depth from the area of application due to shearing resistance developed.

The area over which new stresses develop increase with increase in depth, but have decreasing magnitude of stress (Figure 2.4 ). The sum of the new vertical stresses developed in the soil mass on any horizontal plane should be equal to the weight or force of the surface loading for equilibrium condition to prevail. There exists a fixed ratio between stress and strain within the elastic limit of the material. Hence even if the material is not elastic, the ratio between  $\sigma$  and  $\varepsilon$  should be constant for the theory of elasticity to be applicable. Therefore the elastic theory is assumed to be applicable as long as the stresses induced in the layers are relatively small. As the stresses in the sub-layers of a pavement having adequate safety factor against shear failure are relatively small in comparison with the ultimate strength of the material, the pavement is assumed to behave elastically.

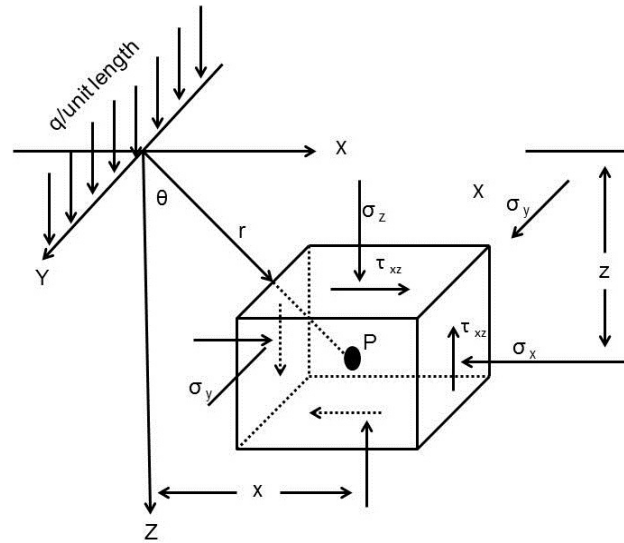


Figure 2.4: Stresses due to vertical line load in rectangular coordinates [130]

Though the increased stress below wheel loading is maximum, it extends indefinitely in all directions. There exist many approaches to compute  $\sigma$  and  $\varepsilon$  in layers with Boussinesq's formula being popular.

### Boussinesq's Approach

It assumes homogeneous, isotropic and semi-infinite soil mass with negligible body weight. The expression to find stress at any point in the soil mass due to a line load (due to wheel loading) of infinite extent acting at the surface is computed assuming plain strain condition. The stress is same at all sections and the shear stresses on those section are zero. Stresses at any point (Figure 2.5 ) is obtained either in polar co-ordinates or in rectangular co-ordinates. The vertical stress ( $\sigma_z$ ) on rectangular co-ordinate is expressed as

$$\sigma_z = \left(\frac{q}{z}\right) \frac{\frac{2}{\pi}}{\left[1 + \left(\frac{x}{z}\right)^2\right]^2} = \frac{q}{z} I_Z \quad (2.16)$$

Where

Q = Vertical loading

Z = Vertical depth of the point from the surface

$X$  = Horizontal distance of the point 'P' from vertical axis

$I_z$  is influence factor = 0.637 at  $x/z = 0$

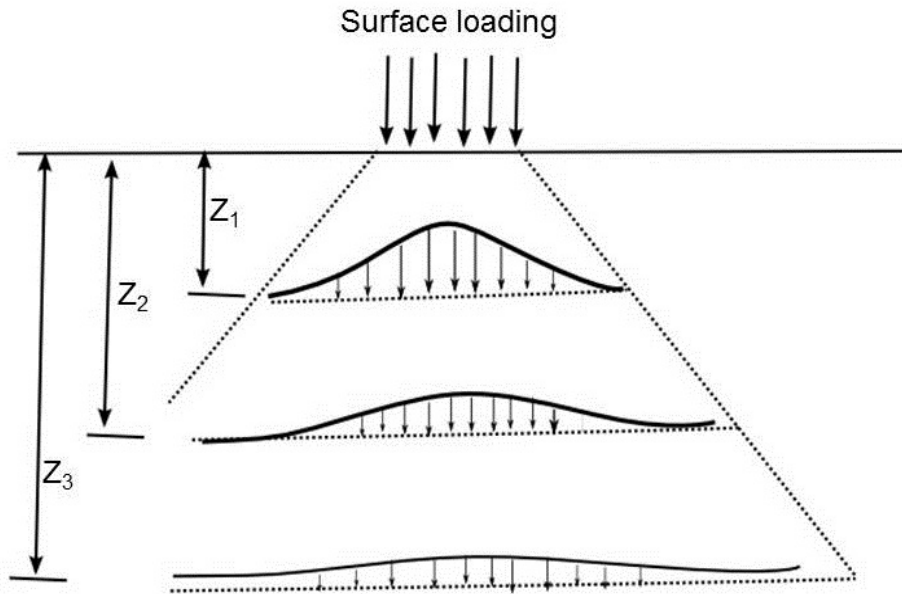


Figure 2.5: Variation of vertical stresses at different depths  $Z$  [110]

The haul road layers undergo deformation that depends on the load applied as well as stiffness of the material. There exists a critical strain which when exceeded causes pavement deformation. The critical strains usually occur under the wheel paths [97]. These are horizontal tensile strains developed at the bottom of the surface layer and base/sub base layer due to axial load which control fatigue cracking, while the vertical compressive strains at the top of the sub-grade layer control the permanent deformation (Figure 2.6 ).



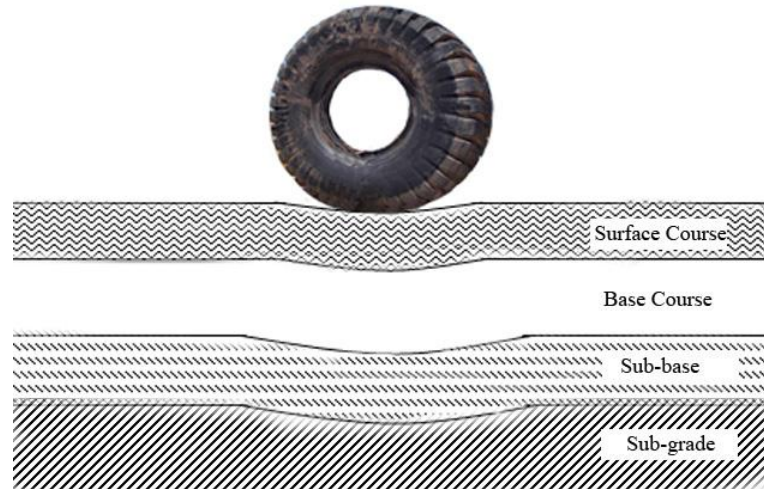


Figure 2.6: Response of pavement layers to load [135]

The failure of a flexible pavement structure supported on a sub-grade soil and subjected to repeated traffic loading can occur through two primary mechanisms-collapse of the pavement structure or cracking of the surface of the pavement. A collapse of the pavement structure occurs due to large plastic (permanent) deformations in the sub-grade soils. At times, even when the loads on the pavement are not excessive but nominal, the pavement surface crack due to fatigue, caused by the reversal of elastic strains at any location in the pavement system. As a result of repeated (cyclic) loads such as those caused by moving traffic, cohesive soils in the sub-grade incur repeated elastic deformations. When these deformations exceed a threshold value, premature fatigue failure of the flexible pavement through cracking of the pavement surface occurs.

### 2.2.3 Critical strain limit

Haul road undergoes/ experiences deformation (strain) when loaded due to running of heavy earth moving machineries. Each layer experience variable strain. The important criterion for haul road design is a critical strain limit for each layer. A road cannot adequately support haul trucks when vertical strain exceeds a critical strain limit as the road ceases to act as a beam [191]. Critical strain limit is around 1500

micro-strains [126]. Thompson and Visser (1997) observed that the critical strain limit was about 2000 micro-strains. The difference in critical strain limits is due to different design life of haul road and traffic density. The strain limit depends on the number of haul trucks running on the haul road over its working life [84].

## **2.3 Symptoms and Causes of Haul Road Deterioration**

Haul road exhibits excessive rutting, potholes, settlement, sinking and overall deterioration. The precipitation/runoff, heavy traffic volume, spring breakup, vehicle spillage and poor compaction are the major causes of haul road deterioration. Lack of sufficient bearing capacity material beneath the surface course exhibits excessive rutting, potholes, settlement, sinking and overall deterioration of the travel way [85, 214, 34, 196, 192]. Potholes are those depressions on the surface course of haul road that occur in the wheel path mostly due to traffic movement. It is due to poor compaction and/or development of shear stress in the sub-grade. Excessive roughness on haul road also causes corrugations. Though it is a surface phenomenon, it is linked to low plasticity materials on the base and sub-base courses, especially those with high sand and gravel fractions [68]. Rutting is the formation of progressive longitudinal depression in the wheel tracks. It primarily originates on mine haul road either due to deformation of surface course materials as due to sub-grade materials. Poor construction materials result in high maintenance cost of road, machines and vehicles with reduction in production and profit.

### **2.3.1 Demerits of base/ sub-base course materials of the haul road**

Base and sub-base layers are constructed either with overburden material or from locally available material found near to the mine boundary. Generally, pit run gravel is used for the base layer. The sub-base is often constructed from overburden, sand,

silt or sandy silt, or other suitable materials. The overburden material often has weathered rock, blasted material, clay or soil. Usually the materials used in base and sub-base layers are not crushed thus a particular particle size distribution is difficult to ensure. As the coarse materials of irregular sizes are placed in the base/sub-base layers, they get surrounded by a ring of soft un-compacted material. It causes uneven stress distribution that result in variable deformation. Some materials also have high plasticity index and cohesive in nature. Common construction materials for haul road base/ sub-base result only in filling the spaces instead of offering total solution to ground stability [29, 52, 8, 197].

### **2.3.2 Haul Trucks**

In past decades the carrying capacity of haul trucks has been increased from 10 T to 170 T and 300 T being envisioned at places, demanding better haul roads to carry such heavy loads. Large capacity haul trucks are being designed, manufactured and accepted by the industry. Large capacity haul trucks have an impact over road design. The haul road width depends upon the width as well as turning radius of the haul trucks. The maximum width of the haul truck has gone up from 9 m to 15 m in last decade. The turning radius of the haul trucks has increased by 12% over earlier generation. Hence larger turning radius and width of road is required to accommodate the large haul trucks.

#### **Haul truck tires**

Haul truck tires have grown with the size and capacity of trucks. The basic materials of a tire are: rubber (synthetic and natural), carbon black, sulphur, steel cable, polyester, nylon, and other chemical agents. A common ratio of rubber to other materials is 50:50 for a radial car tire and about 80:20 for an off-road haul truck tire. For large haul truck tires, about 80% of the rubber comes from natural sources. A higher proportion of natural rubber means a greater capacity to dissipate heat, but lower wear resistance. A higher proportion of carbon black leads to greater wear resistance of tires, but carbon tends to retain heat, thus the tire gets heated more

easily. If the haul road has an abrasive surface, a tire with a greater percentage of carbon black would be desired. But, if the haul road is smooth and free of abrasive materials, a tire with higher percentage of natural rubber would give better service in terms of tonnes per kilometer per hour [191].

There are two major types of tire i.e. bias ply and radial. Bias ply tires use rubber-cushioned nylon to form the carcass and steel wire bundles for beads. Radial tires consist of a ply of steel cables laid radially about the tire as carcass. The bead of the radial tire is formed by a single bundle of steel cables or steel strip. Radial tires have longer tread life, greater stability, more uniform ground pressure, less rolling resistance and less heat buildup from internal friction when the tire is in motion as compared to bias ply tires [114]. Large haul trucks tend to use radial tires due to these reasons. Werniuk (2000) reported that 95% of the tires used on large surface haul trucks were radial tires.

### **Tire foot print area and pressure**

Two important elements of tires that affect haul road design are foot print area and tire pressure. The inflation pressure of new low profile truck tires vary between 586 kPa to 703 kPa [63, 26]. The bearing capacity of the haul road construction materials should be greater than the tire pressure. Thus the bearing capacity of materials should be more than 1 MPa (equivalent to compressive strength of soft rock) used for the surface course [191]. A well designed sub-base and base layers with sufficient bearing capacities and stiffness is very much important because the stress bulb below a tire can extend quite deep due to the large tire footprint areas. The shape of tire footprint is approximated as either a circular or rounded rectangle. The pressure distribution beneath a tire is non-uniform, especially for bias ply tires. However, an assumption of uniform pressure distribution across the tire foot print area for the purpose of stress analysis in haul road layers is suggested [94].

The different wheel loading conditions typically considered are based on (i) maximum wheel load, (ii) contact pressure, (iii) multiple wheel loads or its equivalent, and (iv) repetition of loads. The vertical stresses due to wheel loading on the haul

road have strong influence on pavement strain prediction. There are many approaches to predict the stresses at any point in the pavement mass; one among those is the popular elastic theory. Initially the thickness of the pavement is determined using traffic volume, single wheel load and increased wheel load based on permissible maximum allowable shear stress for specific materials. The dual wheel cases are being considered as equivalent single wheel load (ESWL) where a load is determined that generates the same tire contact area and maximum deflection as would the group of wheels. The concept to consider equivalent single wheel load to multiple wheels give rise to corresponding equivalent deflection. The contact pressure and its distribution between any tire and the pavement depends on tire pressure, wheel load and tire construction. Usually the maximum weight of the haulage machine is considered in designing the road section. Though the true contact area between tire and road surface is elliptical, it is considered circular in shape for case of calculation [72]. The contact area is usually circular for a low ratio between applied load and maximum rated load [109]. Typically the ratio varies between 0.7 and 0.9 for fully loaded mine trucks [63] and the contact area is almost rectangle. Thus

$$\text{Contact Area (m}^2\text{)} A = \frac{\text{Load}}{\text{Tire Pressure}} \quad (2.17)$$

$$\text{Contact radius (m)} r = \sqrt{\frac{A}{\pi}} \quad (2.18)$$

$$\text{Thickness (m)} t = \sqrt{\frac{P}{55.8 \times CBR} - \frac{A}{\pi}} \quad (2.19)$$

The above equation is applicable for CBR less than 12 with multiple wheel groups and the corresponding thickness is given by [192,195]

$$t = \sqrt{A} \left( -0.0481 - 1.1562 \left( \log \frac{CBR}{P_e} \right) - 0.6414 \left( \log \frac{CBR}{P_e} \right)^2 - 0.4730 \left( \log \frac{CBR}{P_e} \right)^3 \right) \quad (2.20)$$

Where  $P_e$  = equivalent tire pressure at depth  $t$

$$P_e = \frac{ESWL}{A} \quad (2.21)$$

Incorporating the repetition factor, the equation to calculate CBR is

$$CBR(\%) = \frac{ESWL}{55.8 \left[ \left( \frac{t}{\alpha} \right)^2 + \frac{A}{\pi} \right]} \quad (2.22)$$

Where  $\alpha$  = repetition factor as determined elsewhere [2]

$$t = \alpha \sqrt{A} \left( -0.0481 - 1.1562 \left( \log \frac{CBR}{P_e} \right) - 0.6414 \left( \log \frac{CBR}{P_e} \right)^2 - 0.4730 \left( \log \frac{CBR}{P_e} \right)^3 \right) \quad (2.23)$$

The deflection under a single wheel load ( $W_s$ ) is

$$W_s = \frac{r_e}{E} b_s F_s \quad (2.24)$$

and deflection for a group of wheels ( $W_d$ )

$$W_d = \frac{r_d}{E} b_d F_d \quad (2.25)$$

Where,

$r_e$  = contact radius for single wheel (m)

$E$  = Elastic modulus of pavement (MPa)

$b_s$  = tire pressure for single wheel (MPa)

$F_s$  = deflection factor for single wheel

$r_d$  = contact radius for multiple wheels (m)

$b_d$  = tire pressure for multiple wheel (MPa)

$F_d$  = deflection factor for group of wheels

Rearranging (Equation 2.22) with input from (Equation (2.17) and Equation 2.18).

We have

$$P_s = \pi r_s^2 b_s \text{ and } P_d = \pi r_d^2 b_d \quad (2.26)$$

Where,  $P_{s,d}$  represent tire pressure for single wheel load and multiple wheel loads

respectively. Equating  $W_s=W_d$  and  $r_s=r_d$

$$\frac{F_s}{F_d} = \frac{b_d}{b_s} \text{ or } \frac{P_s}{P_d} = \frac{F_d}{F_s} \quad (2.27)$$

The (Equation 2.28) shows the relationship between tire load and the deflection factor, which can be obtained from the established curve (Figure 2.7). It was reported that four critical points for stress level exist under a haul truck [218]. The ESWL represents dual assembly and the critical points occur either under the center of one rear load (D) or at the center of the rear axle (C) (Figures 2.8 and 2.9). Two additional critical points (A and B) are also analyzed considering the front axle interaction in proportion to the fully laden axle weight distribution. The influence of each wheel at depth increment is calculated and the maximum ESWL at that depth is determined using (Equation 2.24 and Equation 2.28).

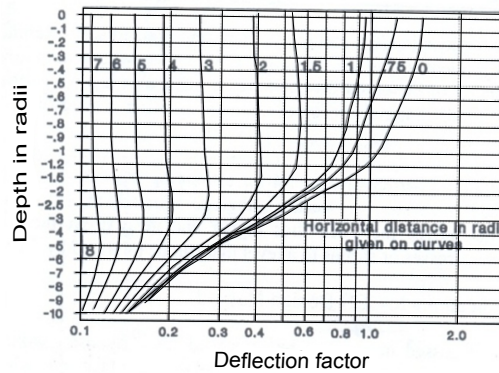


Figure 2.7: Deflection factors for ESWL determination [51]

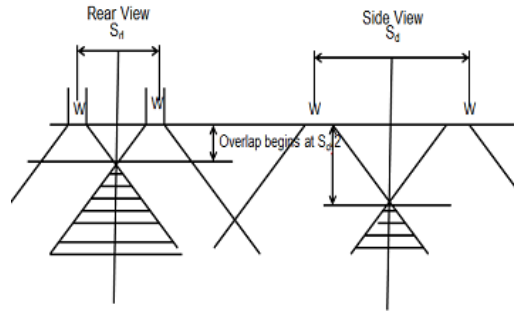


Figure 2.8: Influence of multiple wheels on sub-grade stress for dual and front and rear axles [195]

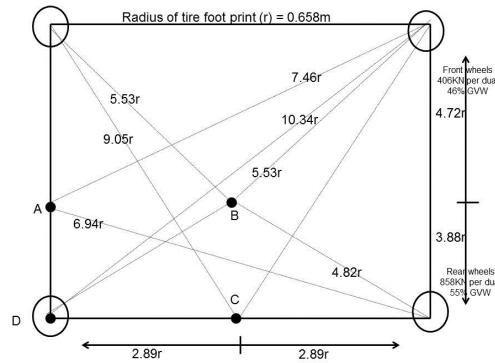


Figure 2.9: Horizontal positions for critical points A, B, C, D for R170 truck (fully laden) [195]

The CBR cover-curve design method developed by Kaufmann and Ault (USBM) is widely adopted for design of mine haul road. CBR value used in haul road design is typically evaluated from soaked test. In CBR cover-curve design method pavement cover thickness of any material with a particular CBR value is determined as a function of applied wheel load and CBR value of the material. The successive layers should have higher CBR value than the preceding layers.

The following equation is also suggested to calculate layer thickness ( $Z_{CBR}$ ) (m)

$$Z_{CBR} = \frac{9.81t_w}{P} [0.104 + 0.331e^{(-0.0287t_w)} [2 \times 10^{-5} (\frac{CBR}{P})]] [(\frac{CBR}{P})^{-0.415 + PX10^{-4}}] \quad (2.28)$$



Where

$t_w$  = Truck wheel load (metric tons)

P = Tire pressure (kPa)

Often the dumpers have dual wheel at rear to cater to excessive loading. The load bearing capacity for those cases are evaluated by considering equivalent single wheel loading to multiple wheels at the rear. It is simplified by assuming the load dispersion in layers beneath the wheel at about  $45^\circ$ . The governing equation suggested for calculating  $Z_{ESWL}$  is

$$Z_{ESWL} = Z_{CBR} + [0.184 + (0.086CBR + \frac{17.76 CBR}{t_w})^{-1}] \quad (2.29)$$

The above equation reflects that as the CBR value increases the thickness of pavement decreases.

## 2.4 Fly ash Generation and Collection

The solid inorganic residue of coal combustion, during process of thermal power generation which is carried away from boiler plant in the flue gas is called fly ash or pulverized fuel ash (PFA). Fly ash is also called coal combustion by-product (CCB) of coal fired thermal power stations. It is a fine material with spherical particles. It closely resembles volcanic ashes and also named as ‘pozzolan’.

Fly ash is generated from various inorganic and organic constituents present in feed coals and is produced at a temperature of 1200-1700°C [208]. The coal which is used in thermal power stations constitutes carbon as major component. It also contains hydrogen, oxygen and some minor elements of nitrogen and sulphur and non-combustible impurities (10-40%) usually present in the form of clay, shale, quartz, feldspar and limestone. When coal is consumed to generate electricity at elevated temperatures, these non-combustible minerals remain as ash products [112].

Indian coal has high ash contents that vary from 30 to 50%. The final result of burning of fossil fuels, particularly coal, is the emission of fly ash. Ash comes from mineral matter present in the fuel. For a pulverized coal unit, nearly 80% of

ash leaves with the flue gas [167]. Electrostatic precipitation (Figure 2.10) is a well-established technique that employs application of electric field to separate out the suspended particles (fly ash or dust) from the flue gas, which comes out of thermal power stations by collecting it in hoppers [133, 143, 89, 20, 67].

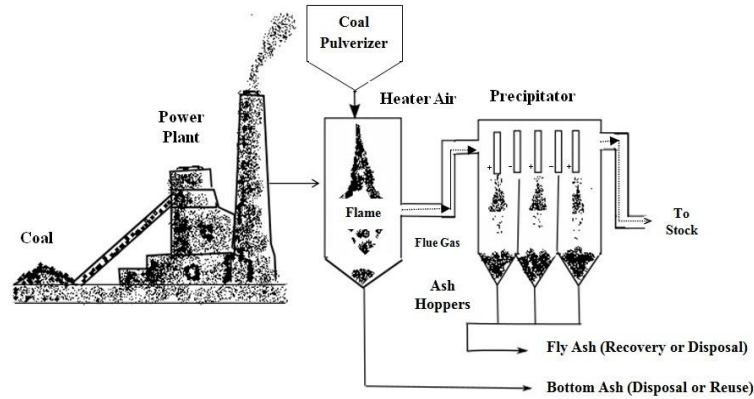


Figure 2.10: A schematic layout of generation and collection of fly ash

### 2.4.1 Problems associated with Fly ash Generation

The problem with fly ash is that its disposal not only requires large quantities of land, water and energy, its fine particles, if not managed well, can become airborne. Currently 160 MT of fly ash is being generated annually in India, with 300 Km<sup>2</sup>. of land being occupied by ash ponds. Such a huge quantity poses challenging problems, in the form of land use, health hazards and environmental damages. The problems associated with fly ash are given below.

1. It is very difficult to handle fly ash in dry state because it is very fine and readily airborne even in mild wind.
2. It pollutes air, water & disturbs the ecology of the surrounding atmosphere.
3. Flying fine particles of ash poses problems for people living near power stations, corrode structural surfaces and affect horticulture.

4. Eventual settlement of fly ash particles over many hectares of land in the vicinity of power station brings about perceptible degeneration in soil characteristics.
5. Long inhalation of fly ash causes silicosis, fibrosis of lungs, bronchitis, pneumonitis etc. (Table 2.2 ).

Table 2.2: Diseases due to the presence of heavy metals in fly ash [164]

Metal	Content (ppm)	Possible Diseases
Chromium (Cr)	136	Cancer
Nickel (Ni)	77.6	Respiratory Problem, Lung Cancer
Lead (Pb)	56	Anaemia
Arsenic (As)	43.4	Skin Cancer, Dermatitis
Antimony (Sb)	4.5	Gastroenteritis
Cadmium (Cd)	3.4	Anaemia, Hepatic Disorder

### 2.4.2 Status of Fly ash Utilization

Fly ash has got various applications in several areas and hence treated as by-product. Due to pozzolanic property, it is used as raw material for cement manufacturing [144, 153]. Some of the other major areas of current fly ash utilization are reclamation of low lying areas, back filling in opencast mines, stowing in underground mines, construction of road and embankments, manufacturing of bricks, structural fills [144, 31, 132].

The present utilization of fly ash is about 50%. Some of the applications include use of fly ash in mine filling, construction of roads/ flyover embankments, hydraulic structures, raising of dykes, manufacture of several building components like bricks, blocks, tiles and use in agriculture (Table 2.3 ). These measures though use fly ash in bulk yet leaves about 80 MT of it unutilized (FAUP, 2010).

Table 2.3: Utilization of fly ash in Various Sectors

Area of Utilization	Utilization(MT)	Utilization (%)
Manufacture of Cement	35	44
Construction of Road Embankments	15	19
Substitution of Cement	10	12
Back Filling in Mines	7	09
Reclamation of low lying Areas	6	07
Raising of Ash Dykes	3	04
Brick Manufacturing	3	04
Agriculture	0.5	0.5
Others	0.5	0.5

## 2.5 Properties of Fly ash

The physical and chemical properties of ash vary depending on origin of coal, type of plant, burning process, inorganic chemical composition of coal, degree of pulverization, types of emission control systems, handling and collection systems etc. Fly ash is of two types i.e. class C and class F. Class F is produced from burning of anthracite and bituminous coal. It contains very small amount of lime (CaO). Class F fly ash (pozzolans) has silicon and aluminum material that itself possess little or no cementitious value. It reacts chemically with lime and cement at room temperature to form cementitious compounds [30].

### 2.5.1 Physical Properties

Fly ash is grayish white in colour and in powder form [101]. Colour of fly ash depends on amount of un-burnt carbon and iron oxide present in ash. The presence of carbon from incomplete combustion of coal gives gray to black colour to fly ash. Carbon free ash is blue-gray to brown in colour due to presence of iron oxide. The overall colour of fly ash is gray.

Particle size distribution represents whether a material is well graded, medium

graded or poorly graded. Fly ash consists of finely divided spheroids of silicious glass that vary between 1 to 50 $\mu$ m in diameter. Majority of these spheroids are considerably finer than Portland cement. Fly ash is a fine grained material consisting of mainly silt-size particles with some clay-size particles of uniform gradation [138]. As fly ash is silt sized non-cohesive material, the effect of dispersion agents on particle size distribution of fly ash is negligible. Hence use of dispersion agents in hydrometer analysis can be dispensed with [184]. The gradation is decided based on co-efficient of uniformity ( $C_u$ ) and co-efficient of curvature ( $C_c$ ) obtained from particle size distribution curve. The co-efficient of uniformity and curvature are calculated as

$$C_u = (D_{60}/D_{10}) \quad (2.30)$$

$$C_c = (D_{30})^2/(D_{10} \times D_{60}) \quad (2.31)$$

Where

$D_{10}$  = Equivalent particle diameter corresponding to 10% fines on particle size distribution curve

$D_{30}$  = Equivalent particle diameter corresponding to 30% fines on particle size distribution curve

$D_{60}$  = Equivalent particle diameter corresponding to 60% fines on particle size distribution curve

Atterberg limits i.e. liquid limit, plastic limit and shrinkage limit are extensively used in the field of geotechnical engineering. Fly ash possesses liquid limit ranging from 26 to 51% [138]. He observed that fly ash is non-plastic in nature.

Free swell index differentiate between swelling and non-swelling soils and determine the degree of soil expansibility. Nearly 70% of Indian coal ashes exhibit negative free swell index which is due to flocculation, low specific gravity and less quantity of clay size particles [138, 184].

Specific gravity is one of the important physical properties required in planning and executing geotechnical applications that involve bulk utilization of fly ash. Specific

gravity of fly ash depends on its chemical composition. Fly ash generally possesses low specific gravity compared to that of soil due to the presence of more number of cenospheres from which the entrapped air cannot be removed, or the variation in the chemical composition, iron content in particular, or both [56, 184]. Specific gravity of Indian fly ash varies in the range of 1.66 to 2.55 [184]. Many factors are responsible for large variation in specific gravity values of fly ash as particle size and shape, gradation, chemical composition and segregation [65]. The specific gravity increases with fineness and the finest fly ash has maximum specific gravity [201].

Classification of any material is based on its physical appearance or chemical composition or some specific characteristics features. The fly ash is classified as fined grained material as it comprises of predominantly silt sized particles. It can belong to one of the five subgroups, namely MLN, MLN-MIN, MIN, MIN-MHN and MHN [184].

### 2.5.2 Chemical Properties

Fly ash is a complex inorganic-organic mixture with unique, polycomponent, heterogeneous and variable composition. There are about 188 minerals or mineral groups have been identified in fly ash [208]. The chemical composition is influenced to a great extent by the geological and geographical factors related to coal deposit, combustion conditions and removal efficiency of controlling devices [162]. Chemically coal is an organic material and primarily contains carbon, hydrogen, nitrogen, oxygen and sulphur. Primary inorganic constituents associated with coal are clay minerals, silica, carbonates and sulphides etc. The alteration, decomposition and transformation by heating of organic and inorganic materials during process of coal combustion produce fly ash. The resulting fly ash consists of compounds of silicon, aluminium, iron and calcium with smaller amount of compounds containing magnesium, titanium, sodium and barium as well as traces of other elements. Since combustion of coal is never complete, fly ash also contains varying amount of unburnt carbon called loss on ignition [90, 31, 199]. The predominant compounds in fly ash are silica ( $\text{SiO}_2$ ), alumina ( $\text{Al}_2\text{O}_3$ ), iron oxide ( $\text{Fe}_2\text{O}_3$ ) and calcium oxide ( $\text{CaO}$ ) [136, 101, 112, 173].

Sum of compounds of silica, alumina, iron oxide, calcium oxide and magnesium oxide is more than 85% [15]. Among those silica and alumina comprises 45% to 80%. The fly ash produced from sub-bituminous and lignite coal has relatively higher percentage of calcium oxide and magnesium oxide and lesser percentage of silicon dioxide, aluminium oxide, and iron oxide as compared to fly ash produced from bituminous coal (Table 2.4 ).

Table 2.4: Range of chemical composition of fly ash from different types of coal

Components	Bituminous	Sub-bituminous	Lignite
SiO <sub>2</sub>	20-60	40-60	15-45
Al <sub>2</sub> O <sub>3</sub>	5-35	20-30	10-25
Fe <sub>2</sub> O <sub>3</sub>	10-40	4-10	4-15
CaO	1-12	5-30	15-40
MgO	0-5	1-6	3-10
SO <sub>3</sub>	0-4	0-2	0-10
Na <sub>2</sub> O <sub>3</sub>	0-4	0-2	0-6
K <sub>2</sub> O	0-3	0-4	0-4
LOI	0-15	0-3	0-5

The chemical properties of fly ash depends upon many factors such as geological factors, the composition of the parent coal, the combustion conditions like the method of burning and control of combustion process, the additives used for flame stabilization, corrosion control additives used, hopper position, flow dynamics of the precipitators and the removal efficiency of pollution control devices etc. The mineral groups present in coal such as hydrated silicates, carbonates, silicates, sulphates, sulphides, phosphates and their varying proportions normally play a dominant role in deciding the chemical composition of the ash. When the pulverized coal is subjected to combustion, the clay minerals undergo complex thermo-chemical transformations. During this process, sillimanite and mullite are crystallized as slender needles along with glass formation. Pyrites and other iron bearing minerals form iron oxides and calcite gets transformed into CaO. The glassy phase formed renders pozzolanicity to the

fly ash. In almost all geotechnical engineering applications, the pozzolanic property of fly ash plays an important role [91]. Fly ash is classified as self pozzolanic, pozzolanic and non-pozzolanic depending on pozzolanic property. Fly ashes can also be classified as reactive and non-reactive fly ashes. Reactive fly ashes are those, which react with lime to give sufficient amount of strength. Non-reactive fly ashes are those, which do not give sufficient strength even on addition of lime. Self pozzolanic and pozzolanic fly ashes are reactive fly ashes where as non-pozzolanic fly ashes are nothing but non-reactive fly ashes.

Fly ash is of two types. Class C and F (ASTM C618 – 08a). The fly ash with silicon dioxide, aluminium oxide and iron oxide more than 70% is class F type. The range of chemical composition of Indian coal ashes together with that for soil is reported in (Table 2.5 ).

Table 2.5: Range of chemical composition of Indian coal ashes and soils [138]

Compounds	Fly ash	Soils
SiO <sub>2</sub>	38–63	43–61
Al <sub>2</sub> O <sub>3</sub>	27–44	12–39
TiO <sub>2</sub>	0.4–1.8	0.2–2
Fe <sub>2</sub> O <sub>3</sub>	3.3–6.4	1–14
MnO	0–0.5	0–0.1
MgO	0.01–0.5	0.2–3.0
CaO	0.2–8	0–7
K <sub>2</sub> O	0.04–0.9	0.3–2
Na <sub>2</sub> O	0.07–0.43	0.2–3
LOI	0.2–3.4	5–16

Loss on ignition is generally equal to the carbon content [156]. Amount of silica or sum of silica and alumina present in fly ash influenced the pozzolanic activity for a longer period of time [198]. A relatively high percentage of carbon decreased the pozzolanic activity [118]. The finer the fly ash, higher was the pozzolanic reactivity [40]. Fly ash collected by ESP was more reactive and consequentially, more suitable as

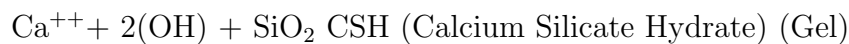
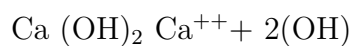
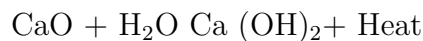


haul road construction material than fly ash collected by mechanical collectors [191].

The investigations on Indian fly ash show that all the fly ash contains silica, alumina, iron oxide and calcium oxide [140]. Quartz and mullite are the major crystalline constituents of low-calcium fly ash ( $\text{CaO} < 5\%$ ), whereas high-calcium fly ash ( $\text{CaO} > 15\%$ ) consists of quartz,  $\text{C}_3\text{A}$ , CS and  $\text{C}_4\text{AS}$  [163, 49, 174, 138, 184, 3]. The morphological studies indicate that the coal ash contains glassy solid spheres (plerospheres), hollow spheres called cenospheres, sub rounded porous grains, irregular agglomerates and irregular porous grains of unburned carbon [49, 184].

When water or any aqueous medium comes in contact with fly ash, iron, aluminum and manganese oxides sink determine the release of the trace elements associated with them into the aqueous medium. The degree of solubility of those oxides in turn depends upon the pH of the aqueous medium [184]. Fly ash with higher free lime and alkaline oxides exhibits higher pH values [138, 184]. About 50% of Indian fly ashes are alkaline in nature [184].

Formation of cementitious materials by the reaction of lime with the pozzolans in presence of water is called hydration. The hydrated calcium silicate or calcium aluminate, join the inert materials together. The typical pozzolanic reactions for stabilization are given below.



Class C type fly ash does not need addition of lime where as class F does [165].

### 2.5.3 Engineering Properties

A thorough understanding of the engineering behaviour of fly ash is very much essential for the bulk use of fly ash in geotechnical applications. The density of fly ash is an important parameter since it controls the strength, compressibility and permeability. Densification of ash improves the engineering properties. The compacted unit weight of the material depends on the amount and method of energy application, grain size

distribution, plasticity characteristics and moisture content at compaction [91, 138]. Compaction is a process of densification of the material by packing the particles closer together with reduction in the volume of air voids.

#### 2.5.4 Compaction Characteristics

Compaction of fly ash is required to improve its engineering properties. The compacted unit weight of the material depends on the amount of energy applied, grain size distribution, plasticity characteristics and moisture content at compaction [138]. Optimum moisture content decreases and maximum dry density increases with increase in fineness of fly ash [201]. Das and Yudhbir opined that presence of porous particles e.g. (unburnt carbon, plerosphere and cenospheres) was responsible for high optimum moisture content value [39]. Maximum dry density is related to mean size (mm) of fly ash by the following correlation (Equation 2.32 ) [201]

$$\gamma_d(Proctor) = 7.5486D_{50}^{-0.1072} \quad (2.32)$$

The variation of dry density with moisture content for fly ash is less compared to that for a well-graded soil, both have the same median grain size [128, 184]. The tendency for fly ash to be less sensitive to variation in moisture content than for soils can be explained by the higher air void content of fly ash. Soils normally have air void content ranging between 1% and 5% at maximum dry density, whereas fly ash contains 5% to 15%. The higher void content tend to limit the buildup of pore pressures during compaction, thus allowing the fly ash to be compacted over a larger range of water content [200]. Compaction tests were carried out on coal ashes and the obtained maximum dry density varied between 11.4 kN/m<sup>3</sup> and 45 kN/m<sup>3</sup> with the corresponding optimum moisture contents ranging between 28% and 36% [55]. Maximum dry density varied between 11.9 kN/m<sup>3</sup> and 18.7 kN/m<sup>3</sup> and optimum water content varied between 13% and 32% [44]. Typically maximum dry density of Indian fly ash vary in the range 8.9 kN/m<sup>3</sup> to 13.8 kN/m<sup>3</sup> and optimum moisture content in the range 17.9% to 62.3% [184, 39, 184]. Fly ashes originating from different

sources themselves show large variations in OMC and MDD due to their specific gravity depends on iron and carbon contents [174, 91].

### 2.5.5 Unconfined Compressive Strength

It is an important engineering property that is necessary for using fly ash in many geotechnical applications is its strength. The unconfined compressive strengths for fine ash are higher than those for the coarser ash specimens [99]. The unconfined compressive strength (UCS) increased from 390 kPa to 900 kPa at 7 days curing and 400 kPa to 1200 kPa at 90 days curing of British fly ashes compacted at Proctor's maximum dry densities [65]. The fraction of lime, present as free lime in the form of calcium oxide or calcium hydroxide, controls self-hardening characteristics of fly ashes [171]. The unconfined compressive strength of fly ashes act as a function of free lime present [174]. The unconfined compressive strength of fly ash increased exponentially with the free lime content [219]. They also reported that the carbon content in fly ashes reduced the strength which was attributed to the lower frictional resistance of carbon particles at the inter particle level. The class-F fly ash achieved unconfined compressive strength of 126 kPa at 7 days and 137 kPa at 28 days curing [56].

The major advantage of fly ashes with regard to shear strength in the compacted and saturated condition is that the variation of effective friction angle is negligibly small, irrespective of whether it is obtained from consolidated drained test or consolidated un-drained test [184]. The shear strength of class F fly ash primarily depended on cohesion component when it was in partially saturated [111]. When the sample was fully saturated or dried, it lost its cohesive part of the strength. When density of fly ash increases its friction also increases [25]. The shear strength parameters as angle of internal friction and cohesion of typical Indian fly ashes obtained by drained test under compacted condition are in the range of  $33^\circ$  to  $43^\circ$  and 16 kPa to 93 kPa respectively. Similar results are obtained by un-drained test under compacted condition in the range of  $27^\circ$  to  $39^\circ$  and 16 kPa to 96 kPa respectively [184, 138, 184]. The general relationship between UCS and quality of sub-grade soil are used in pavement construction (Table 2.6 ).

Table 2.6: Relationship between UCS and quality of sub-grade soil [37]

Quality of Sub-grade	UCS (KPa)
Soft sub-grade	25-50
Medium sub-grade	50-100
Stiff sub-grade	100-200
Very stiff sub-grade	200-380
Hard sub-grade	> 380

### 2.5.6 California Bearing Ratio

CBR test is an empirical test. The results of the test are case specific. CBR values are useful in evaluating the suitability of the material for use in road construction. It is the ratio of force per unit area required to penetrate a specimen with a circular plunger of standard size at a standard rate to that required for the corresponding penetration in a standard material.

Compacted coal ashes tested in un-soaked condition had higher CBR values than those of fine grained soils [184]. High CBR values are due to capillary forces that exist in partial saturated state. These capillary forces become zero on submerge in water. CBR values reduce drastically after soaking. Investigation was carried out on the engineering behavior of low carbon, pozzolanic fly ash and reported that CBR values at soaked condition were less than those at un-soaked condition and also concluded that properly compacted and cured fly ash samples obtained excellent CBR values [73]. They reported CBR values of about 325% and 280% for un-soaked and soaked samples respectively. The CBR values of typical Indian fly ashes vary from 11.3% to 20.6% for un-soaked condition and 0.2% in soaked condition [184, 138, 184]. The general relationship between CBR and quality of sub-grade soil are used in pavement construction (Table 2.7).

Table 2.7: Relationship between CBR and quality of sub-grade soil [16]

Quality of Sub-grade	CBR (%)
Very poor sub-grade	0-3
Poor to fair sub-grade	3-7
Fair sub-grade	7-20
Good sub-grade	20-50
Excellent sub-grade	75

### 2.5.7 Ultrasonic Velocity

Ultrasonic pulse velocity test is a non-destructive testing method. It is used to determine the dynamic properties of materials. This method is valid for wave velocity measurement of both anisotropic and isotropic materials though velocities obtained in anisotropic materials may be influenced by several factors such as direction, material composition, dampness, weakness, travel distance and diameter of transducer.

The ultrasonic pulse velocity test is a measurement of transit time of a longitudinal vibration pulse through a sample which has a known path length. It is carried out by applying two transducers (transmitter and receiver) to the opposite end surfaces of the samples. If any discontinuity surface lies in the pulse path, the measured time corresponds to the pulse that follows shortest path, because any discontinuity causes a time delay compared to travel time of pulses in homogeneous mass. The schematic representation of Ultrasonic velocity measurement system (Figure 2.11 ). The electrical pulses of a specified frequency are generated by pulse generator. These pulses are converted into elastic waves which propagate through the sample by transmitter. The mechanical energy of the propagating waves that propagate through the sample are received by the second transducer called receiver placed at opposite end of the sample and then turns it into electrical energy of same frequency. The signal travel time is measured electronically through the sample and is registered in the oscilloscope.

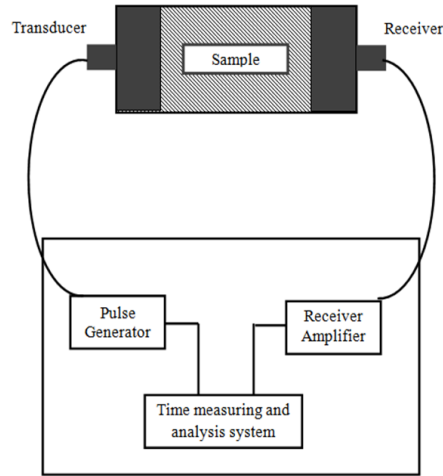


Figure 2.11: Typical arrangement of Ultrasonic velocity measurement [108]

The relationship between various parameters on pulse velocity, density, elastic constants, modulus values are given by the following equations

$$\mu = \frac{V_p^2 - 2V_s^2}{2(V_p^2 - V_s^2)} \quad (2.33)$$

$$E = \frac{\rho V_s^2 (V_p^2 - 4V_s^2)}{V_p^2 - V_s^2} \quad (2.34)$$

$$K = \frac{\rho (V_p^2 - 4V_s^2)}{3} \quad (2.35)$$

$$G = \rho V_s^2 \quad (2.36)$$

Where

$V_p$  = compression P wave velocity, m/s

$V_s$  = shear S wave velocity, m/s

$\rho$  = density, kg/m<sup>3</sup>

$\mu$  = Poisson's ratio

E = Young's Modulus, Pa

K = Bulk Modulus, Pa

G= Shear (Rigidity) Modulus, Pa

Ultrasonic non-destructive testing is a versatile technique which is applied to a wide variety of material analysis applications. The ultrasonic velocity of fly ash-cement composites increased over time [119]. The ultrasonic velocity increased with increase in curing period of the masonry composite material made of limestone powder and fly ash [202]. It was reported that the ultrasonic pulse velocity increased from 1150 m/s to 1800 m/s in the composite containing 10% fly ash at 7 days curing. The increase in fly ash percentage from 0% to 75% causes a decrease in ultrasonic velocity [45]. The ultrasonic velocity of the mixture containing 25% fly ash was 2.06 km/s and with 75% fly ash was 1.36 km/s. It was also reported that the ultrasonic velocity increases with increase in density of the material.

Various investigations were carried out to determine rock properties as unconfined compressive strength, static elasticity modulus by Portable Non-destructive Digital Indicating Tester (PUNDIT) [66, 205, 207, 11]. Investigation was carried out on mine cemented paste backfill material by ultrasonic wave and reported that ultrasonic non-destructive test results could be correlated with other laboratory test results [53]. Ultrasonic testing method was used to determine the quality of grout in the grouted rock bolts in place of costly, time consuming and over coring destructive method [105, 220]. Indirect in-situ measurements were done by ultrasonic method to obtain data for rock mass classification because classical methods are expensive and time consuming [54, 102, 82]. Ultrasonic method has been used in determination of properties of concrete mixes [107]. Ultrasonic method was used to evaluate properties of a mixture of cement, fly ash and lime [217].

## 2.6 Uses and Strength Behaviour of Fly ash

Investigations and laboratory studies have been carried out for utilizing fly ash in bulk to minimize environmental as well as disposal problems. Fly ash has been proposed for various applications as soil stabilization, land reclamation, filling material, manufacturing of brick, construction of road and embankment etc. There are many

instances on bulk utilization of fly ash in road constructions [96, 13, 212, 125]. The addition of fly ash reduced the volume change characteristics and improved the sub-grade strength. Fly ash provides silica and alumina needed for cementitious reaction with lime to increase the strength, stiffness, and durability of the stabilized base layer [23, 104].

Engineering properties of compacted fly ash was observed and concluded that properly compacted and stabilized fly ash had the requisite properties for use in load-bearing fills or highway sub-bases [65]. Plasticity index of clay was decreased with the addition of lime and fly ash [79].

The use of fly ash to stabilize soils should have multiple benefits to their use in haul roads improving mining productivity [69]. The suitability of fly ash as construction material in road base and sub-base construction on stabilizing the ash with 5% and 10% lime or cement [146]. There exist a couple of road projects, especially in rural sectors where cementitious fly ash has been used as sub-base material [96]. Incorporation of fly ash in the clay material improves the mechanical properties of the clay [150, 193]. The gain in strength and modulus is dependent on the fly ash and cement contents in the fly-soil mixture [81].

Government regulation has put severe restrictions on disposal of fly ash near the coal power plants as practiced earlier (MOEF, 2009). It necessitates exploration of new avenues to cater to the huge generation of fly ash.

Bulk utilization of fly ash is possible only through geotechnical applications [184]. Fly ash, mine spoil/ coal partings and kiln dust were mixed at 25:70:5 and found that the composite was suitable for use in base and sub-base layers of mine haul road [192]. The unconfined compressive strength of developed composite increased from 0.4 MPa to 0.6 MPa after 7 days curing and 0.6 MPa to 1.1 MPa at 28 days curing with elastic modulus varying between 150 MPa and 350 MPa after 14 to 28 days. The composite showed Young's modulus values high enough to meet the reduced strain for haul road construction.

In recent years, for economic and environmental reasons, focused attention has been given to the use of solid wastes in lieu of conventional aggregates in pavements



[22]. Higher amount of fly ash is needed for effective pozzolanic activity in case of poorly graded material [160]. Unconfined compressive strength and Brazilian tensile strength characteristics were observed for fly ash mixed with varying percentages of soil and carbide lime [35]. Unconfined compressive strengths and Brazilian tensile strengths obtained were between 410 kPa and 1924 kPa and between 17 kPa and 200 kPa respectively at 7 to 90 days curing for the mixes containing soil and 25% fly ash stabilized with 4%, 7% and 10% of lime. It was reported that the compressive strength of fly ash-lime-soil were between 410 kPa and 634 kPa at 7 days, 822 kPa and 1,243 kPa at 28 days and 6.9 MPa and 9.4 MPa at 180 days curing.

Recycled plastic strip mixed with soil-cement-fly ash can develop a sufficient bond which delay the propagation of tensile cracks in the base course of the road structure and can be suitable for haul road construction [180]. Strength characteristics of fly ash mixed with varying percentage of phosphogypsum were obtained [115]. Unconfined compressive strengths increased from 3.04 MPa to 3.13 MPa at 7 days curing for the fly ash contents from 12% to 52% in the mixes and then increase in fly ash content from 62% to 72%, the strength value decreased from 2.76 MPa to 2.56 MPa.

Soil-fly ash mixtures prepared with 18% fly ash and compacted at 7% wet of optimum water content showed significant improvement compared to the untreated soils, with CBR ranging from 15% to 31% [1].

Fly ash has good potential use in geotechnical applications. Its low specific gravity, freely draining nature, ease of compaction, insensitiveness to changes in moisture content, good frictional properties etc. can be gainfully exploited in the construction of roads, embankments etc. Fly ash was mixed with soil and concluded that the addition of fly ash reduces the dry density of the soil due to low specific gravity and unit weight [149]. It was concluded that the soils with CBR values 4.7%, 2.03% and 3.53% increased up to 11.41% by adding fly ash up to 46%. Thus, fly ash can be effectively utilized in the soil to improve shear strength, cohesion and the bearing capacity.

The engineering properties of Class F fly ash amended soils as highway base materials were evaluated [6]. They mixed fly ash (40%) with sandy soils with plastic fines

contents and activated the mixture with 7% cement and obtained CBR and UCS values of 140% and 3.2 MPa respectively. Similar observations were obtained when silty and sandy soils were stabilized with lime-activated Class F fly ash for highway bases [211].

The plasticity index and linear shrinkage of all types of soil decreased from 15% to 1% and 7% to 1% respectively, but the CBR value increased from 36% to 162% which enhanced the suitability of the soils for construction of base and sub-base in road works by conducting a laboratory investigation on four types of soil samples as clayey sand, gneiss with calcrete, quartz and schist and friable calcrete, each mixed with 4%, 8%, 16% and 20% fly ash [160].

Many attempts have been made to use fly ash in road construction, particularly in rural road construction [212, 174]. 60,000 m<sup>3</sup> of unutilized fly ash was successfully used in the construction of a 3.4 km long and 7.3 m wide road [31].

Fly ash utilization resulted in maximum savings in the sub-base course limited to about 60 to 90 km of lead for rigid and flexible pavements [94]. Most of our power plants are situated within this range of most coal mines. One conservative estimate puts the unutilized fly ash occupying about 65000 acres of land [39] which demands increase the utilization percentage.

Unconfined compressive strength and California bearing ratio values increased due to increase in fly ash percentage (10% - 20%) in the soil-fly ash mixtures [165]. It was concluded stabilized fly ash-soil mixtures offer an alternative for soft sub-grade improvement in highway construction. The class-F fly ash stabilized with only lime (10%) and lime (10%) with gypsum (1%) achieved compressive strength of 552 kPa and 5902 kPa at 28 days curing and 4046 kPa and 6308 kPa at 90 days curing [56]. It was reported that the CBR value of the specimens stabilized with only lime (10%) and lime (10%) with gypsum (1%) result 77% and 172% at 28 days curing period compared to 34% at 28 days for un-stabilized fly ash.

Fly ash provides silica and alumina needed for cementitious reaction with lime to increase strength, stiffness, and durability of the stabilized base layer [23]. Fly ash acted as a mineral filler to fill the voids in the granular pulverized pavement mix,

reducing the permeability of the Full Depth Reclamation (FDR) stabilized base layer. Lime, phosphor-gypsum and fly ash was mixed in the ratio of 8:46:46 and observed a continuous increase in strength value of 2.4 MPa at 7 days to more than 16 MPa at 365 days curing [168]. It was observed that fly ash mixture was a better material for semi-rigid road base material.

Fly ash and steel slag mixed with 2.5% of phospho-gypsum resulted in enhanced strength value [168]. Investigation was carried out with solidified material by comparing with some typical road base materials and observed increase in strength value of 8 MPa at 28 days to 12 MPa at 360 days curing respectively has higher strength than lime-fly ash and lime-soil road base material and opined the material as a road base application.

Bottom ash and fly ash was used successfully for pavement construction [75]. With increase in height of compacted fly ash layer over soft soil layer, the CBR value of compacted fly ash increased[56]. The silica and alumina in the fly ash reacts with lime to form hydration products which increase the strength, stiffness and durability of the stabilized base layer [104].

CBR values of unpaved road material stabilized with fly ash (10% and 20%) and lime kiln dust (2.5% and 5%) were found to be between 69% and 142% at 7 days curing and more than 164% at 28 days curing [27].

## 2.7 Inference

The exhaustive literature review carried out reflects the attributes of fly ash in geo-technical applications. It also brought the deficiencies in using the overburden material alone in haul road construction. Availability of free lime in the mixture along with presence of moisture enhanced the strength values. Hence in the investigation development of suitable road base/ sub-base material have been experimented with fly ash, overburden and commercially available additive.

# Chapter 3

## Methodology

### 3.1 General

The aim of the investigation was to enhance bearing capacity of surface coal mine haul road as well as to achieve bulk utilization of fly ash. This chapter presents methods adopted and materials used to achieve the goal. The major ingredients were fly ash, mine overburden and clinker. Sample preparation, various methods followed for characterization of ingredients and development of different composite materials are reported.

### 3.2 Materials and Methods

#### 3.2.1 Materials

The details of ingredients used in this investigation are discussed.

#### **Fly ash**

Fly ash, a by-product of coal combustion was collected from CPP-II of Rourkela Steel Plant (RSP), SAIL. The reasons involved in selecting RSP fly ash for the investigation are:

1. It is situated near the two major coalfields i.e. IB Valley, Talcher and Basundhara coal field
2. It produces huge amount of fly ash creating acute environmental as well as disposal problems.

Rourkela Steel Plant is an integrated steel plant of Steel Authority of India Limited commissioned in 1958. It has a captive power plant that consumes 2230 tonne of coal per year and generates 120 MW electricity. It produces about 600 tonne of fly ash per year. The fly ash so generated is typically dumped in nearby pond areas.

1. Collection method

The fly ash used in the present study was collected in dry state from electrostatic precipitators of CPP-II, RSP. During the combustion of pulverized coal in suspension-fired furnaces of thermal power unit, the volatile matter is vaporized and the majority of the carbon is burnt. The mineral matter associated with the coal, such as clay, quartz and feldspar disintegrates. The finer particles that escape with flue gases are collected using electrostatic precipitators in hoppers. The hoppers have small outlets. Gunny bags made of strong poly-coated cotton of 50Kg capacity were used to collect the dry fly ash. Each bag was sealed immediately after fly ash collection and the same was again inserted in another bag to prevent atmospheric influences. The bags were transported with care from the plant to laboratory and kept in a controlled environment.

### **Overburden Material**

Overburden from a surface coal mine is an important ingredient for the investigation. It was sourced from an active mine Basundhara opencast coal mine, MCL, Odisha (Figure 3.1). It is situated at about 150 km from Rourkela. The coal belongs to Gondwana sequence. Major part of the area is covered by Barakar / Karharbari formation. The typical overburden material consists of alluvium, laterite, fine to medium grained sandstone, shaly sandstone, shale, carbonaceous shale, fire clay etc. The mine produces about 7 MT per annum. The length of main haul road is around 8

Km and branch haul roads are 1-1.5 Km at different locations of the mine. Haul roads are basically flexible pavement type which are designed by California Bearing Ratio (CBR) method. The mine follows drilling, blasting, loading and dumping operations. Shovel and dumper combinations are used to handle overburden materials. 50 T to 80 T dumpers (make: BEML) are used to haul overburden material.

1. Collection method

The O/B dump area is around 2 km from the benches in operation. The O/B dump area spreads about 400 m long and 500 m wide. Dumpers dump the overburden material which is evenly spread by dozers. Samples of overburden material were collected from different areas of the dumping yard including freshly dumped material so as to have the representative samples. All the materials so collected were again mixed at the site thoroughly discarding pebbles, rock fragments, gravel etc. The samples were then placed in air tight packs and transported and kept in a controlled environment. Limited amount of samples were taken out for each experiment.

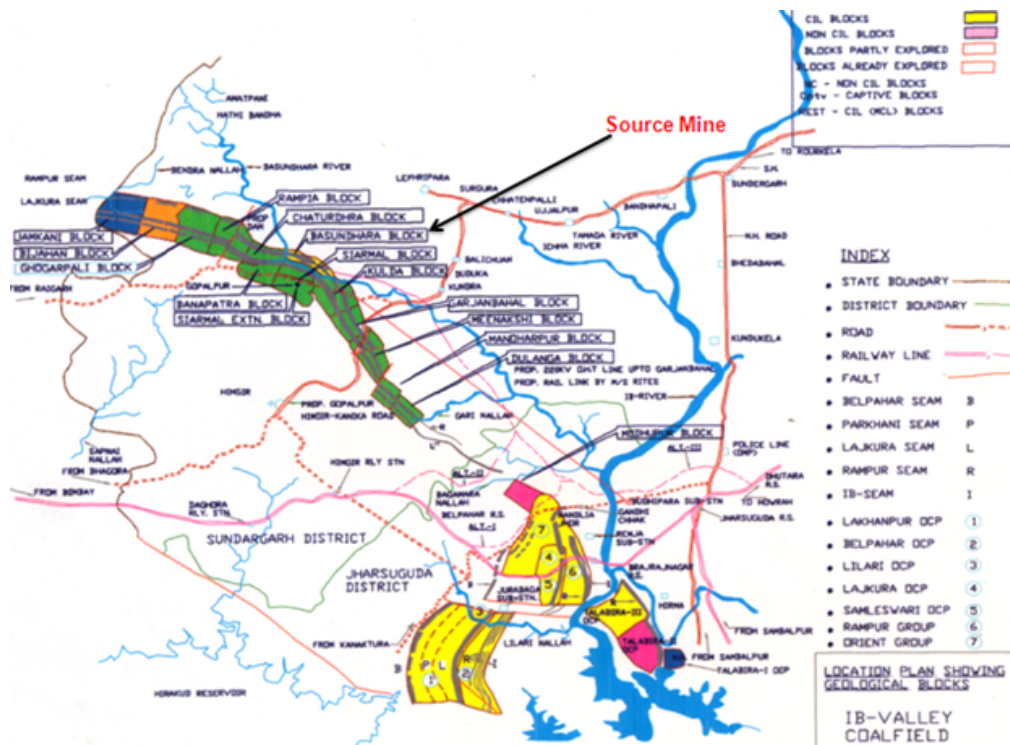


Figure 3.1: Map of IB Valley coal field showing Basundhara Coal Mine



Figure 3.2: Collection of mine overburden samples

### 3.2.2 Methods

#### Sample preparation

There are many published reports of evaluating the performance of soil stabilization with fly ash [47, 27, 14, 154, 159]. The soil chosen in those investigations were more or less uniform. Overburden material is heterogeneous in nature. The overburden disposal is not only a challenge, but also has many disadvantages in its use as construction material for haul roads. As the aim of the investigation was not only to enhance haul road strength behaviour, but also to maximize fly ash utilization percentage, it was decided to evaluate composites with more than 50% fly ash content (Table 3.1).

Table 3.1: Various proportions of flyash, mine overburden and clinker

Fly ash (%)	Overburden (%)	Clinker (%)	Fly ash (%)	Overburden (%)	Clinker (%)
90	10	0	70	30	0
88	10	2	68	30	2
86	10	4	66	30	4
84	10	6	64	30	6
82	10	8	62	30	8
80	20	0	60	40	0
78	20	2	58	40	2
76	20	4	56	40	4
74	20	6	54	40	6
72	20	8	52	40	8

Availability of free lime enhances the pozzolanic activity of materials. Therefore clinker a commercially available additive was chosen for the investigation. Clinker mainly consists of calcium oxide, silica, alumina and iron oxide. The mineral phases are very fine, usually in the range of 30-60 $\mu$ m. It consists mainly of alite, belite, calcium aluminate and aluminoferrite. In this investigation a varying percentage of clinker 2%, 4%, 6% and 8% were used in preparing the fly ash-overburden composites (Table 3.1). Modified Proctor compaction test was carried as per IS: 2720-Part (1983) to determine the maximum dry density and optimum moisture content of the fly ash-mine overburden-clinker mixes for preparation of sample. The samples were prepared at their respective OMC and MDD. The ingredients such as fly ash, mine overburden and clinker were blended in the required proportion in dry condition. The dry mixed ingredients were put in a poly pack, covered and left for about an hour for homogenization. Then required amount of water was added to the mixture and mixed thoroughly. The mixture was left in a closed container for uniform mixing and to prevent loss of moisture to atmosphere. The wet mixture was compacted in the proctor mould.



**Sample preparation for CBR Test**

The California bearing ratio (CBR) test samples were prepared using standard CBR mould of 150mm diameter and 175mm height as per IS: 2720-Part 16 (1987). The sample was statically compacted in the mould, such that the height was maintained at 127mm. A circular metal spacer disc of 148 mm diameter and 47.7mm height was used to compact the sample.

**Sample preparation for UCS Test**

Mould of 38 mm diameter and 76 mm length was used for preparation of the unconfined compressive strength (UCS) test samples as per IS: 2720-Part 10 (1991). Samples were prepared with uniform tamping. Two circular metal spacer discs of height 5 mm and diameter 37.5mm each with base (7 mm height, 50 mm diameter) were used at top and bottom ends of the mould to compact the sample such that the length of the specimen was maintained at 76 mm. Then the discs were removed and another spacer disc of height 100 mm and diameter 37.5 mm with a base (height 7 mm, 50 mm diameter) was used to remove the sample from mould. The final prepared specimen had length to diameter ratio of 2.

**Sample preparation for Tensile Strength Test**

The tensile strength is determined as per ASTM D3967. The sample for Brazilian tensile strength test was prepared using the same mould of UCS test samples. For this purpose, two circular metal spacer discs of 5 mm and 62 mm heights and 37.5 mm diameters with base (height 7 mm, 50 mm diameter) were used. The final prepared specimen had length to diameter ratio of 0.5.

**Sample preparation for Ultrasonic Pulse velocity Test**

Ultrasonic P- wave velocity test was carried out as per IS: 10782 (1983). Mould of 38 mm diameter and 76 mm length was used for preparation of the Ultrasonic test. The procedure for the sample preparation of the above test is same as unconfined

compressive strength (UCS) test samples. The final prepared specimen had length to diameter ratio of 2.

### **Sample preparation for SEM, EDX and XRD Analyses**

The raw materials after oven dried were taken for scanning electron microscopy (SEM), energy dispersive X-ray (EDX) and X-ray diffraction studies. Fractured pieces of composites retrieved from CBR moulds after CBR tests were taken for the above analyses. For SEM and EDX analyses, fragments of the specimens were collected and oven dried to constant mass. For XRD analyses, fractured pieces of the samples after oven dried were crushed and sieved by 75 $\mu$ m sieve.

## **3.2.3 Experimental methods**

### **Grain Size Distribution**

Grain size distribution was carried out through a standard set of sieves as per IS: 2720-Part 4 (1985). The material passing through the 75 $\mu$ m size was collected carefully and grain size distribution analysis was performed by using Hydrometer test . The overburden and fly ash have been classified based on particle size (IS: 1498, 1970).

### **Atterberg Limits**

The Atterberg limits of the mine overburden were determined as per IS: 2720-Part 5 (1985) and Part 6 (1972). The liquid limit is the minimum moisture content at which the soil type material can flow under a specified small disturbing force, the disturbing force being defined by the method of testing. The liquid limit of mine overburden was determined using Casagrande apparatus. The liquid limit of fly ash was determined by the cone penetration method as per BS: 1377-Part 2 (1990) due to difficulty in cutting a groove using Casagrande device. The plastic limit is the minimum water content at which soil ceases to behave as a plastic material. It was determined by rolling about 5 gm of wet soil pat into a thread on the glass plate with tips of the fingers of one hand to 3mm diameter. The shrinkage limit is the maximum water

content below which the soil ceases to decrease in volume on further drying. It was determined using shrinkage limit dish.

### **Free Swell Index**

Free swell index of the overburden and fly ash was determined as per IS: 2720-Part 40 (1977).

### **Specific Gravity**

The specific gravity of the mine overburden and fly ash were determined using volumetric flask method as per IS: 2720-Part 3 (1980).

### **X-ray Diffraction (XRD) Analysis**

X-ray diffraction provides a powerful tool to study the structure of the materials which is a key requirement for understanding materials properties. X-ray diffraction is based on constructive interference of monochromatic X-rays and a crystalline sample. X-ray powder diffraction is most widely used for the identification of unknown crystalline materials (e.g. minerals, inorganic compounds). It is a technique for analyzing structures unknown solids which is critical to studies in geology, environmental science, material science, engineering and biology. X-ray beam hits a crystal, scattering the beam in a manner characterized by the atomic structure. Even complex structures can be analyzed by x-ray diffraction, such as DNA and proteins. In the present investigation, XRD analysis was performed on a Philips diffractometer (PANalytical X-ray B.V., UK) employing Cu K $\alpha$  radiation in the range  $2\theta = 0^{\circ}$  to  $90^{\circ}$  at a goniometer rate of  $2\theta = 2^{\circ}/\text{min}$  to detect the mineral phases.

### **SEM and EDX Studies**

Scanning Electron Microscopy (SEM) is a powerful analytical technique for the evaluation of particulate matter. Scanning electron microscope uses a beam of energetic electrons to examine objects on a very fine scale. It is capable of performing analyses of selected point locations on the sample and is especially useful for determining

chemical compositions. The SEM analyses were conducted in a JEOL JSM 6480 LV, (Japan) model operated at 15 kV and linked with an energy dispersive X-ray (EDX) attachment. Microstructure and chemical composition of the samples were examined by SEM and EDX techniques.

### **Loss On Ignition (LOI)**

Loss on ignition of overburden and fly ash were determined as per IS: 1760-Part 1 (1991).

### **pH Test**

The pH value was determined as per IS: 2720-Part 26 (1987) to identify the acidic or alkaline characteristic of overburden and fly ash. The measurement of pH was carried out using pH meter (make: Systronics, India) with accuracy up to  $\pm 0.02$  units. The instrument was standardized with three standard buffer solutions of pH 7.00, 4.00 and 10.00 at  $25^{\circ}\text{C}$ . The suspension was stirred well and allowed to come to room temperature ( $25 \pm 1^{\circ}\text{C}$ ) before taking the pH measurement.

### **Triaxial Compression Test**

The un-drained, triaxial compression test was carried out as per IS: 2720-Part 11 (1993) to determine the shear strength parameters of the mine overburden and fly ash. Three identical samples of 38 mm diameter and 76 mm length were prepared at optimum moisture content and maximum dry density of the materials obtained from the modified Proctor compaction test. The samples were tested by giving confining pressures  $1\text{kg}/\text{cm}^2$ ,  $2\text{kg}/\text{cm}^2$  and  $3\text{kg}/\text{cm}^2$  respectively. Average values of three tests for each type were considered for analysis. Mohr-Coulomb relation between two normal stresses ( $\tau = C + \sigma_n \tan \varphi$ ) has been used to determine Cohesion and angle of internal friction of the materials.

**Compaction Test**

Higher compaction is needed to meet the bearing capacity for heavy vehicle transportation and typically the machineries operating in surface coal mines weigh about 80 T. Modified Proctor compaction test is typically used to give a higher standard of compaction. It was performed to determine the maximum dry density and optimum moisture content of the material. The sample was compacted in the mould in five layers using a rammer of 4.9 kg mass with a fall of 450 mm by giving 25 blows per layer [39]. The compacted energy value given was 2674 kJ/m<sup>3</sup>.

**California Bearing Ratio Test**

The samples were statically compacted to 95% of maximum dry density in CBR mould for the test. The samples were soaked for four days in water and were allowed to drain for 15 min before test. The curing periods adopted were immediate, 7 days (3 days moist curing + 4 days soaking) and 28 days (24 days moist curing + 4 days soaking) [91]. Two surcharge disks, each weighing 2.5 kg, were placed over the sample. A plunger of 50 mm diameter was used to penetrate the sample at a rate of 1.25 mm/min during test. The prepared CBR samples, soaking of CBR samples in the water tank and experimental set up for CBR test (Figure 3.3).

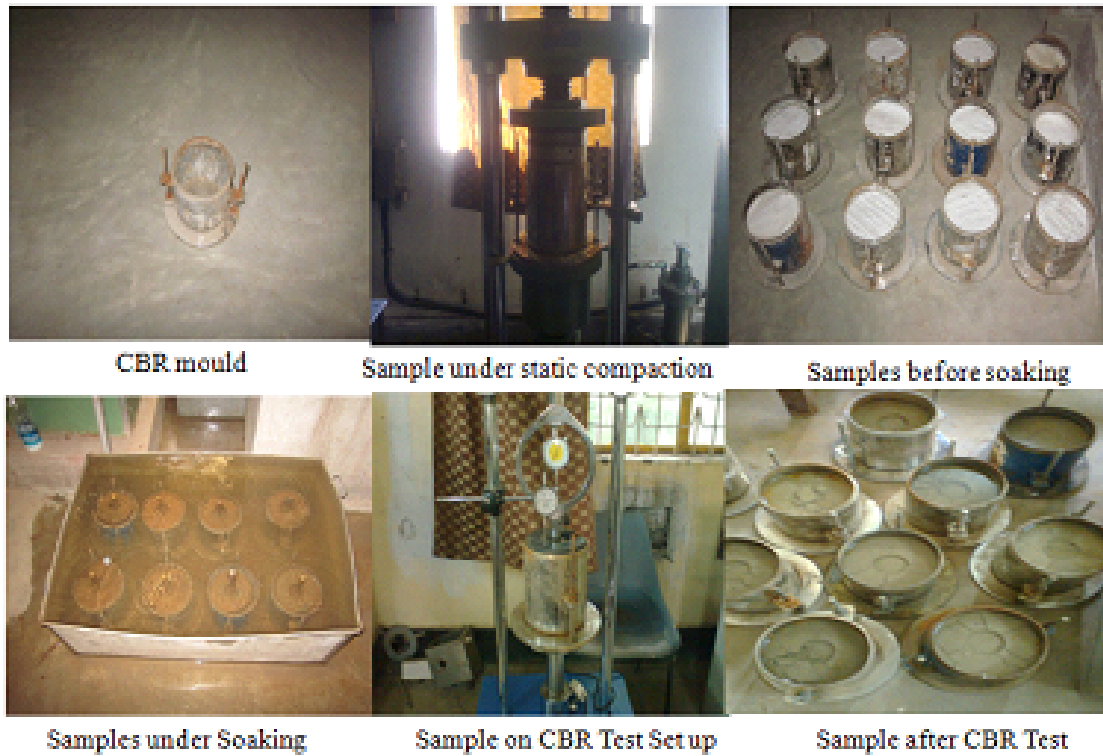


Figure 3.3: California Bearing Ratio Test

### Unconfined Compressive Strength Test

Unconfined compressive strength is carried out to determine the resistance of material to any external loading. The availability of free lime and reactive silica and aluminum etc. plays a vital role in strength gain. Moisture content has direct effect on reactivity. Hence it is preserved by curing the sample in a controlled chamber with  $>95\%$  humidity at  $30 \pm 2^{\circ}\text{C}$  (Figure 3.4). The unconfined compressive strength tests were conducted at a strain rate of 1.2 mm/min. Load and deformation data were recorded till failure of the specimen. The experimental set up and prepared sample for unconfined compression test (Figure 3.4).

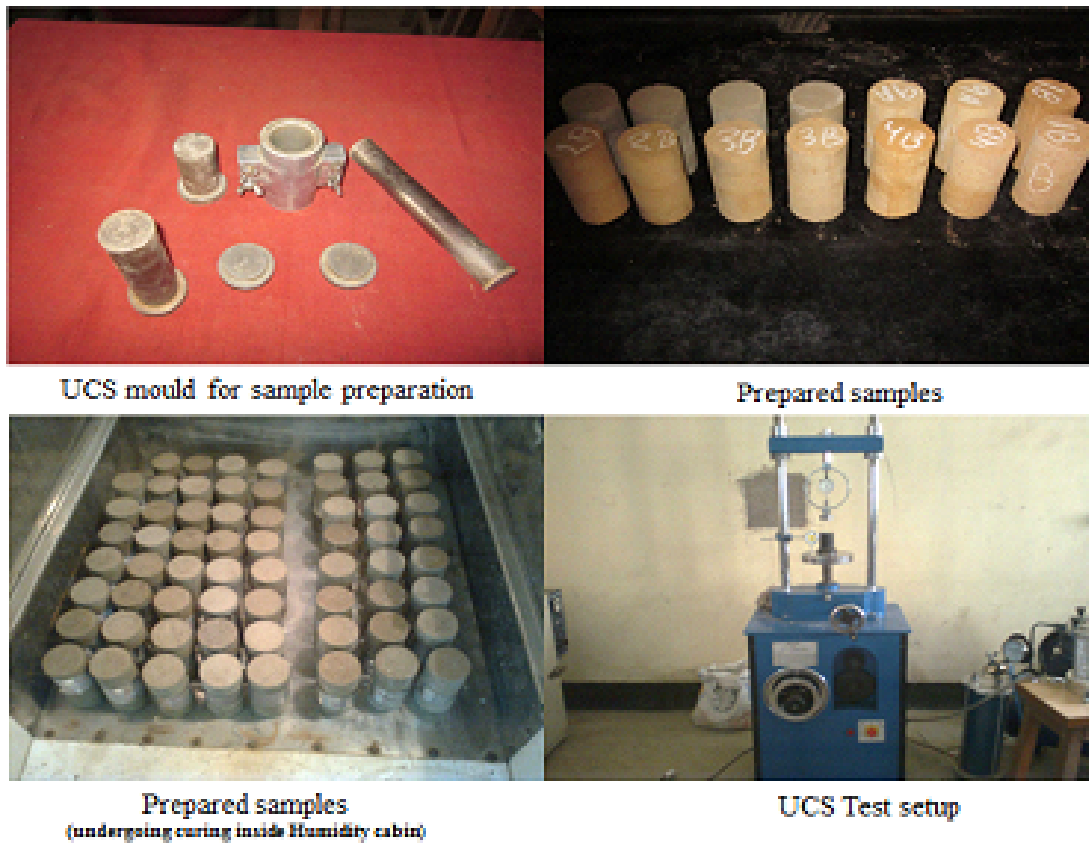


Figure 3.4: Unconfined Compressive Strength Test

### Brazilian Tensile Strength Test

Determination of direct tensile strength of soil or rock mass is difficult. So, indirect test i.e. Brazilian tensile test is practiced (Figure 3.5). The Brazilian tensile test make the sample fail under tension though the loading pattern is compressive in nature. The samples were placed diametrically during test. The sample fails diametrically in tension by application of load. The indirect tensile strength is calculated as:

$$\sigma_t = \frac{2P}{\pi Dt}$$

Where

$\sigma_t$  = Brazilian Tensile Strength

P = Failure Load

D = Diameter of the sample

$t$  = thickness of the sample

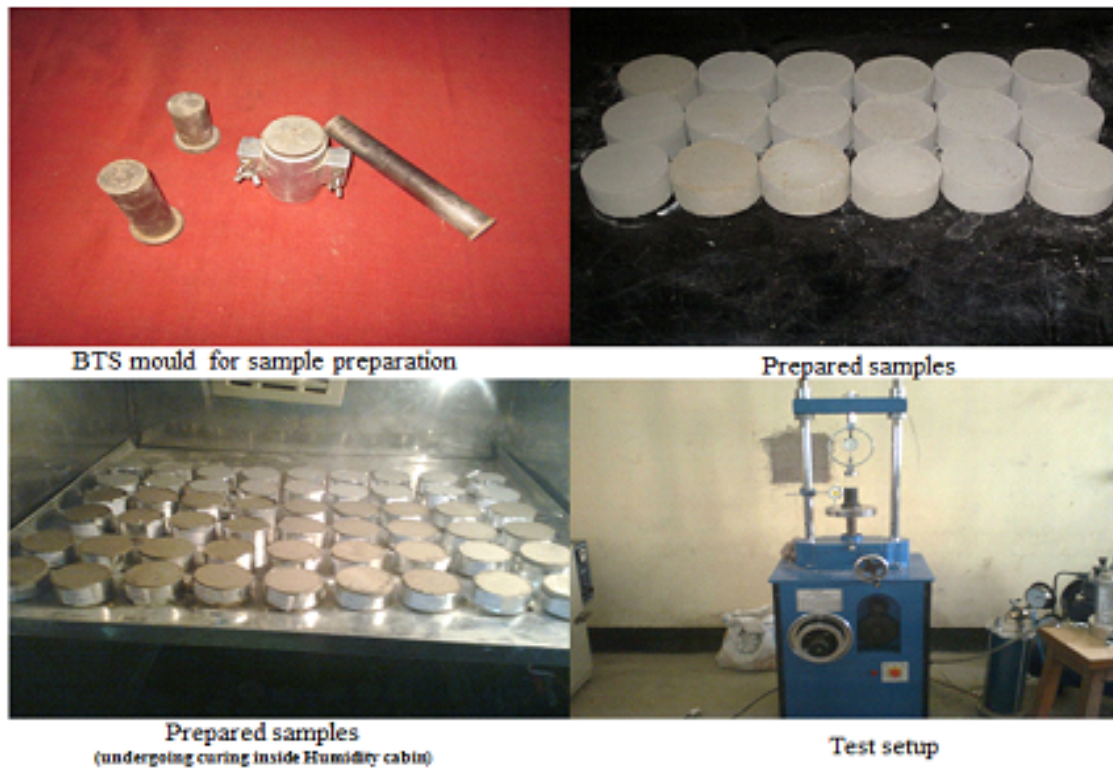


Figure 3.5: Brazilian Tensile Strength Test

### Ultrasonic Pulse Velocity Test

P-wave velocity values of developed composites were determined using an Ultrasonic Velocity Measurement System (make: GCTS, USA; Figure 3.6). This system includes 10 MHz bandwidth receiver pulse raise time less than 5 nano seconds, 20 MHz acquisition rate with 12bit resolution digitizing board, transducer platens with 200 kHz compression mode and 200 kHz shears mode. The test was carried out by applying two sensors to opposite surfaces of the specimen. Sufficient surface contact between the sensors and the specimen was maintained by a couplant as honey.



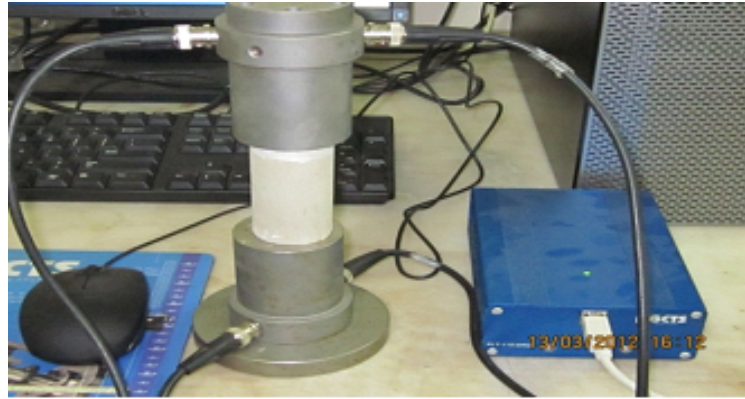


Figure 3.6: Ultrasonic Pulse Velocity Test Instrument and view of Test in Progress

### 3.2.4 Experimental Size

The investigation included many characterization studies including major laboratory tests as compaction, California bearing ratio (CBR), unconfined compressive strength (UCS), Brazilian tensile strength (BTS), Ultrasonic tests in addition to other index tests. The reported results represent average values of three to four samples for each test type except that for compaction to determine MDD and OMC. The test results that were not within 5% to 10% of each other were discarded and fresh samples were prepared and tested. The total number of tests were 220 and about 800 samples were tested (Table 3.2).

Total number of Tests

Proctor Compaction	CBR	UCS	BTS	P-wave velocity
20	60	60	20	60
Total=20+60+60+20+60=220				

Total Number of samples Tested

Proctor Compaction	CBR	UCS	BTS	P-wave velocity
$20 \times 3 = 60$	$60 \times 3 = 180$	$60 \times 3 = 180$	$20 \times 4 = 80$	$60 \times 3 = 180$
Total=60+180+180+80+180=680 (Excluding tests for characterization = 100 samples)				

Table 3.2: Experimental Design Chart

Sl. No.	Compositions (FA+O/B+CL) *CL= Clinker	Compaction	CBR			UCS			BTS			P wave velocity		
			Soaked	7 Days	28 Days	7 Days	14 Days	28 Days	7 Days	14 Days	28 Days	7 Days	14 Days	28 Days
1	90FA+100/B+0CL	✘	*	*	*	+	+	+	×	×	×	•	•	•
2	88FA+100/B+2CL	✘	*	*	*	+	+	+	×	×	×	•	•	•
3	86FA+100/B+4CL	✘	*	*	*	+	+	+	×	×	×	•	•	•
4	84FA+100/B+6CL	✘	*	*	*	+	+	+	×	×	×	•	•	•
5	82FA+100/B+8CL	✘	*	*	*	+	+	+	×	×	×	•	•	•
6	80FA+200/B+0CL	✘	*	*	*	+	+	+	×	×	×	•	•	•
7	78FA+200/B+2CL	✘	*	*	*	+	+	+	×	×	×	•	•	•
8	76FA+200/B+4CL	✘	*	*	*	+	+	+	×	×	×	•	•	•
9	74FA+200/B+6CL	✘	*	*	*	+	+	+	×	×	×	•	•	•
10	72FA+200/B+8CL	✘	*	*	*	+	+	+	×	×	×	•	•	•
11	70FA+300/B+0CL	✘	*	*	*	+	+	+	×	×	×	•	•	•
12	68FA+300/B+2CL	✘	*	*	*	+	+	+	×	×	×	•	•	•
13	66FA+300/B+4CL	✘	*	*	*	+	+	+	×	×	×	•	•	•
14	64FA+300/B+6CL	✘	*	*	*	+	+	+	×	×	×	•	•	•
15	62FA+300/B+8CL	✘	*	*	*	+	+	+	×	×	×	•	•	•
16	60FA+400/B+0CL	✘	*	*	*	+	+	+	×	×	×	•	•	•
17	58FA+400/B+2CL	✘	*	*	*	+	+	+	×	×	×	•	•	•
18	56FA+400/B+4CL	✘	*	*	*	+	+	+	×	×	×	•	•	•
19	54FA+400/B+6CL	✘	*	*	*	+	+	+	×	×	×	•	•	•
20	52FA+400/B+8CL	✘	*	*	*	+	+	+	×	×	×	•	•	•

# Chapter 4

## Results and Discussion

### 4.1 Introduction

A typical surface coal mine in India has about 5 km of permanent haul road with a life span of 25 to 30 years. The carrying capacity of haul trucks as well as heavy earth moving machineries undergoes many up-gradations within the life period of an operating coal mine as the demand for coal continues to increase. However the design pattern of haul road and its construction do not undergo corresponding enhancement. It is often observed that mine authority simply fill haul roads with the locally available materials to save money. In acute adverse conditions, only the wearing or surface course of the haul road is repaired. So, it is very much important to design and construct the haul road sub-base with material of adequate bearing capacity. The engineering properties of a material are dependent on the composition of material to a large extent. There exists wide variation in the composition of fly ash depending on coal types, types of furnace, temperature, collection technique etc. [119, 138, 184]. The overburden material over coal strata in the Gondwana basin is heterogeneous in nature. The geotechnical properties of the developed composite materials were determined as per established methods. All the results of the current investigation and their corresponding analyses have been presented in different sections as mentioned below:

1. Mine Site Observations

2. Characterization of ingredients as Fly Ash, mine overburden and Clinker
3. Development of Different Composite materials
4. Determination of geotechnical Properties of developed composite materials
5. Micro-structural analyses of the developed composite materials
6. Simulation of the application of developed composite materials
7. Development of model equations and prediction of fly ash usage volume

## 4.2 Mine Site Observations

Frequent visits were made to the chosen surface coal mine for various reasons i.e. to collect overburden material, to collect mine data, to inspect the haul road conditions, to study the haul road construction mechanism, to discuss with mine officials and haul truck operators as well as to observe critically the various problems associated with haul road etc. The mine used 50 to 80T dumper for hauling overburden material. It uses CBR approach of haul road design. The haul road surface is very poor. some of the features observed are (Figure 4.1).



Figure 4.1: Uneven surfaces and potholes observed in the haul roads

## 4.3 Characterization of Ingredients

The aim was to develop fly ash based composite material suitable for sub-base course. So a detail analysis of the constituent materials as well as the developed composites was carried out. The results of the characterization are reported here.

### 4.3.1 Physical Properties

The fly ash was collected in dry state and was in loose stage. Its average water content was less than 1%. The fly ash used had a powdery structure with medium to dark grey colour indicating low lime content [113].

The physical properties of fly ash and mine overburden are reported in Table 4.1. The specific gravity of fly ash and mine overburden obtained are 2.10 and 2.63. The specific gravity of fly ash is found to be less than that of mine overburden, due to the presence of cenospheres and less iron content. The materials with higher iron content have relatively high specific gravity [184].

The particle size distribution of the construction material has strong influence over the density. The overburden contains sand size fraction with appreciable amount of non-plastic fines or fines with low plasticity (Figure 4.2). It is typically described as poorly graded sand-silt mixtures and belongs to SM group. It contains 27% of sand, 57% of silt and 8% of clay size particles.

The United States classification systems (USCS) of soils do not classify the coal ashes satisfactorily because of its non-plastic nature. Hence geotechnical classification system developed for the purpose has been followed (Sridharan and Prakash, 2007). The fly ash belongs to non-plastic inorganic coarse silt sized fractions (MLN) group as it contains more than 50% of fines is in the range  $20\mu\text{m}$  to  $75\mu\text{m}$ . The coefficient of uniformity ( $C_u = D_{60}/D_{10}$ ) is 4.47.

Specific surface area is a measure of the fineness of the material which influences the reactivity with other ingredients. The low value of fly ash is due to more percent of silt particle as compared to that in overburden material [184].

Atterberg limits as liquid limit (LL), plastic limit (PL), plasticity index (PI)

Table 4.1: Physical properties of fly ash and mine overburden

<b>Property</b>	<b>Fly ash</b>	<b>O/B</b>
Specific Gravity	2.10	2.63
Atterberg Limits		
	Liquid Limit (%)	31.57
	Plastic Limit (%)	Non-plastic
	Shrinkage Limit (%)	...
	Plasticity Index (%)	...
Sieve Analysis (%)		
	Gravel (>4.75mm)	...
	Sand (4.75mm-0.075mm)	18
	Coarse Sand	0
	Medium Sand	0
	Fine Sand	18
	Silt (0.075mm-0.002mm)	79.8
	Coarse Silt	52
	Medium Silt	16
	Fine Silt	11.8
	Clay (<0.002mm)	2.2
	Coefficient of Uniformity ( $C_u$ )	4.47
	Coefficient of Curvature ( $C_c$ )	1.82
pH Value	7.10	5.5
Free Swell Index	Negligible	18.18

and shrinkage limit are important factors in material identification and classification. These parameters reflect a few geotechnical problems as swelling potential and workability. The respective values of LL for fly ash and overburden are 31.57% and 26.90% respectively. Though both values are close overburden material is less workable than that for fly ash. The tests also confirm that fly ash is non-cohesive and has negligible shrinkage limit thus better suited to geotechnical application. Free swell index of the fly ash is found to be negligible due to flocculation which confirms to that reported elsewhere [138].

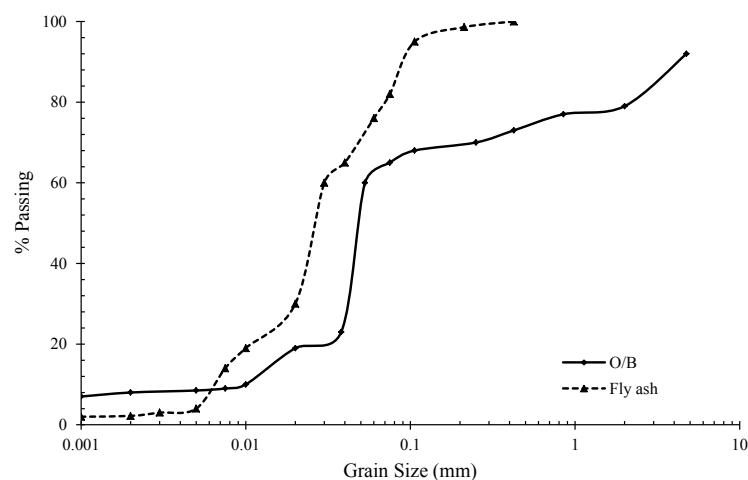


Figure 4.2: Grain size distribution curves of fly ash and mine overburden

### 4.3.2 Chemical Properties

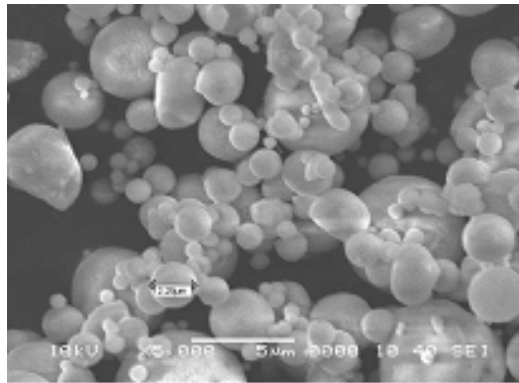
The chemical composition of fly ash, overburden and clinker are important indicators of suitability of a material for geotechnical applications. The chemical composition of fly ash indicates that it has not only less calcium content but also the quantity of  $(\text{SiO}_2 + \text{Al}_2\text{O}_3 + \text{Fe}_2\text{O}_3)$  exceeds 70% (Table 4.2). Thus, it is classified as “Class F” type (ASTM 618). The fly ash and mine overburden mainly consist of silica ( $\text{SiO}_2$ ), alumina ( $\text{Al}_2\text{O}_3$ ) and iron oxide ( $\text{Fe}_2\text{O}_3$ ). Oxides of calcium, magnesium, potassium, titanium, sodium are also present in small quantities. The major constituent of clinker is calcium oxide at (67%).

The morphology of fly ash indicates the presence of glassy solid spheres, hollow spheres (cenospheres), rounded and smooth porous grains as well as irregular agglomerates (Figure 4.3 (a)). These particles affect the compaction behaviour [99, 42]. The micrograph is without any formation of cementitious compound. It confirms that the fly ash used in the investigation has low calcium content. It compares favorably to those observed elsewhere [10, 91].

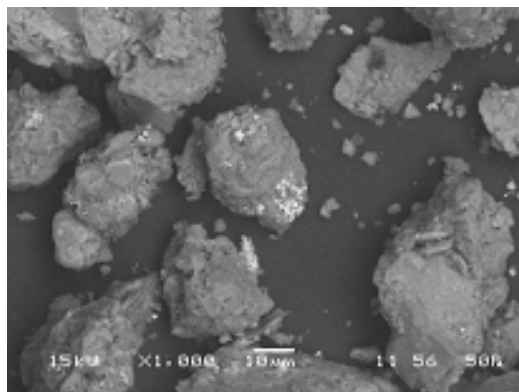
The morphology of overburden indicates the presence of irregular shape solid particles. The X-ray diffraction profiles of the overburden and fly ash indicate the presence of crystalline phases (Figure 4.4(a) and 4.4(b)). It is noticed from the XRD analysis

that Kaolinite and Quartz are the major mineral constituents of the overburden. The major mineral constituents of fly ash are Quartz, Silliminate and Mullite. Quartz is the most prominent mineral present in both overburden and fly ash materials.

The pH of overburden and fly ash are found to be 5.5 and 7.1. The pH values indicate that fly ash is slightly alkaline and overburden is acidic depending on alkaline oxide content and free lime content. The silica lime reaction is pH dependent. The higher the pH, the better is the solubility of silica and lime-silica reaction in producing pozzolanic products. The pH of the solution increases if presence of lime is in excess of the amount required for the silica to react. But addition of lime in excess than that required for the reactions makes pH constant as the solution becomes saturated [179].



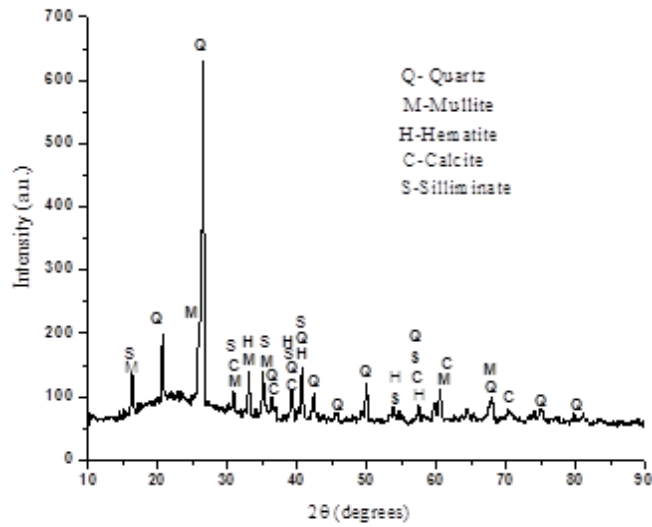
(a)



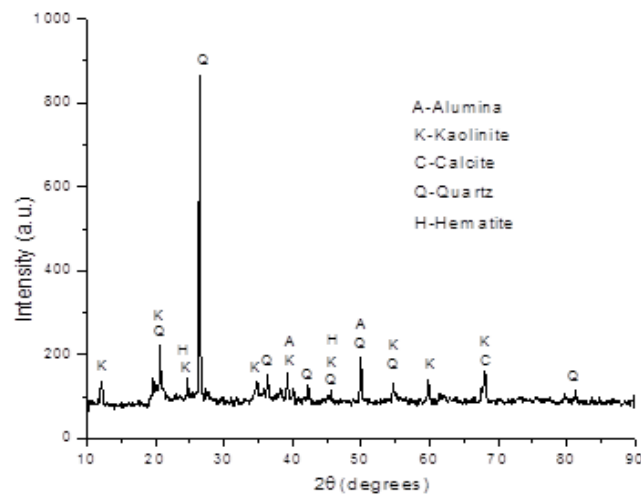
(b)

Figure 4.3: SEM Image of (a) fly ash; (b) mine overburden





(a)



(b)

Figure 4.4: XRD of (a) fly ash; (b) mine overburden

Table 4.2: Chemical Compositions of Fly ash, Mine overburden and Clinker

Constituents	SiO <sub>2</sub>	Al <sub>2</sub> O <sub>3</sub>	Fe <sub>2</sub> O <sub>3</sub>	CaO	K <sub>2</sub> O	MgO	TiO <sub>2</sub>	Na <sub>2</sub> O	SO <sub>3</sub>	LOI
Mine O/B	48.24	29.18	8.36	1.10	0.40	1.30	0.69	—	—	10.73
Fly Ash	53.11	33.64	6.44	0.55	1.45	0.83	2.05	0.13	—	1.8
Clinker	20.46	4.52	3.57	66.38	0.68	2.01	—	0.16	1.39	0.75

### 4.3.3 Engineering Properties

The engineering properties of a material such as compressive strength, tensile strength, CBR etc. are dependent on the moisture content and density. Typically the higher the compaction the better is its geotechnical characteristics. Hence it is necessary to achieve the desired degree of compaction which is necessary to meet the expected properties [134].

Compaction is the process of increasing the density of material by the application of mechanical energy such as tamping, rolling and vibration. It is achieved by forcing the particles closer with a reduction in air voids. Optimum moisture content (OMC) is the moisture content at which compacted material reaches the maximum dry density of solid particles. The compaction characteristics of ingredients as fly ash and mine overburden were carried out to determine the optimum moisture content and maximum dry density (Figure 4.5). The maximum dry density of flyash was lower than that obtained for mine overburden due to low specific gravity and non-cohesive in nature. Fly ash has higher optimum moisture content due to the fact that particles themselves are hollow or cenospheres and holds a considerable quantity of water internally. The compaction curve of fly ash is almost flat and indicates it's insensitive to moisture variation. It confirms to similar observations reported elsewhere [187, 39, 184]. The maximum dry density of fly ash is less than that of overburden due to less iron content and specific gravity of the fly ash. The MDD of overburden and fly ash were  $1941 \text{ kg/m}^3$  and  $1296 \text{ kg/m}^3$  respectively (Table 4.3). Corresponding values for OMC were 14.2% and 22.3% respectively. The low density value of fly ash was due to the high moisture content, unlike the overburden which has less water content.

The shear strength parameters of compacted overburden and fly ash are represented in (Table 4.3). As the sand and clay contents of overburden are more than that of fly ash, the cohesion and angle of internal friction of overburden are relatively higher than that of fly ash. Angle of repose is the maximum inclination of the sloping surface of a material exhibiting the limiting stability. The angle of repose of overburden material is close to its angle of internal friction value. It is very low for fly

ash as fly ash exhibits pseudo-cohesion, even in its dry state by virtue of its fineness.

Unconfined compressive strength (UCS) of a material is its resistance to any externally applied load. It reflects inter granular cohesion as well as strength of cementing material holding those grains. The UCS values of fly ash and overburden material are 132.76KPa and 343.91KPa respectively (Table 4.3 ). The value of overburden is more than twice to that of fly ash due to presence of high quantity binding material (CaO) as compared to fly ash.

The California Bearing Ratio values for overburden and fly ash materials in unsoaked condition are 18% and 26% respectively. But the values reduce drastically at soaked condition. CBR values of Mine Overburden and fly ash were 2.53% and 0.7% respectively. Both these values are less than 3 % that make the materials unsuitable for sub-base application [16].

Table 4.3: Engineering Properties of Overburden and Fly ash

Property	Overburden	Fly ash
1. Compaction characteristics (Modified Proctor Test)		
Maximum Dry Density (kg/m <sup>3</sup> )	1941	1296
Optimum Moisture Content (%)	14.2	22.3
2. Shear strength parameters		
Cohesion (kPa)	60.40	33.25
Angle of Internal Friction	37.03 <sup>0</sup>	27.5 <sup>0</sup>
3. Angle of Repose	35.0 <sup>0</sup>	11 <sup>0</sup>
4. Unconfined Compressive Strength (kPa)	343.19	132.76
5. CBR value(%) Un-soaked condition	26.0	18.0
Soaked condition	2.53	0.70

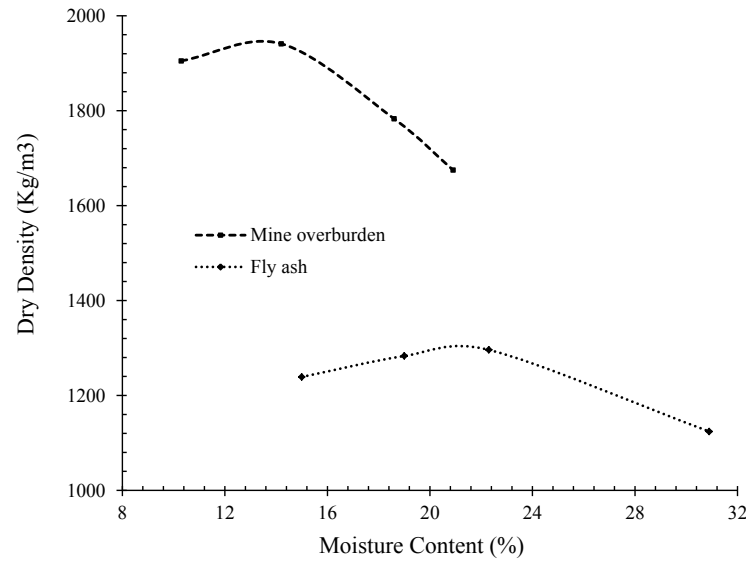


Figure 4.5: Compaction curves of fly ash and mine overburden

## 4.4 Geotechnical Properties of Developed FCMs

The developed composite materials were subjected to various engineering tests as compaction behaviour, UCS, CBR, Brazilian tensile strength, ultrasonic pulse velocity and micro- structural analyses.

### 4.4.1 Compaction Characteristics

The maximum dry density values of untreated composites varied between  $1330 \text{ kg/m}^3$  to  $1566 \text{ kg/m}^3$  (Figure 4.6). It reduced as the quantity of fly ash increased. As the fly ash percentage was increased the values for OMC increased.

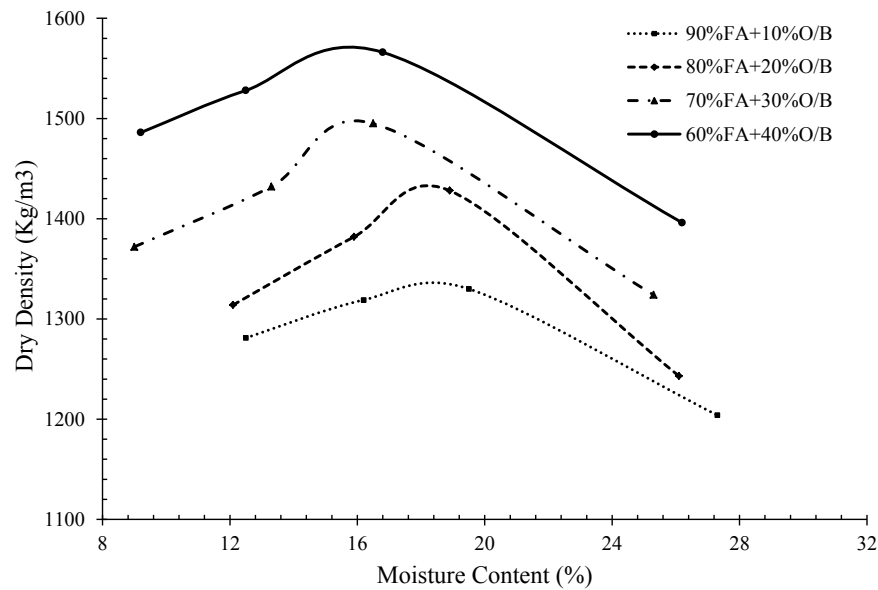


Figure 4.6: Compaction curves of untreated composites

The aim of the investigation was to develop an alternative engineering material with mine overburden and fly ash stabilized with clinker. Accordingly samples were prepared (Table 3.1). The specimen behaviour changed when clinker was added in various proportions. The maximum dry density values of all composite materials increased with increase in clinker content (Figures 4.7 and 4.8). It confirms to similar observations for fly ash-soil-lime mixtures [35, 6, 81, 91, 160, 76].

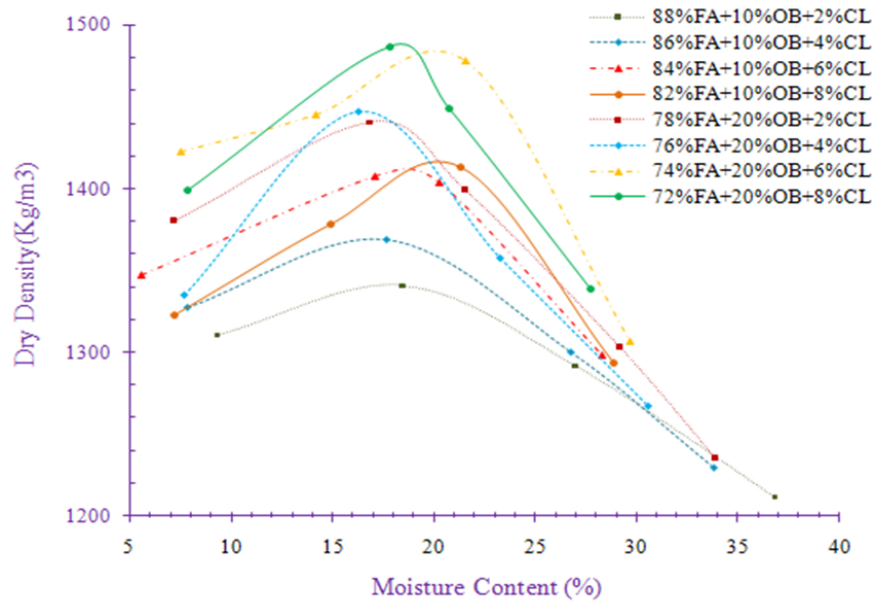


Figure 4.7: Compaction curves of the composites containing 10% and 20% O/B

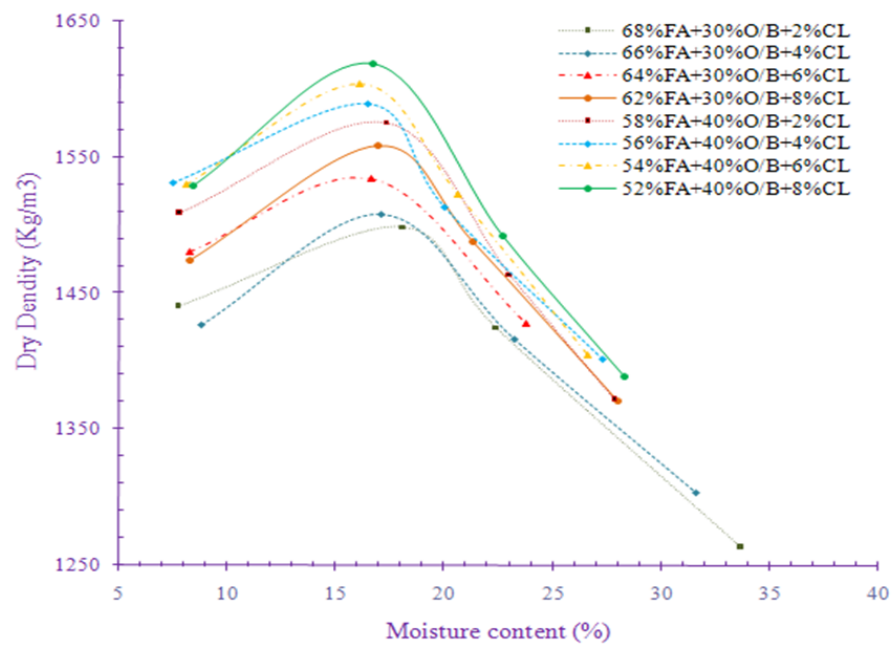


Figure 4.8: Compaction curves of the composites containing 30% and 40% O/B

### 4.4.2 California Bearing Ratio Behaviour

CBR value is used as an index of material strength. This method is well established and popular for design of the base and sub-base material for road pavement. In this investigation CBR tests were carried out to characterize the bearing capacity of the untreated fly ash-overburden composite as well as clinker treated fly ash-overburden composite materials.

#### **Effect of curing on the CBR of Untreated fly ash and mine overburden mixes**

The variation of CBR of fly ash-overburden mixes for both un-soaked and soaked conditions (Figure 4.9). The CBR values of untreated fly ash-overburden composite materials vary from 21.46% to 23.74% in un-soaked condition. The higher CBR value in un-soaked condition is due to the capillary forces created at optimum moisture content and maximum dry density condition in addition to the friction resisting the penetration of the plunger (Mishra et al., 2003). However when the samples were tested after 4 days soaking, the CBR values were very low due to the destruction of the capillary forces. Soaked condition though a conservative estimate, yet considered for worst scenario. The obtained CBR value less than 3% is unsuitable for sub-grade material [16] and hence need to be stabilized with additive for haul road application.

The CBR values of composites when tested at different curing periods exhibited little change over uncured results (Figure 4.10 ). The CBR values of 28 days cured samples almost doubled to that at soaked conditions i.e. with a range of 2% to 4%, but still unsuitable for sub-base material. Hence it was decided to improve the CBR of fly ash and mine overburden mixes using additive.

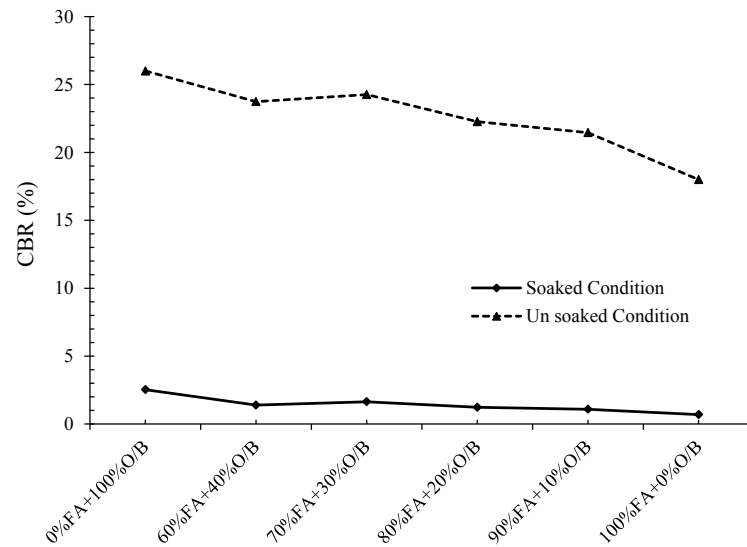


Figure 4.9: CBR values of fly ash-mine overburden mixes

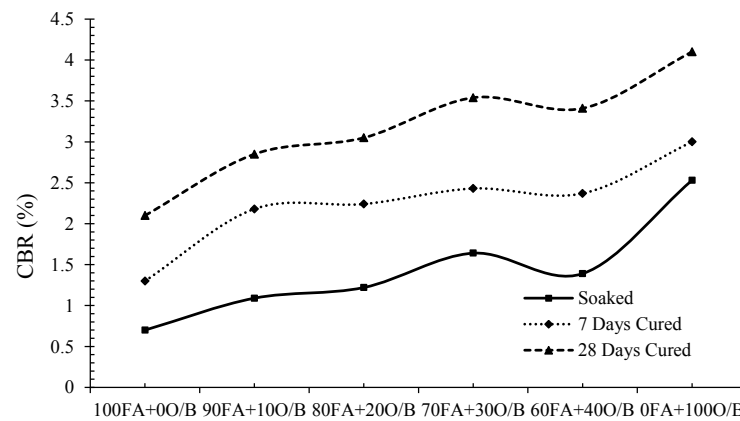


Figure 4.10: CBR values of fly ash-mine overburden mixes

### CBR Behaviour of Clinker Stabilized Fly ash Composites

Generally additives like cement or lime enhance the strength of the soil or fly ash [35, 56, 104]. Clinker is an input material for cement preparation. Lime available commercially is relatively expensive. Hence it was decided to develop and evaluate the performance with clinker. CBR values were determined for fly ash-overburden material stabilized with clinker. Clinker was added between 2% and 8%. As clinker



was added, each composite showed significant enhancement in CBR values. In soaked condition the composite with 88% fly ash exhibited CBR value 8.44% with 2% clinker (Figure 4.11). However as clinker percentage increased the composites with higher fly ash content showed higher CBR values (Figure 4.12). Thus confining that availability of silica and alumina adds to strength gain over time. The composite with 80% fly ash produced 20%, 32% and 45% CBR at 4, 6 and 8% clinker content respectively. The maximum CBR value obtained was 139.3% for the composite 62%FA+30%O/B with 8% clinker at 28 days curing (Figure 4.13). The results showed curing period and clinker percentage have strong effect on enhancement of the bearing capacity of developed composites. It confirms to the observation reported elsewhere for soil with class C fly ash [74].

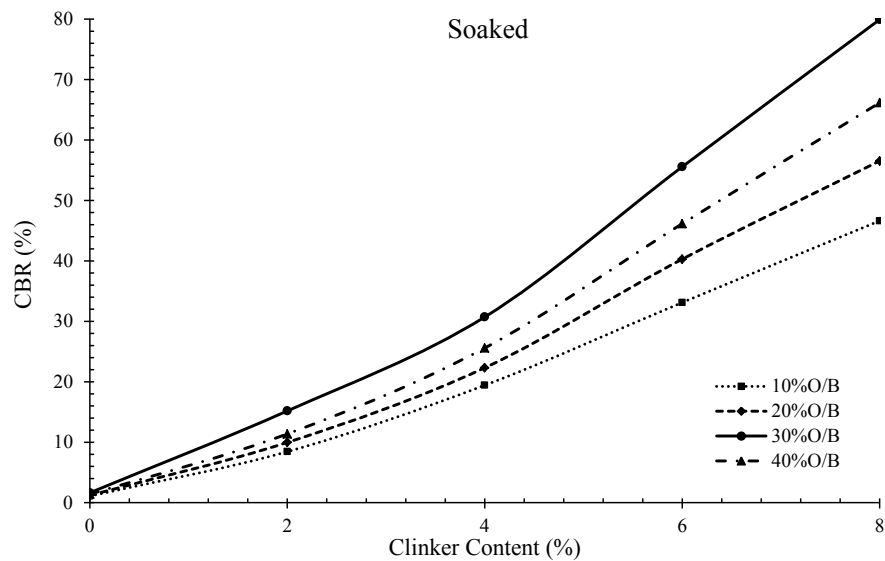


Figure 4.11: CBR values of developed composites in soaked condition

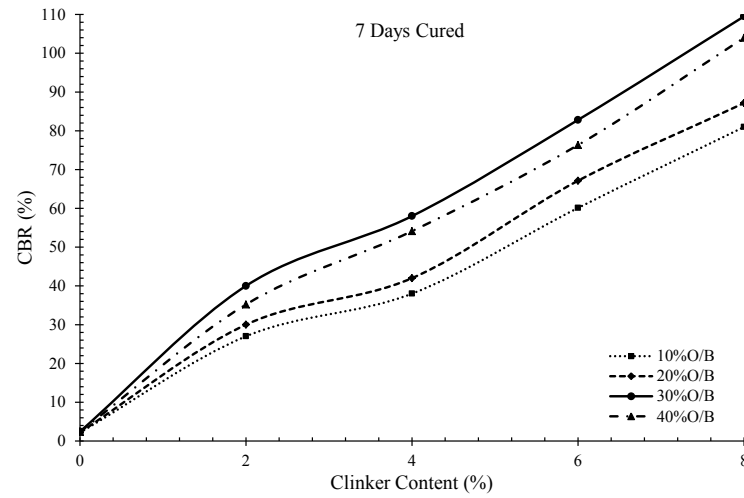


Figure 4.12: CBR values of developed composites at 7 days curing

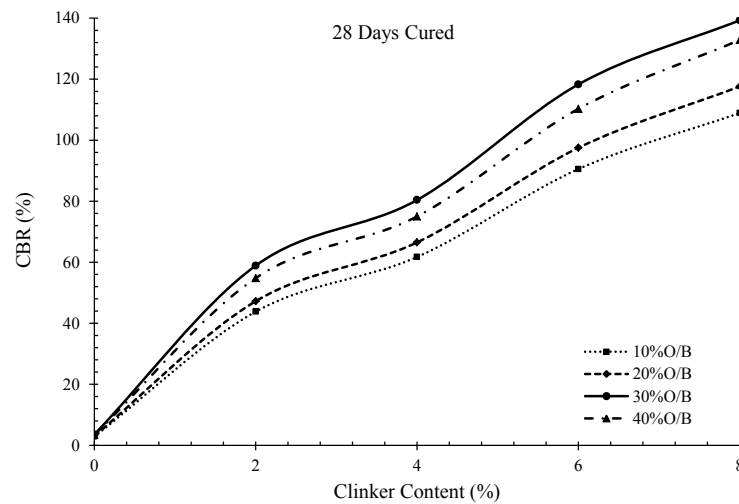


Figure 4.13: CBR values of developed composites at 28 days curing

It is observed that the CBR values increased from 15.18% to 79.94% and 58.88% to 139.3% at 7 and 28 days of curing respectively as clinker percentage increased from 2% to 8% for 70%FA+30%O/B. Thus, increase in curing period increased the CBR value. Hydration of clinker forms calcium silicate hydrate gel that depends on the availability of free lime, the more the lime the better the gel formation. Continuous increase in the CBR values with different curing period (Figure 4.14). The fly ash mixed with 30% mine overburden and 8% clinker shown highest CBR values among all developed composites at 7 and 28 days curing respectively. There is strong bond

between the fly ash and mine overburden particles by the cementitious products and hence higher CBR in the composite. The value compares favorably with the CBR result of the soil stabilized with fly ash (10% and 20%) and lime kiln dust (2.5% and 5%) to be 69 to 142% at 7 days curing and greater than 164% at 28 days curing [27].

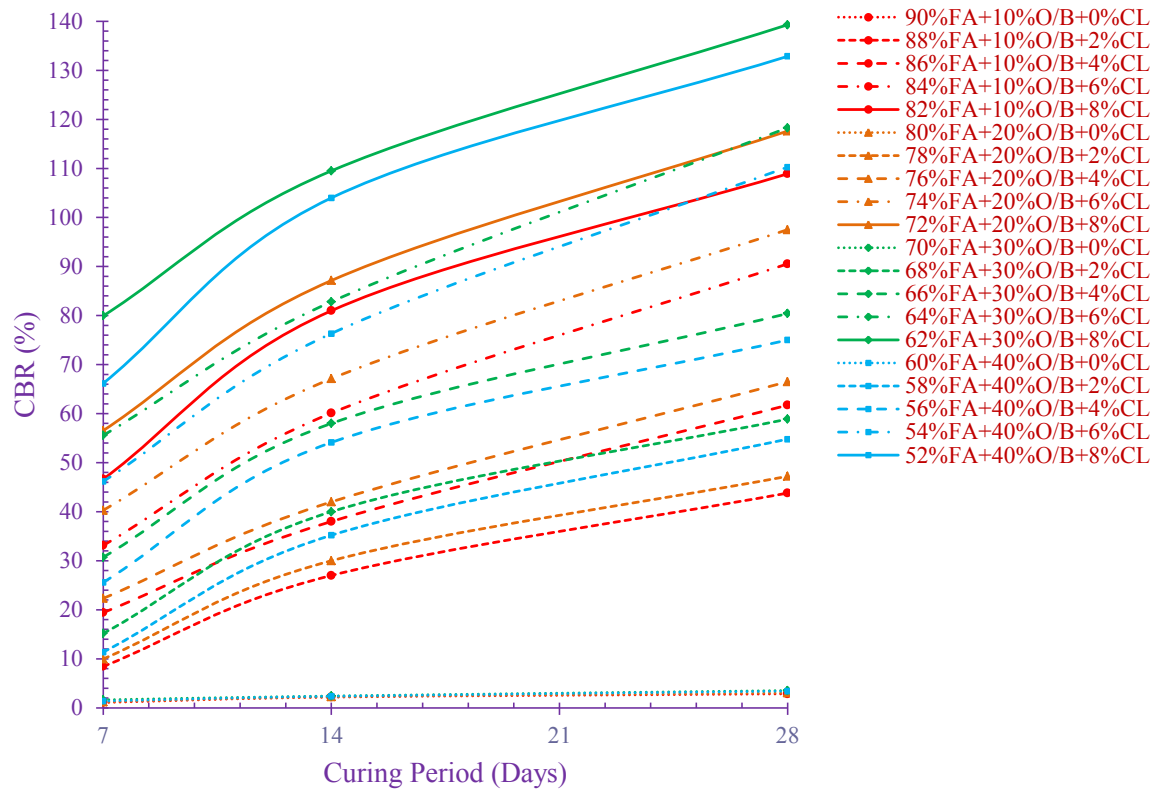


Figure 4.14: Effect of curing period on CBR

CBR gain is the strength enhancement due to addition of clinker in the treated composites with respect to that of untreated composites. The maximum CBR gain was 39.35 for composite 62%FA+30%OB+8%CL and the minimum CBR gain was 15.36 for the composite 88%FA+10%OB+2%CL at 28 days curing (Table 4.4).

Table 4.4: CBR Gain of Fly ash-Mine overburden-Clinker Composites

FA (%)	O/B (%)	CL (%)	Curing Period (Days)	CBR (%)	CBR Gain
90	10	0	28	2.85	1
88	10	2	28	43.8	15.36
86	10	4	28	61.72	21.65
84	10	6	28	90.54	31.76
82	10	8	28	108.9	38.21
80	20	0	28	3.05	1
78	20	2	28	47.22	15.48
76	20	4	28	66.5	21.8
74	20	6	28	97.51	31.97
72	20	8	28	117.62	38.56
70	30	0	28	3.54	1
68	30	2	28	58.88	16.63
66	30	4	28	80.4	22.71
64	30	6	28	118.29	33.41
62	30	8	28	139.3	39.35
60	40	0	28	3.41	1
58	40	2	28	54.8	16.07
56	40	4	28	75.01	21.99
54	40	6	28	110.28	32.34
52	40	8	28	132.86	38.96

#### 4.4.3 Unconfined Compressive Strength

The unconfined compression test is one of the widely used laboratory tests in pavement design and soil stabilization applications. It is often used as an index to quantify the strength enhancement of materials due to treatment. The results of UCS tests for both untreated and treated composites are reported.

### Unconfined Compressive Strength of Untreated composites

The UCS values of untreated fly ash and overburden composites immediately after preparation could not be obtained as they failed immediately after loading. Marginal increase in UCS values was observed at different curing periods (Figure 4.15).

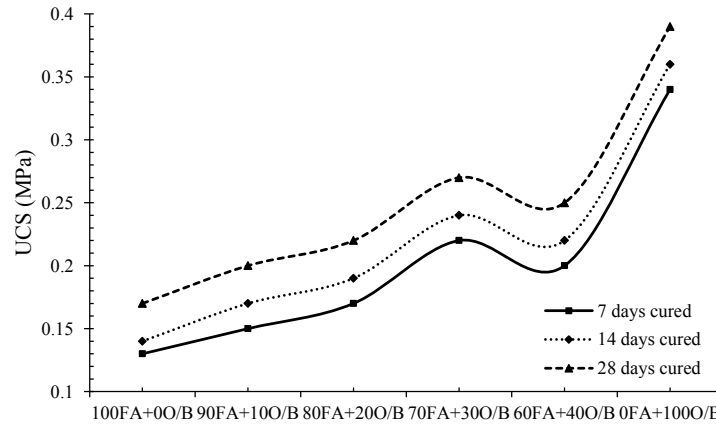


Figure 4.15: UCS values of fly ash-mine overburden mixes

### Unconfined Compressive Strength of Treated Composites

The compressive strength values changed dramatically with addition of clinker. The composites achieved UCS value between 0.15 to 1.1MPa which were significantly dependent on clinker content as well as on curing period. The composite 70%FA+30%O/B with 2% to 8% clinker shown highest strength (0.32 to 1.09MPa) as compared to other composites at 7 days curing (Figure 4.16). The composite 62%FA+30%O/B stabilized with 8% clinker achieved UCS value of 1.4MPa at 28 days curing (Figure 4.18). It showed availability of additional clinker produced enhanced bonding between reactive elements. Each composition exhibited higher strength values with an increase in clinker content and curing period. These values are far above the minimum values suggested for sub-grade [37].

The composite containing 62% fly ash and 30% mine overburden with 8% clinker exhibited maximum compressive strength as compared to other composites at 7, 14, 28 days of curing (Figures 4.16 , 4.17 and 4.18). Typically the stress values at

the base/sub-base layers of mine haul road for 35-170T dumpers are 300 to 650 KPa respectively [191]. The strength achieved by almost all the mixes in this study is above these values after curing and hence suitable for mine haul road construction.

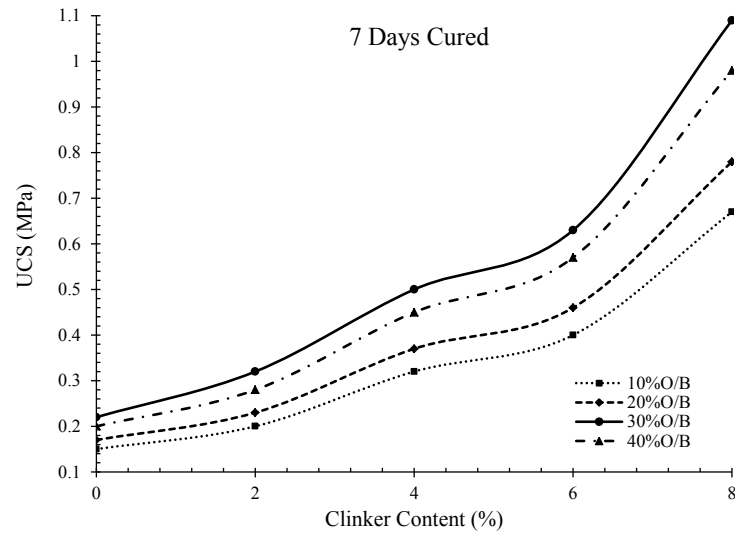


Figure 4.16: UCS values of developed composites at 7 days curing

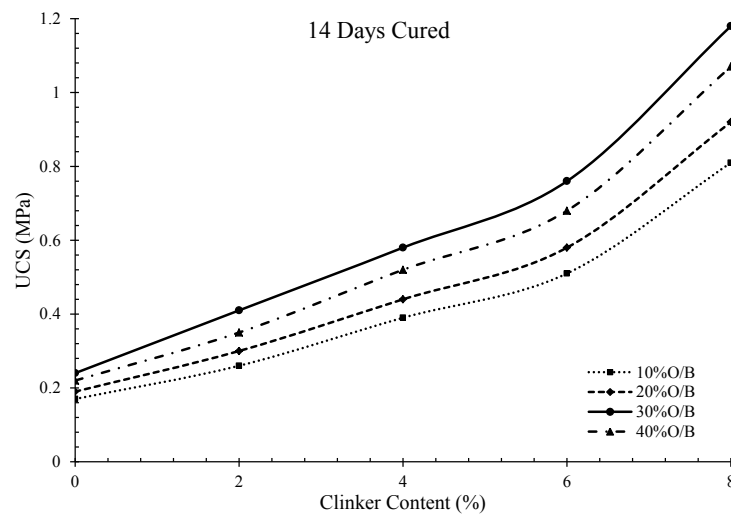


Figure 4.17: UCS values of developed composites at 14 days curing

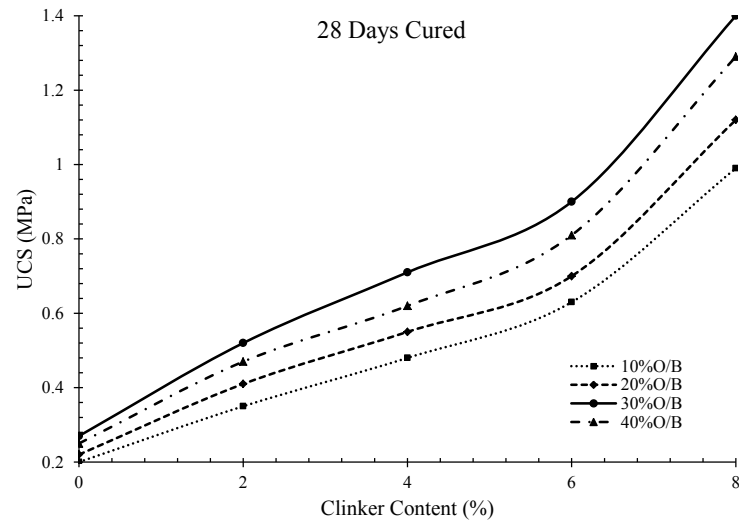


Figure 4.18: UCS values of developed composites at 28 days curing

All the samples in unconfined compressive loading conditions exhibited shear type failure (Figure 4.22). Except a few samples all samples failed by shear which reflect the combined influence of sample and machine characteristics [175]. Load bearing capacity and longitudinal displacement recording were done till failure i.e. peak strength of all the samples. The axial strain values could not be recorded for post failure investigation as the weakened sample got disintegrated soon after its peak strength. The Young's modulus values (stress/strain) were calculated for every sample (Figure 4.19 , 4.20 and 4.21 ).

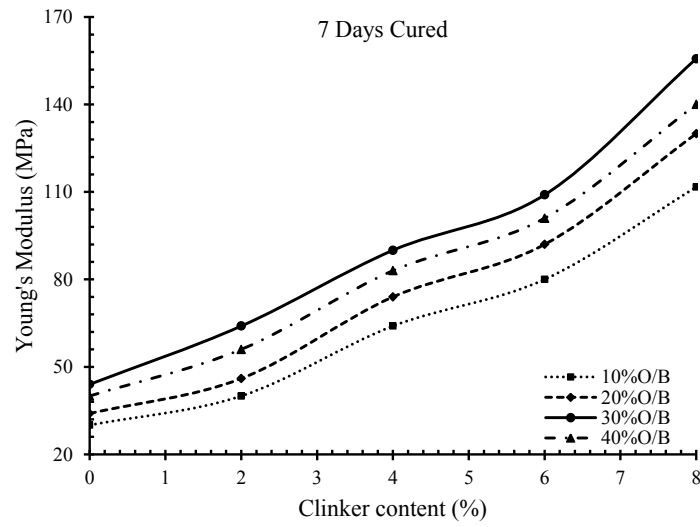


Figure 4.19: Young's modulus values of developed composites at 7 days curing

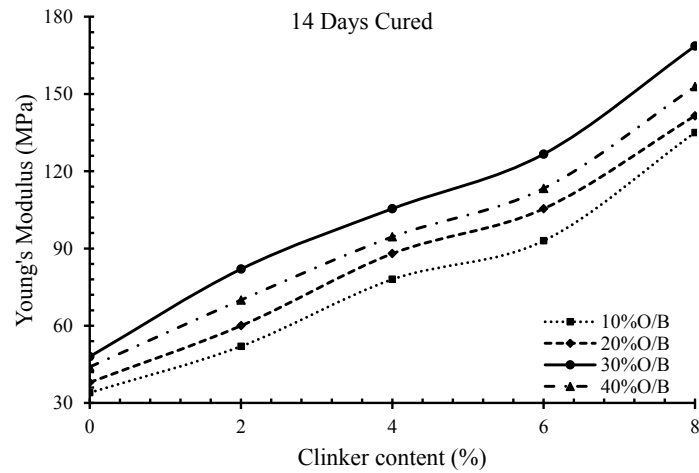


Figure 4.20: Young's modulus values of developed composites at 14 days curing



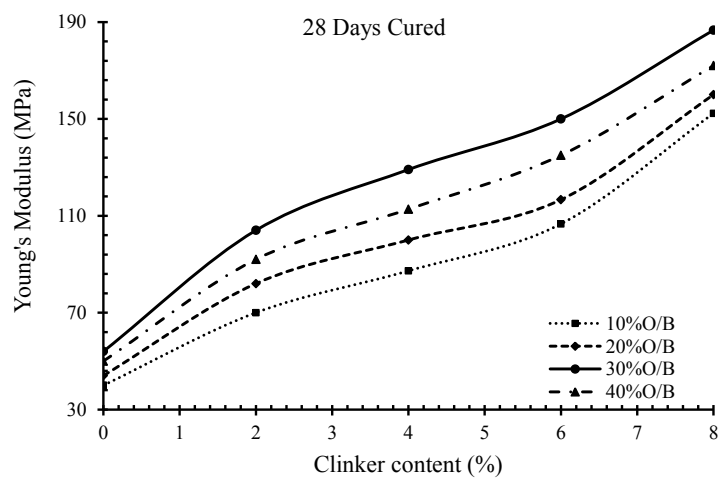


Figure 4.21: Young's modulus values of developed composites at 28 days curing



Figure 4.22: Post failure profiles of few UCS samples

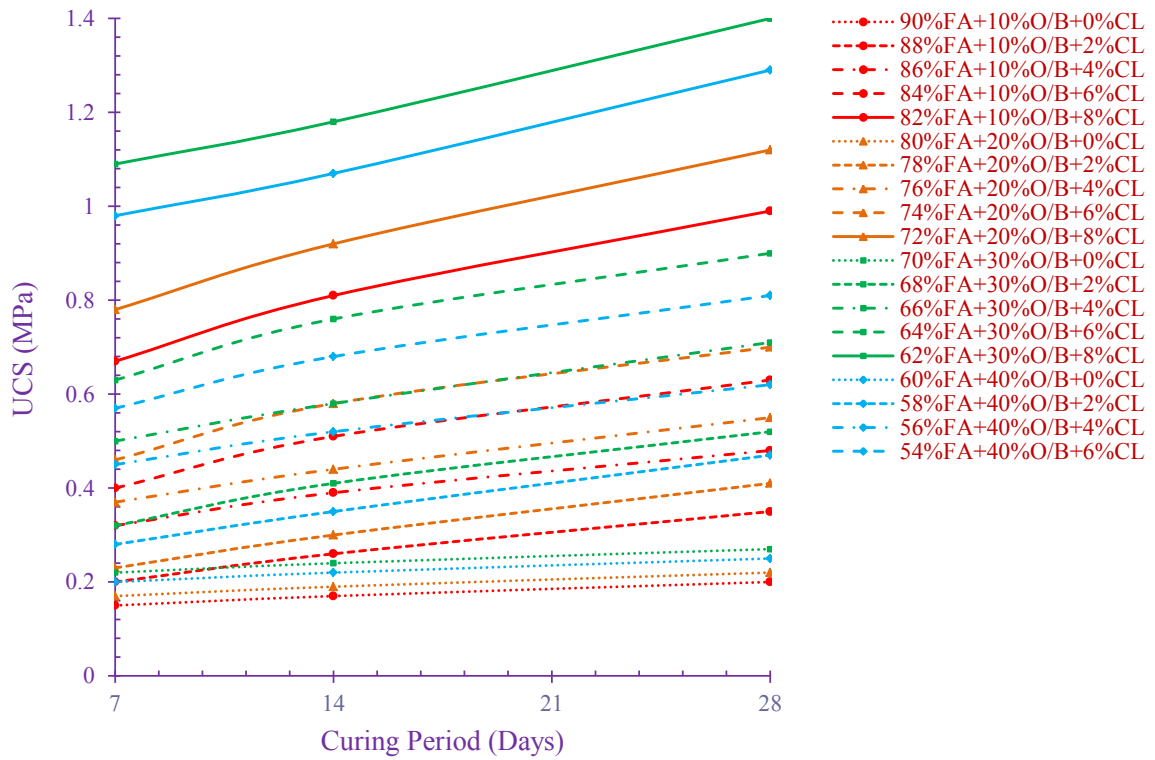


Figure 4.23: Effect of curing period on UCS

UCS Gain is the ratio of UCS value of clinker treated composite to untreated composite. The UCS gain values obtained were between 1.75 and 5.18 for 28 days cured composites (Table 4.5). There exist optimum quantities of CaO, Al<sub>2</sub>O<sub>3</sub> and SiO<sub>2</sub> to react among themselves and exhibit maximum CBR value.

Table 4.5: UCS Gain of Fly ash-Mine overburden-Clinker Composites

FA (%)	O/B (%)	CL (%)	Curing Period (Days)	UCS (MPa)	UCS Gain
90	10	0	28	0.2	1
88	10	2	28	0.35	1.75
86	10	4	28	0.48	2.4
84	10	6	28	0.63	3.15
82	10	8	28	0.99	4.95
80	20	0	28	0.22	1
78	20	2	28	0.41	1.86
76	20	4	28	0.55	2.5
74	20	6	28	0.7	3.18
72	20	8	28	1.12	5.09
70	30	0	28	0.27	1
68	30	2	28	0.52	1.92
66	30	4	28	0.71	2.62
64	30	6	28	0.9	3.33
62	30	8	28	1.4	5.18
60	40	0	28	0.25	1
58	40	2	28	0.47	1.88
56	40	4	28	0.62	2.52
54	40	6	28	0.81	3.24
52	40	8	28	1.29	5.16

#### 4.4.4 Brazilian Tensile Strength Characteristics

Tensile strength is an important property to predict the cracking behaviour of pavement, structures using stabilized soils [9]. The tensile strength is a vital parameter to evaluate the suitability of stabilized soil or fly ash as road base material. In the present study tensile test was conducted on developed composites to evaluate the tensile strength as well as the cracking behaviour of clinker treated fly ash-overburden

material. The tensile strength of untreated fly ash, untreated overburden as well as untreated fly ash–overburden composite materials was very low and hence not reported here. However the behavior of composites changed dramatically and values could be recorded as clinker was added. The treated fly ash–overburden composite materials at 7 and 14 days exhibited marginal values due to low strength and hence not reported here. All the specimens failed more or less at the middle through an induced force which is tensile in nature (Figure 4.24). The failure occurred within 60 to 100 seconds.

At 28 days curing all composites showed more than 40 kPa strength values with maximum values at 8% clinker with 62% fly ash and 30% overburden. The sample (62%FA+30%OB+8%CL) exhibited 150 kPa at 28 days curing (Figure 4.25). Brazilian tensile strength of all the composites were between 40 to 150 kPa at 28 days of curing. The fly ash mixed with 30% mine overburden and 8% clinker exhibited maximum tensile strength as compared to that of other composites at 28 days of curing. The strength achieved in all the composites in this investigation is above these values after a period of curing and hence useful for mine haul road construction.

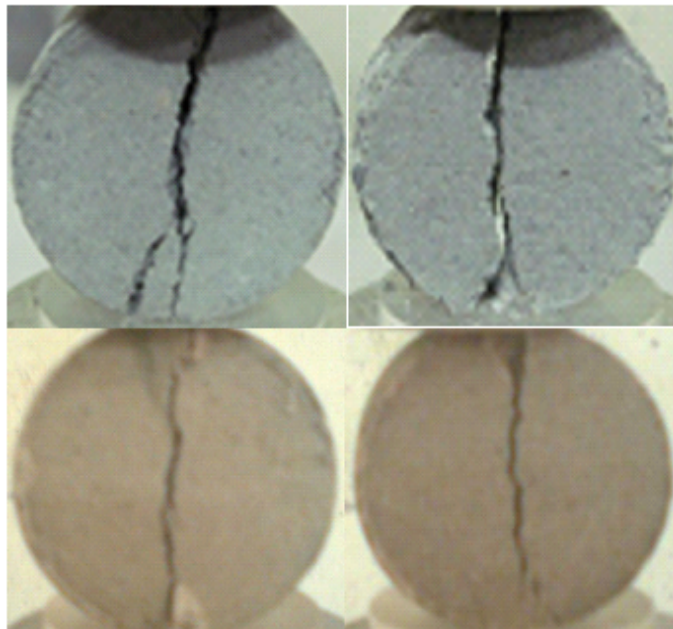


Figure 4.24: Post failure profiles of few Brazilian tensile test samples

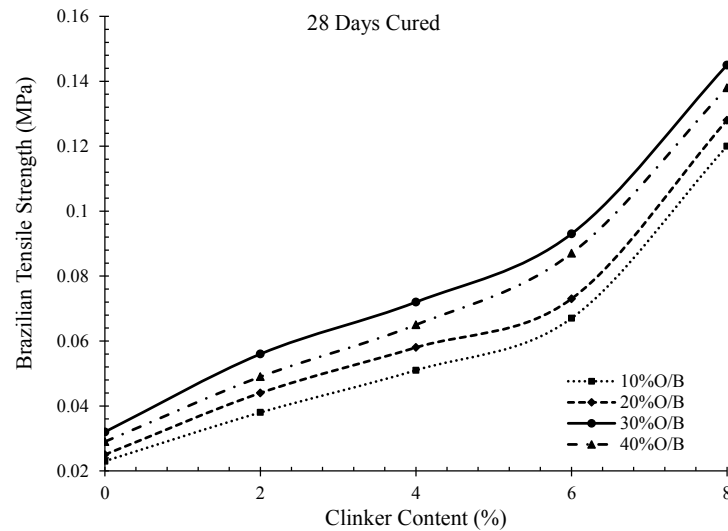


Figure 4.25: Tensile Strength values of developed composites at 28 days curing

#### 4.4.5 Ultrasonic Pulse Velocity

The P-wave velocity depends on the quality of transmission, cohesiveness of constituent materials, dampness, presence of weaknesses as crack, voids, etc. Its accuracy also depends on the homogeneity of the specimen. The P wave velocities of untreated fly ash-overburden composites did not exhibit any significant strength values.

The ultrasonic pulse velocities varied between 812 m/s and 1785 m/s for varying curing periods. Maximum values were obtained at 28 days curing, thus confirming the increased conductivity in the sample (Figure 4.28). The conductivity is a result of enhanced pozzolanic reaction due to enhanced reaction between calcium oxide (CaO), alumina ( $Al_2O_3$ ) and silica ( $SiO_2$ ). The rise is marginal after 7 days curing (Figure 4.26). The maximum P wave velocity values were obtained for the composite 62%FA +30%O/B+8% clinker which is similar to the results obtained in UCS, UTS and CBR tests. P wave velocities obtained at 7, 14, 28 days curing were between 812 and 1649 m/s, 855 and 1692 m/s, 887 and 1785 m/s respectively (Figures 4.26 , 4.27 and 4.28 ). Addition of clinker improved the P-wave velocity of developed composites.

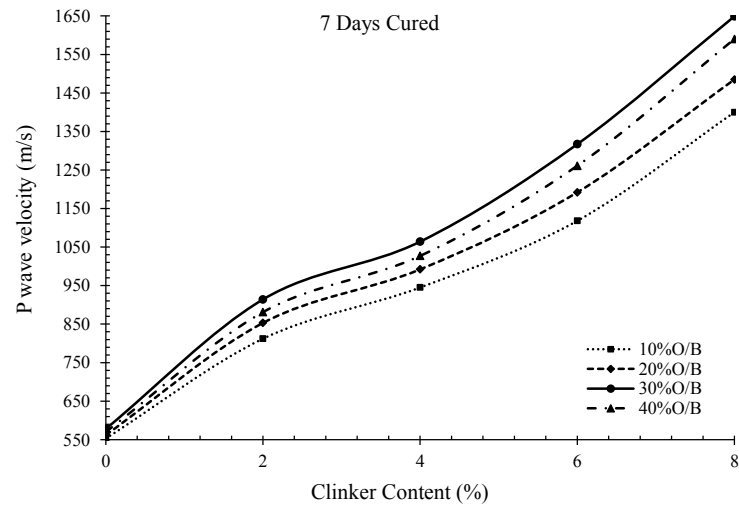


Figure 4.26: P wave velocity values of developed composites at 7 days curing

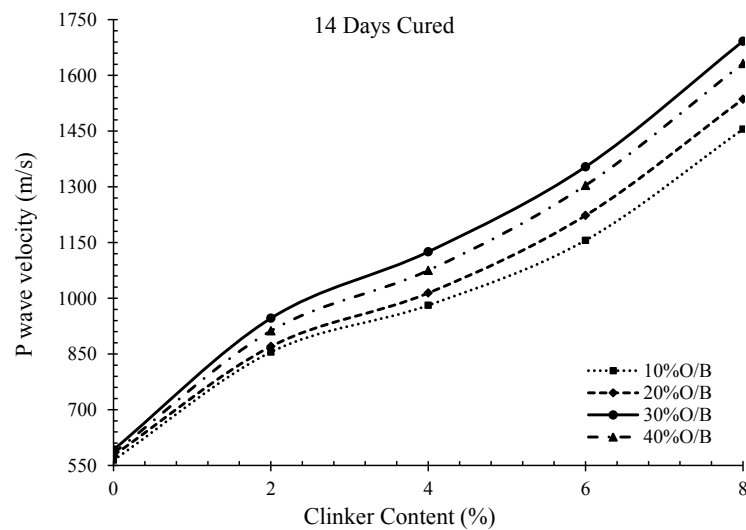


Figure 4.27: P wave velocity values of developed composites at 14 days curing

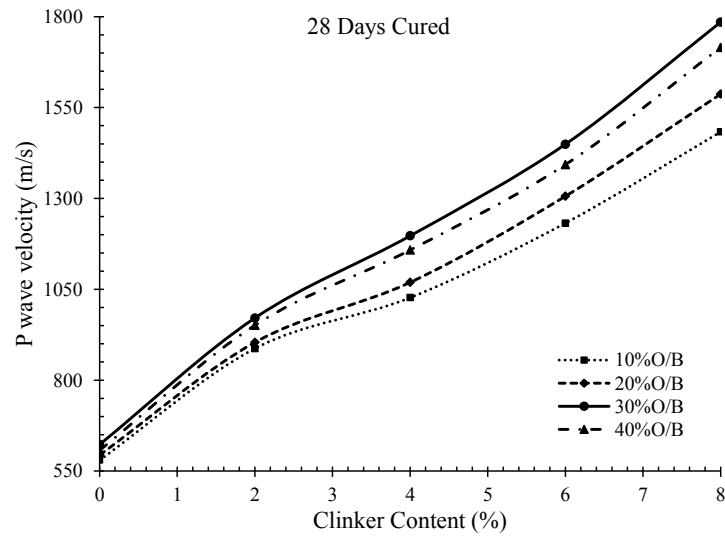


Figure 4.28: P wave velocity values of developed composites at 28 days curing

The Poisson's ratio is an important parameter of a material under loading. The Poisson's ratio values were obtained from ultrasonic pulse velocity test. The Poisson's ratio values of each composite decreased with increase in clinker percentage. The Poisson's ratio values varied between 0.36 and 0.20 of all developed composites cured at 7, 14 and 28 days (Table 4.6 ).

Table 4.6: Poisson's Ratio Values of Developed Composite Materials

Compositions (FA+O/B+CL) *CL= Clinker	Poisson's ratio		
	Curing Period (Days)		
	7 Days	14 Days	28 Days
90FA+10O/B+0CL	0.36	0.34	0.31
88FA+10O/B+2CL	0.33	0.31	0.29
86FA+10O/B+4CL	0.31	0.30	0.28
84FA+10O/B+6CL	0.30	0.29	0.27
82FA+10O/B+8CL	0.29	0.28	0.26
80FA+20O/B+0CL	0.35	0.33	0.30
78FA+20O/B+2CL	0.32	0.30	0.28
76FA+20O/B+4CL	0.30	0.29	0.27
74FA+20O/B+6CL	0.28	0.27	0.25
72FA+20O/B+8CL	0.27	0.26	0.24
70FA+30O/B+0CL	0.33	0.31	0.28
68FA+30O/B+2CL	0.30	0.28	0.26
66FA+30O/B+4CL	0.28	0.27	0.24
64FA+30O/B+6CL	0.27	0.25	0.23
62FA+30O/B+8CL	0.25	0.23	0.20
60FA+40O/B+0CL	0.34	0.31	0.29
58FA+40O/B+2CL	0.31	0.29	0.27
56FA+40O/B+4CL	0.29	0.28	0.25
54FA+40O/B+6CL	0.27	0.26	0.24
52FA+40O/B+8CL	0.26	0.24	0.22

## 4.5 Microstructural Analysis

It is observed that the glassy portions of the spheres of the composite are potentially attacked by calcium oxide. The SEM images show development of gel at different stages of pozzolanic reaction. It confirms to the observation that during early stages, the reactive particles in the fly ash-overburden-clinker composite served as nucleation sites for hydration and pozzolanic reaction products as (C-S-H, C-A-H, C-A-S-H) [97].

The cementitious compounds formed around the fly ash and overburden particles (Figures 4.29, 4.30, 4.31, 4.32 ). The composite (62%FA + 30%O/B+8%CL) at 28 days exhibited dense gel - like mass covering all reactive particles completely and filling up the inter-particle spaces with blurred grain boundaries (Figure 4.29). It appears like a massive unit compared to the other composites. The dense gel acted



as a binding substance and appears to be evenly distributed to form compact structure, thus creating more contact and higher cohesion that in turn reflects in greater strength values. It was observed from static laboratory tests that all samples exhibited maximum strength values at 28 days. So its SEM analysis was carried out to understand the microstructural aspects. The CBR of lime kiln dust amended soil-fly ash mixtures increased with increasing curing time due to the formation of calcium silicate hydrate (CSH) and calcium aluminate silicate hydrate gels (CASH) around soil and fly ash particles [27].

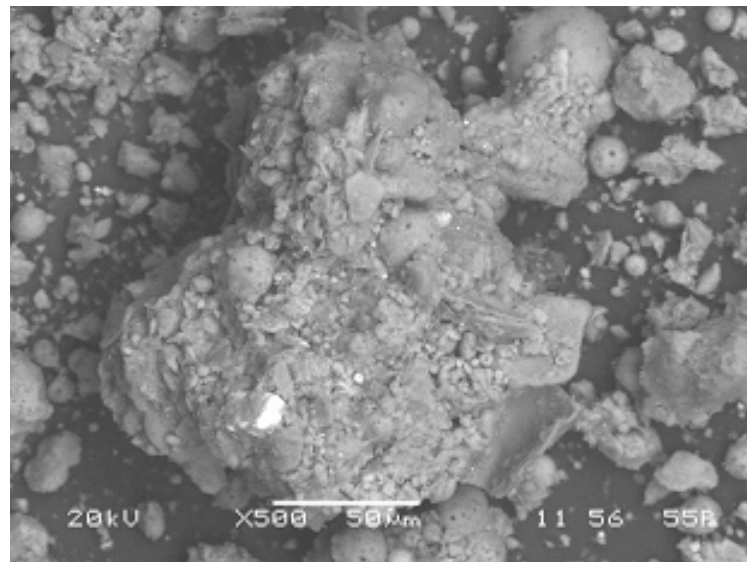


Figure 4.29: SEM image of 68%FA+30%O/B+2%CL

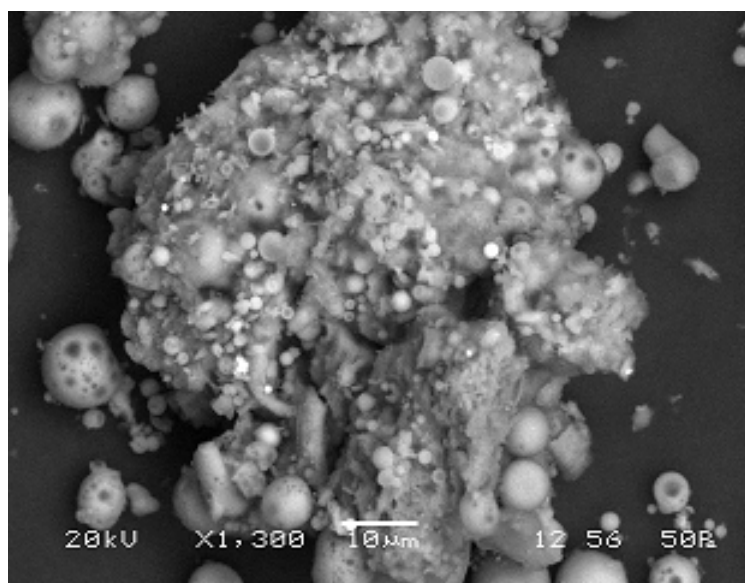


Figure 4.30: SEM image of 66%FA+30%O/B+4%CL

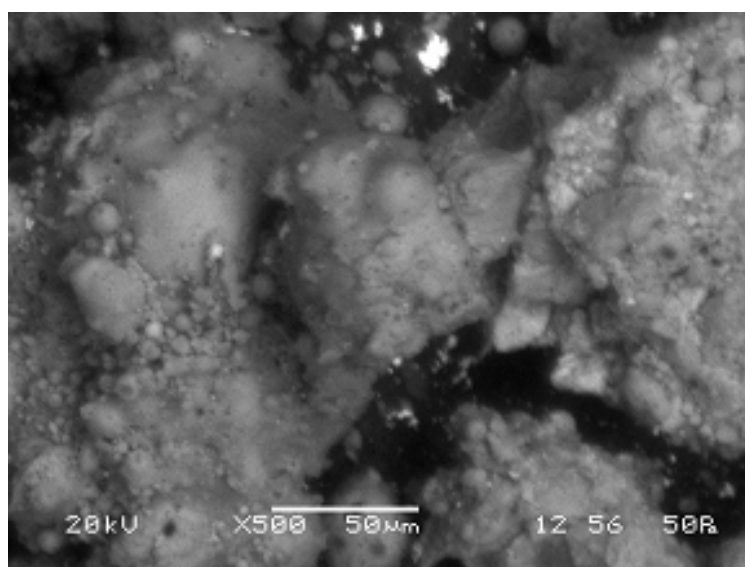


Figure 4.31: SEM image of 64%FA+30%O/B+6%CL

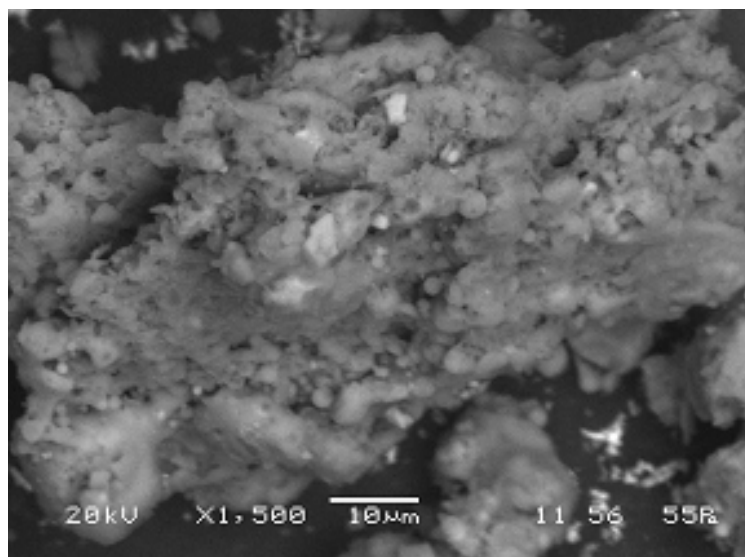


Figure 4.32: SEM image of 62%FA+30%O/B+8%CL

#### 4.5.1 Energy Dispersive X-ray Analysis

EDX is an analytical method for chemical characterization. The EDX analyses of all the composites were carried out to observe the effect of hydration at 28 days of curing. There were variations in elemental composition of composites (Table 4.7). In all composites calcium content increased due to increase in clinker content. Alumina content also increased with increase in fly ash content in composites. But, increase in clinker content reduced the alumina percentage in all composites. These results confirm to similar observation reported elsewhere [27]. All the mixes contain very small or negligible percentages of Na, Mg, S and K. The chemical composition of all composites indicates that they contain high percentages of silica ( $\text{SiO}_2$ ), alumina, iron and calcium oxides as well as small percentages of other elements. Among all these oxides, calcium oxide ( $\text{CaO}$ ) is very reactive. In the presence of aqueous solution, calcium oxide undergoes hydration. The formation of calcium silicate hydrate (CSH) gel and calcium aluminate hydrate (CAH) gel leads to increase in calcium content. The effectiveness of the lime treatment depends on the quality and quantity of lime as well as the chemical composition of the soil/fly ash. The strength developed is obviously influenced by the quantity of cementitious gel produced and consequently

by the amount of lime consumed.

Basicity index i.e.  $\text{CaO}/\text{SiO}_2$  is a good indicator of pozzolanic reactions which yields higher strength values [157]. The  $\text{CaO}/\text{SiO}_2$  ratios ranged from 0.065 to 0.693 in the composites. The composite containing 62% fly ash and 30% overburden treated with 8% clinker produced  $\text{CaO}/\text{SiO}_2$  ratio of 0.693 which exhibited maximum strength value. The CaO content is more (i.e. 25%) in the composite containing 62% fly ash and 30% overburden treated with 8% clinker as compared to other composites. The observations confirm to that reported elsewhere [27].

#### 4.5.2 X-ray Diffraction Analysis

The mineralogical analyses of the composites are very important to determine the changes in the mineralogical phases due to pozzolanic reactions. Cementing compounds such as CSH, CAH and CASH were identified in 3% cement stabilized fly ash only and fly ash – black cotton soil mixes at 28 days curing by XRD analysis [91]. The strength development is also dependent on the amount of hydration products as well as their interlocking mechanisms [97].

The formation of reaction products such as calcium silicate hydrate (CSH), calcium aluminate hydrate (CAH) and calcium aluminate silicate hydrates (CASH) confirmed from X-ray diffraction analysis. These new cementitious compounds induce aggregation effect in fly ash and overburden particles, bind the particles together to form fly ash-overburden clusters and resulted in overall enhanced behaviour of composites. The X-ray diffraction analysis of the selected composite (62%FA+30%O/B+8%CL) show the influence of clinker content on the hydration products (CAH, CSH, CASH). The intensity increased with increase in clinker content, maximum being at 8% clinker. The peaks for the composite vary with the clinker contents (Figure 4.33). Quartz, the primary mineral present in fly ash is indicated by sharp peaks.

Table 4.7: Chemical Compositions of the Composites, cured for 28 days

Elements in oxide form	(88FA+100/B+2CL)	(86FA+100/B+4CL)	(84FA+10/B+6CL)	(82FA+100/B+8CL)	(78FA+200/B+2CL)	(76FA+200/B+4CL)	(74FA+200/B+6CL)	(72FA+200/B+8CL)	(68FA+300/B+2CL)	(66FA+300/B+4CL)	(64FA+300/B+6CL)	(62FA+300/B+8CL)	(58FA+400/B+2CL)	(56FA+400/B+4CL)	(54FA+400/B+6CL)	(52FA+400/B+8CL)
Na	0.21	0.13	0.28	0.15	0.07	0.2	0.12	0.11	0.09	0.23	0.14	0.25	0.15	0.18	0.14	0.29
Mg	1.67	0.97	0.44	0.88	0.99	1.23	0.97	0.55	1.11	1.33	1.68	0.69	0.98	1.34	1.42	0.98
Al	29.4	26.53	24.11	20.2	29.8	27.1	21.6	20.3	31.2	26.1	24.7	22.5	31.6	28.7	26.3	22.5
Si	48.8	52.3	47.83	49.5	48.4	50.7	46.7	45.2	44.6	47.5	42.2	36.5	49.3	46.7	40.7	37.8
S	1.08	0.85	0.73	1.12	0.98	1.2	1.08	1.03	0.41	1.2	0.76	0.59	0.74	0.71	0.06	0.87
K	1.17	2.67	3.32	1.56	2.34	1.74	2.58	0.95	2.15	2.33	1.89	1.21	2.24	2.34	1.25	1.82
Ca	3.19	4.06	9.19	15.3	3.24	5.2	11.5	17.8	4.1	7.8	14.7	25.3	3.56	7.1	13.3	20.6
Ti	1.78	2.07	1.37	1.64	1.15	1.06	0.89	2.32	0.52	0.51	0.97	2.26	2.17	2.4	2.7	2.74
Fe	10.1	8.09	11.2	7.45	8.5	7.25	10.2	7.9	9.39	6.9	7.15	4.93	4.37	5.53	9.68	8.1
LOI	2.1	2.13	2.06	1.93	3.9	3.76	3.58	3.43	5.89	5.77	5.62	5.45	4.6	4.49	4.33	4.21

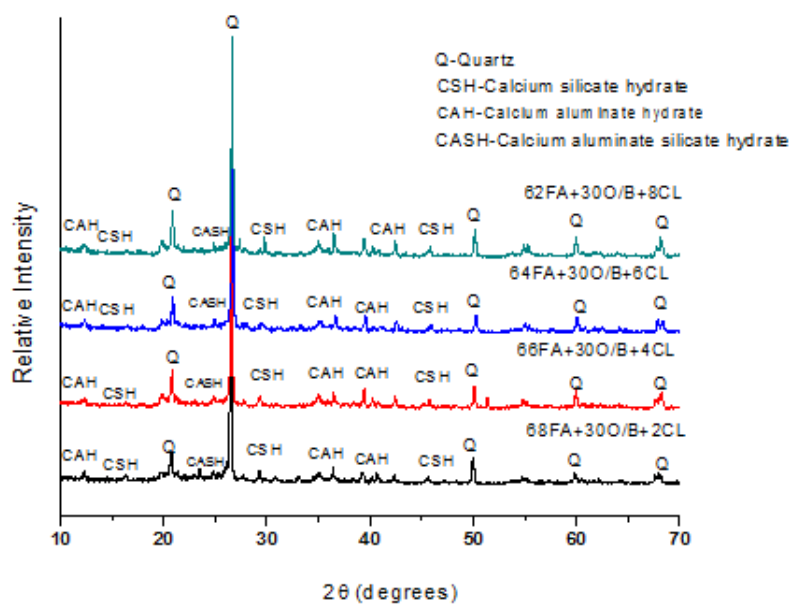


Figure 4.33: XRD of (70FA+30O/B) stabilized with 2, 4, 6, 8% clinker at 28 days curing

## 4.6 Development of Empirical Models

A part of the objectives was to develop model equations for the investigation with the parameters like UCS, CBR, BTS, P-wave velocity and  $\text{CaO}/\text{SiO}_2$ . Those are reported for the best fit correlations.

### 4.6.1 Relationship between CBR, UCS, BTS and P-wave velocity

The investigation involved samples for various parametric determinations. Each parameter has been discussed separately earlier. A few empirical models have been developed to establish mutual relationships between UCS and P-wave velocity, CBR and P-wave velocity, BTS and P-wave velocity, CBR and UCS, CBR and BTS.

The data are analyzed using multiple regression models by the method of least squares. There exists relation between compressive strength of fly ash-lime and fly

ash-lime-gypsum mixes with chemical composition, loss on ignition, CBR and tensile strength using power model [56]. It is observed that power equations suit for the fly ash and overburden mixes stabilized with clinker. It confirms that the relationship between compressive strength and P-wave velocity become stronger with increasing curing period. Similar results were also observed between CBR and unconfined compressive strength (Figure 4.34, 4.35, 4.36, 4.37, 4.38 ). The results of regression model between California bearing ratio values, unconfined compressive strength, brazilian tensile strength and P-wave velocity at 28 days curing period are reported (Table 4.8).

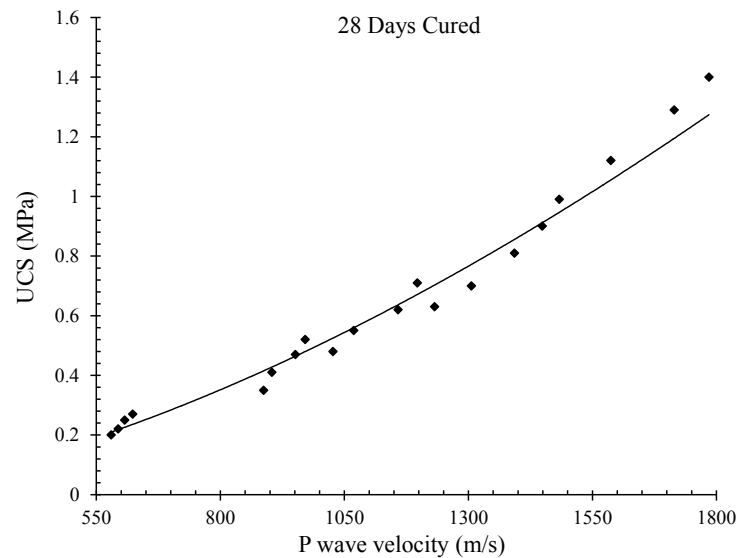


Figure 4.34: Relationship between unconfined compressive strength and P wave velocity

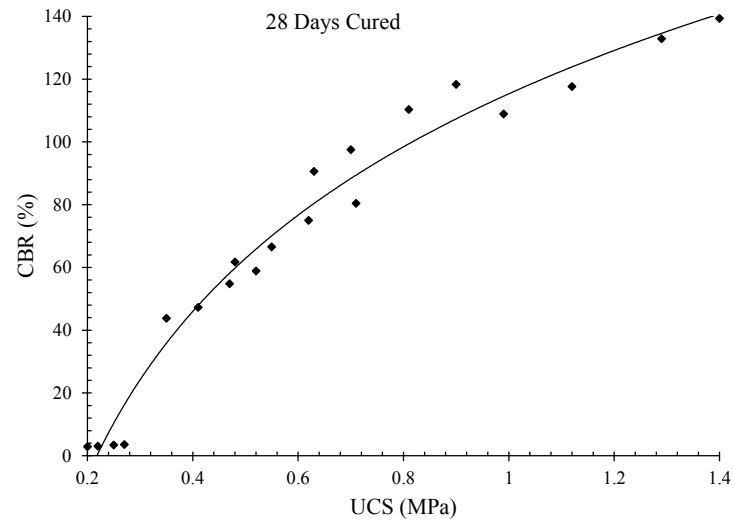


Figure 4.35: Relationship between CBR and unconfined compressive strength

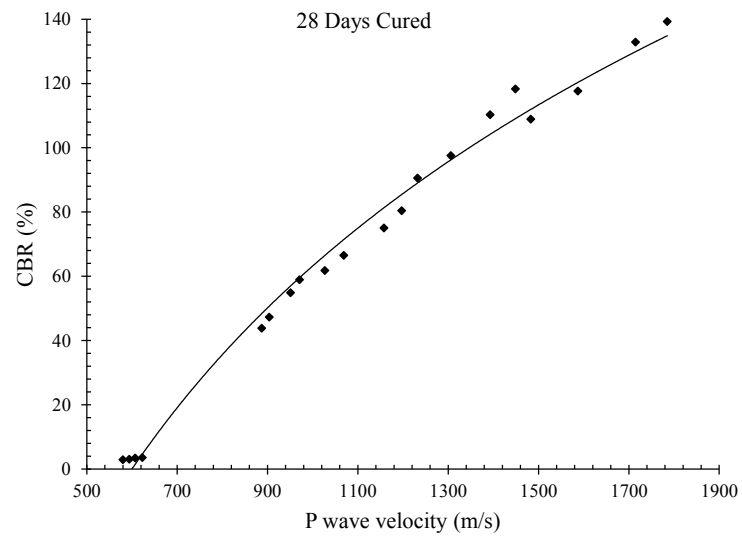


Figure 4.36: Relationship between CBR and P wave velocity



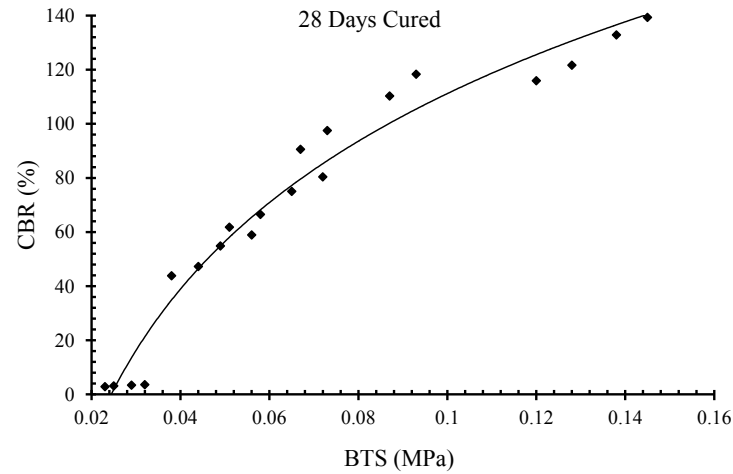


Figure 4.37: Relationship between CBR and BTS

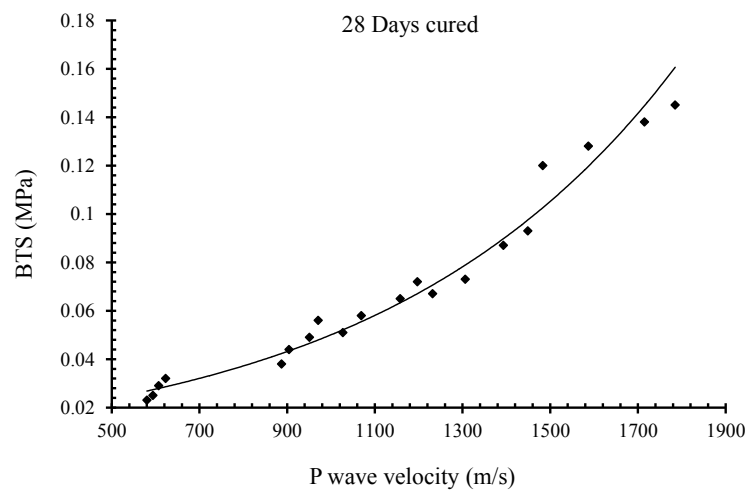


Figure 4.38: Relationship between BTS and P wave velocity

#### 4.6.2 Effect of Chemical composition on CBR, UCS, BTS and P-wave Velocity Values

In order to evaluate the effect of chemical composition of the mixtures on observed CBR, UCS, BTS and P-wave velocity values, the best fit regression model at 28 days curing were plotted against CaO content, CaO/SiO<sub>2</sub> ratios of the mixes (Figure 4.39, 4.40, 4.41, 4.42, 4.43, 4.44 ) and results were reported in Table 4.8. The best fit curves to the data produced high and modest correlation coefficients (R) for CBR,

UCS, BTS and P-wave velocity values. It is confirmed from the regression model that the CaO content, CaO/SiO<sub>2</sub> ratios exhibited good correlation with CBR, UCS, BTS and P-wave velocity values. Cetin et al. (2010) observed that the CBR value increased with increasing CaO content as well as with CaO/SiO<sub>2</sub>.

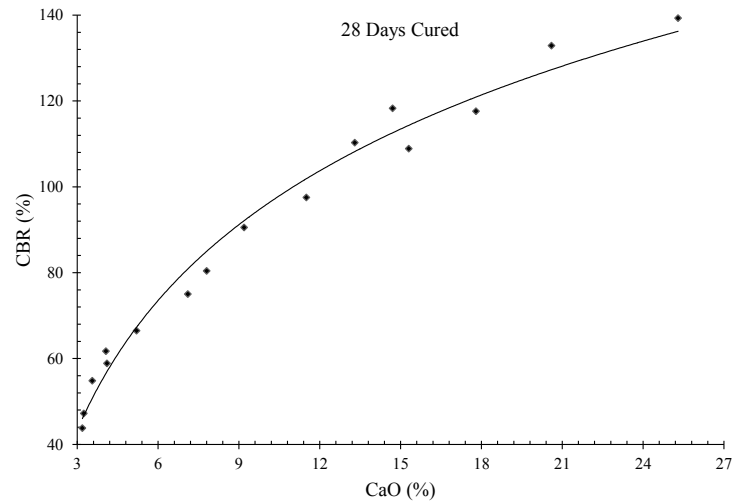


Figure 4.39: Effect of CaO content on CBR

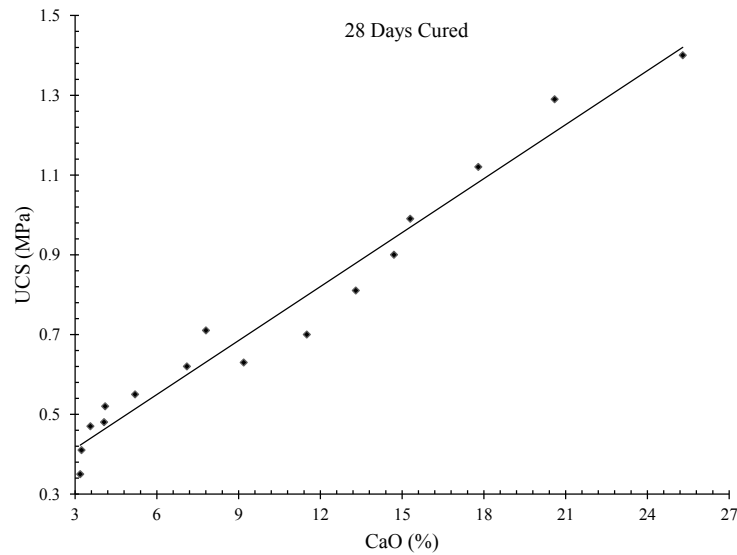


Figure 4.40: Effect of CaO content on UCS

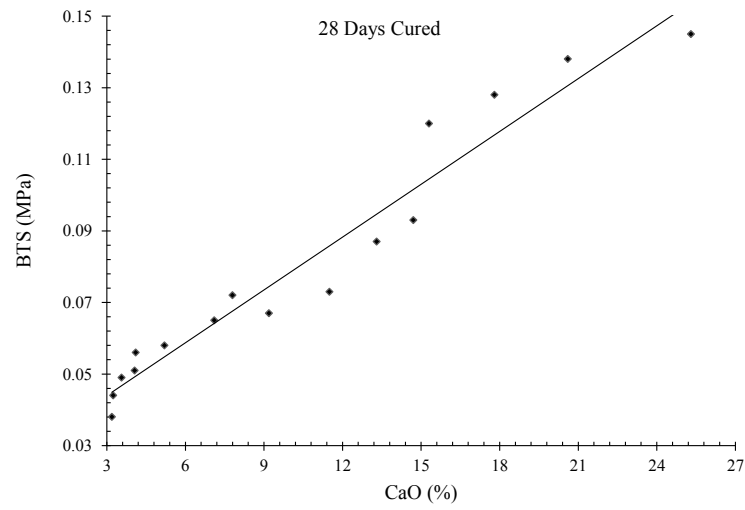
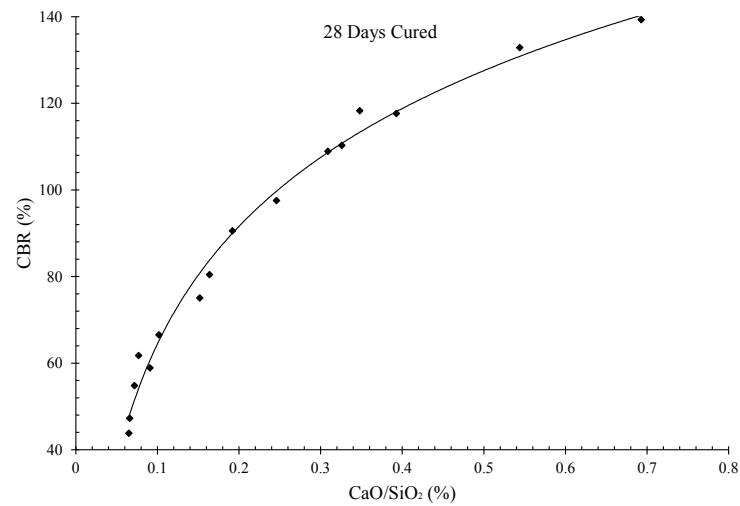


Figure 4.41: Effect of CaO content on BTS

Figure 4.42: Effect of CaO/SiO<sub>2</sub> on CBR

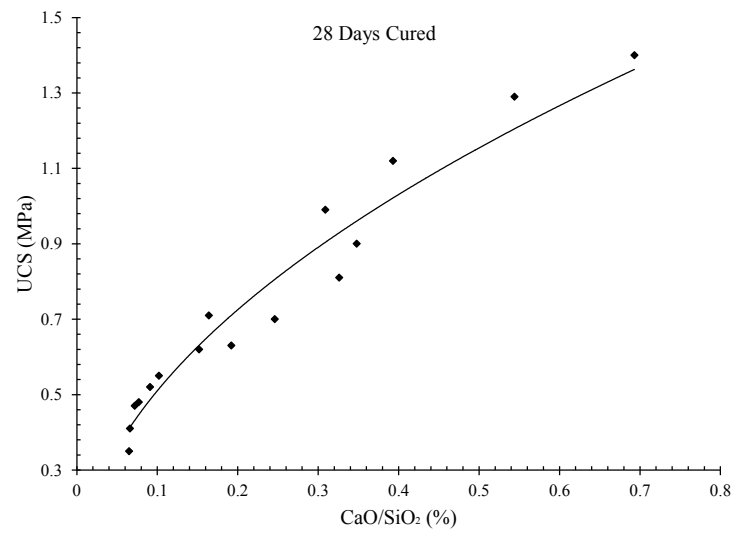
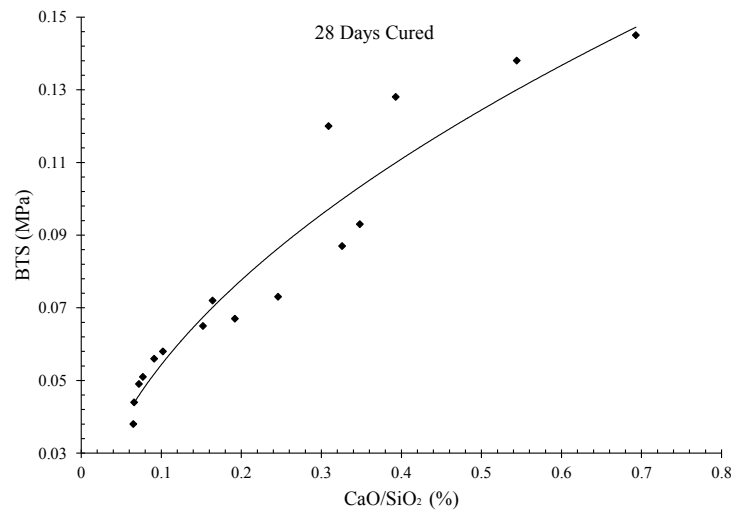
Figure 4.43: Effect of CaO/SiO<sub>2</sub> on UCSFigure 4.44: Effect of CaO/SiO<sub>2</sub> on BTS

Table 4.8: The developed correlation among various parameters of fly ash-mine overburden-clinker mixes

Parameters to be related	Best fit equation	R <sup>2</sup> value	Curing period (Days)
UCS vs. CaO (%)	$y=0.045x+0.279$	0.968	28
CBR vs. CaO (%)	$y=43.573\ln(x)-4.537$	0.982	28
BTS vs. CaO (%)	$y=0.004x+0.029$	0.946	28
UCS vs. CaO/SiO <sub>2</sub> (%)	$y=1.641x^{0.507}$	0.947	28
CBR vs. CaO/SiO <sub>2</sub> (%)	$y=39.221\ln(x)+154.72$	0.988	28
BTS vs. CaO/SiO <sub>2</sub> (%)	$y=0.177x^{0.515}$	0.930	28
UCS vs. P wave velocity	$y=8E-06x^{1.604}$	0.980	28
CBR vs. P wave velocity	$y=123.71\ln(x)-791.37$	0.989	28
BTS vs. P wave velocity	$y=0.011e^{0.001x}$	0.975	28
CBR vs. UCS	$y=75.679\ln(x)+115.33$	0.972	28
CBR vs. BTS	$y=78.845\ln(x)+292.72$	0.964	28

# Chapter 5

## Numerical Investigation

### 5.1 General

High-speed computer has revolutionized the scope of analysis by numerical methods like Finite Element Method (FEM), Finite Difference Method (FDM) for design of structures. FEM is flexible in adopting variables like irregular geometric shape, unusual loading conditions, varying material properties etc. Finite element method is capable of addressing all complicated aspects like non-linearity, non-homogeneity, anisotropy etc. It involves two approaches i.e. force approach and displacement approach. Displacement approach is more popular in mining applications [137, 216, 103, 119].

FEM analysis typically consists of breaking the model into number of small elements. Each element is modeled as a completely self-contained system, typically in its elastic range though other approaches are also carried out. The simplest element is defined by nodes at each corner that also depend on the order of element. Nodal points are defined as the joint of adjacent elements. The complete system is evaluated as a series of equations to maintain equilibrium in terms of force and displacement. The measurement of force or stress and displacement or strain at the boundary of the model is governed by specific boundary conditions. The FEM formulation is expressed either in one, two (planar or axisymmetric) or three dimensions.

First FEM analysis of a pavement structure with axisymmetric formulation was

reported by [46]. FEM allows the model to accommodate load dependent stiffness of materials though most of the models use linear elastic theory as constitutive relationship.

Simulation of road pavement constructed with cement stabilized fly ash was observed to exhibit low strain [97]. There are many reports on both linear and non-linear analysis of road pavement [89, 86, 80, 131].

## 5.2 Axisymmetric solutions

Various problems can be solved using axi-symmetric solids subjected to axially symmetric loading. Due to symmetry of the problem, the stress components are independent of angular coordinate  $\theta$ . The problem is similar to that in plane stress and plane strain. By virtue of symmetry, state of stress and strain is fully defined by two components of displacement in any plane along symmetry axis. The strain components all derivatives with respect to  $\theta$  become zero for all stress and strain components i.e.  $\mu$ ,  $\gamma_{r\theta}$ ,  $\gamma_{\theta z}$  and  $\tau_{\theta}$  are zero. The radial and axial coordinates are denoted as  $r$  and  $z$  with  $u$  and  $w$  being corresponding displacement. The non-zero stress components are  $\sigma_r$ ,  $\sigma_\theta$ ,  $\sigma_z$  and  $\tau_{rz}$ .

In plane stress or plane strain components either stress or strain in direction normal to plane is zero. The strain energy of the plate is associated with three strain components. Any displacement in radial direction will induce strain in circumferential direction. The circumferential stress is not zero.

Problems involving three dimensional solids subjected to axisymmetric loading reduce to two dimensional problems. Isoparametric elements have proved their effectiveness on two dimensional problems. In isoparametric element, geometry and displacement are described in same parameters and are of same order.

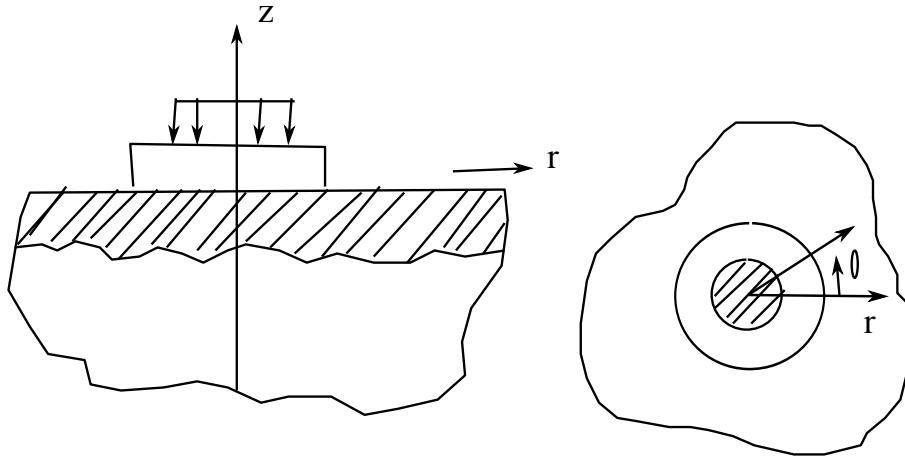


Figure 5.1: Haul road cross-section under axisymmetry loading [43]

Axi-symmetric structures are those which can be generated by rotating a line or curve about an axis. If such structures are subjected to axisymmetric loadings like uniform internal or external pressures, uniform self-weight or live load uniform over the surface, there exist symmetry about any axis (Figure 5.1). The advantage of symmetry is used to simplify the analysis where stress components are independent of the angular ( $\theta$ ) coordinate. Hence all derivatives with respect to  $\theta$  vanish.

### 5.2.1 Elastic Equations

Elasticity equations are used for solving structural mechanics problems. These equations must be satisfied if an exact solution to a structural mechanics problem is to be obtained. The types of elasticity equations are

1. Strain-Displacement relationship equations

$$e_x = \frac{\partial u}{\partial x}; e_y = \frac{\partial v}{\partial y}; \gamma_{xy} = \frac{\partial u}{\partial y} + \frac{\partial v}{\partial x}; \gamma_{xz} = \frac{\partial u}{\partial z} + \frac{\partial w}{\partial x}; \gamma_{yz} = \frac{\partial v}{\partial z} + \frac{\partial w}{\partial y} \quad (5.1)$$

$e_x$  = Strain in x-direction

$e_y$  = Strain in y-direction

$\gamma_{xy}$  = Shear strain in xy-plane

$\gamma_{xz}$  = Shear strain in xz-plane



$\gamma_{yz}$  = Shear strain in yz-plane

## 2. Stress-strain relationship equation

$$\begin{bmatrix} \sigma_x \\ \sigma_y \\ \sigma_z \\ \tau_{xy} \\ \tau_{yz} \\ \tau_{zx} \end{bmatrix} = \frac{E}{(1+\mu) \times (1-2\mu)} \begin{bmatrix} (1-\mu) & \mu & \mu & 0 & 0 & 0 \\ & (1-\mu) & \mu & 0 & 0 & 0 \\ & & (1-\mu) & 0 & 0 & 0 \\ & & & \frac{1-2\mu}{2} & 0 & 0 \\ & & & & \frac{1-2\mu}{2} & 0 \\ & & & & & \frac{1-2\mu}{2} \end{bmatrix} \begin{bmatrix} e_x \\ e_y \\ e_z \\ \gamma_{xy} \\ \gamma_{yz} \\ \gamma_{zx} \end{bmatrix} \quad (5.2)$$

*Symmetrical*

$\sigma$  –Stress,  $\tau$  –Shear stress, E-Young's modulus,  $\mu$ -Poisson's ratio, e-strain,  $\gamma$ -shear strain

## 3. Equilibrium equations

$$\frac{\partial \sigma_x}{\partial x} + \frac{\partial \tau_{xy}}{\partial y} + \frac{\partial \tau_{xz}}{\partial z} + B_x = 0; \quad \frac{\partial \sigma_y}{\partial y} + \frac{\partial \tau_{yz}}{\partial z} + \frac{\partial \tau_{xy}}{\partial x} + B_y = 0; \quad \frac{\partial \sigma_z}{\partial z} + \frac{\partial \tau_{xz}}{\partial x} + \frac{\partial \tau_{yz}}{\partial y} + B_z = 0 \quad (5.3)$$

$\sigma$  –Stress,  $\tau$  –Shear stress,  $B_x$ -Body force in at x-direction,  $B_y$ -Body force in at y-direction,  $B_z$ -Body force in at z-direction

## 4. Compatibility equations

There are six independent Compatibility equations, one of which is

$$\frac{\partial^2 e_x}{\partial y^2} + \frac{\partial^2 e_y}{\partial x^2} = \frac{\partial^2 \gamma_{xy}}{\partial x \partial y} \quad (5.4)$$

The other five equations are similarly second order relations.

### 5.2.2 Axisymmetric elements

Most of the three dimensional problems are symmetry about an axis of rotation. Those types of problems are solved by a special two dimensional element called as axisymmetric element.

### 5.2.3 Axisymmetric formulation

The displacement vector  $u$  is given by

$$u(r, z) = \begin{bmatrix} u \\ w \end{bmatrix} \quad (5.5)$$

Where  $r$  and  $z$  represent radial and axial co-ordinates with  $u$  and  $w$  being corresponding displacement. The stress  $\sigma$  is given by

$$[\sigma] = \begin{bmatrix} \sigma_r \\ \sigma_\theta \\ \sigma_z \\ \tau_{rz} \end{bmatrix} \quad (5.6)$$

Where  $\sigma_r, \sigma_\theta, \sigma_z, \tau_{rz}$  are non-zero stress components. The strain  $e$  is given by

$$[e] = \begin{bmatrix} e_r \\ e_\theta \\ e_z \\ \gamma_{rz} \end{bmatrix} \quad (5.7)$$

$$\varepsilon_r = \frac{u}{r}, \varepsilon_\theta = \frac{u}{r}, \varepsilon_z = \frac{w}{z}, \tau_{rz} = \frac{u}{z} + \frac{w}{r} \quad (5.8)$$

In this case stress-strain relationship is

$$\begin{bmatrix} \sigma_r \\ \sigma_z \\ \sigma_\theta \\ \tau_{rz} \end{bmatrix} = \frac{E}{(1 + \mu) \times (1 - 2\mu)} \begin{bmatrix} 1 - \mu & \mu & \mu & 0 \\ & 1 - \mu & \mu & 0 \\ & & 1 - \mu & 0 \\ \text{Symmetrical} & & & \frac{1-2\mu}{2} \end{bmatrix} \begin{bmatrix} \varepsilon_r \\ \varepsilon_z \\ \varepsilon_\theta \\ \gamma_{rz} \end{bmatrix} \quad (5.9)$$

Where

$r, \theta$  and  $z$  = Radial, Circumferential and Cartesian coordinate respectively

$E$  = Young's modulus,  $\mu$  = Poisson's ratio

$\varepsilon$  = Normal strain,  $\{\varepsilon\}$  = Strain vector

$\sigma$  = Normal stress,  $\{\sigma\}$  = Stress vector

$\tau$  = Shear stress,  $\gamma$  = Shear strain

$u, w$  = Displacement in Cartesian coordinates

### 5.3 Tire Pressure Calculation

The dumper load that is borne by the tires is calculated as below.

$$\text{Tire pressure} = \frac{\text{Gross vehicular weight of Dumper}}{\text{Number of tires} \times \text{Tire foot print area}}$$

Dumpers of 80 T, 200 T and 300 T are considered.

For 80T dumper

Gross vehicular weight = 160T (make: Caterpillar)

Number of tires = 6

Diameter of area of contact = Tire width = 0.8m

$$\text{The Tire pressure} = \frac{160 \times 9.81}{6 \times \pi (0.4)^2} = 520 \text{ kPa}$$

Similarly tire pressure for 200T and 300T dumper capacity are 555 kPa and 700 kPa respectively.

### 5.4 Modelling

A schematic layout of existing haul road pavement is shown in Figure 5.2

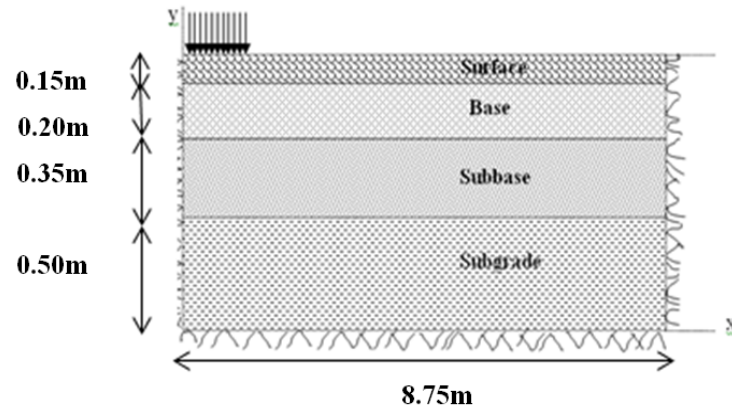


Figure 5.2: A schematic layout of existing haul road pavement

Simulation models were developed to determine the stress-strain behaviour of haul road pavement. Material properties like Young's modulus and Poisson's ratio of both conventional material and developed fly ash based composite materials were used to develop the models (Table 5.1 ). Typically dense sand, gravel, silty sand, sandy clay, clay shale, medium clay, soft clay, silty clay, etc. are used in haul road pavement. The elastic constants of these road construction materials vary over a large scale. As observed from field visits, loose overburden materials consisting of clay, broken rocks, pebbles, sandstone, shale etc. are used for haul road construction. The surface course is reinforced with crushed stone and compacted. As it was not possible to measure their elastic modulus, it was assumed from the published literature [110]. Corresponding values for surface course, base course, sub-base, sub-grade of the haul road pavement considered for simulation are 180, 90, 60 and 50MPa respectively. Poisson's ratio value was assumed 0.4 for each layer [191, 97, 110].

The aim of the investigation was to evaluate the performance of developed fly ash composite to replace the conventional sub-base material. The developed composite material exhibiting maximum strength value was considered for the purpose i.e. 62%FA+30%O/B+8%CL. Its elastic modulus and Poisson's ratio are 186MPa and 0.2 respectively.

Table 5.1: Young's modulus, E (MPa) and Thickness, t (m) of the pavement layers for Conventional material and sub-base replaced with FCM

Case ID	Construction Materials	Layer							
		Surface		Base		Sub-base		Sub-grade	
		E	t	E	t	E	t	E	t
A	Conventional Material	180	0.15	90	0.2	60	0.35	50	0.5
B	Only Sub-base replaced with FCM	180	0.15	90	0.2	186	0.35	50	0.5

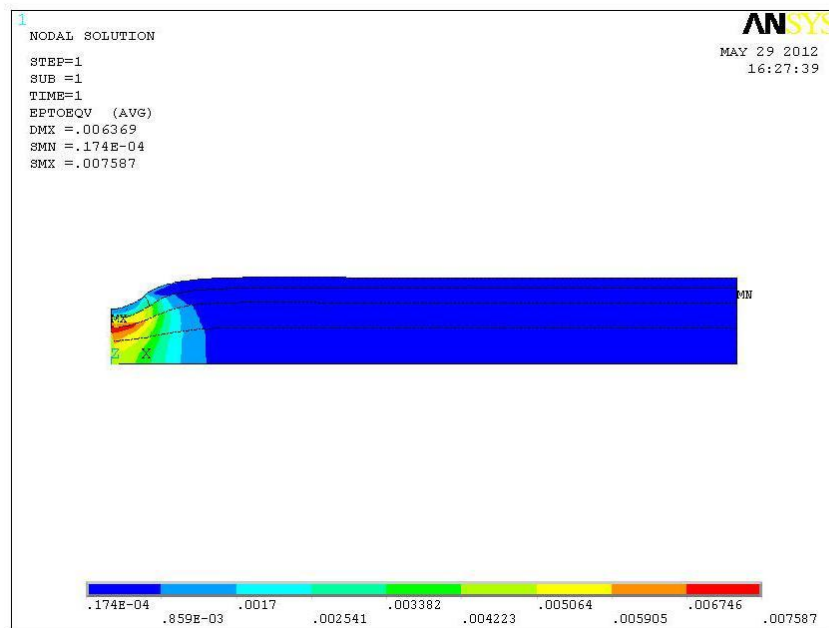


Figure 5.3: Maximum strain of haul road pavement with conventional material

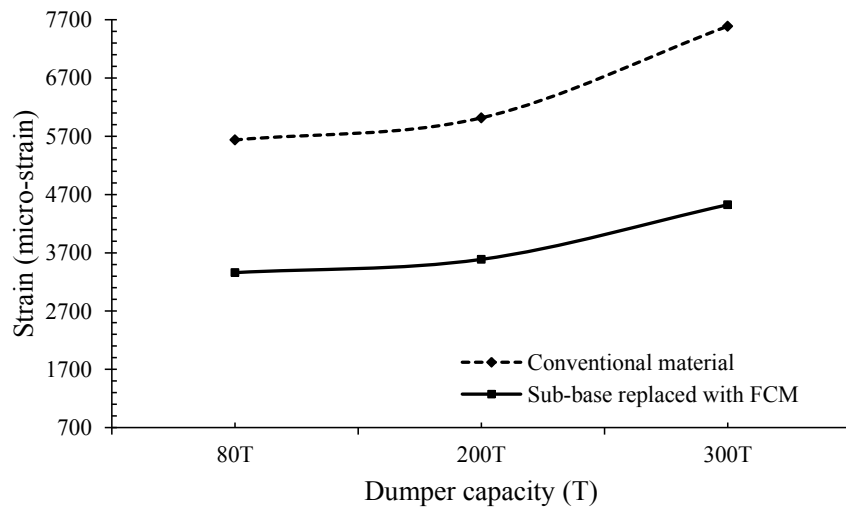


Figure 5.4: Strain behaviour vs. dumper capacity

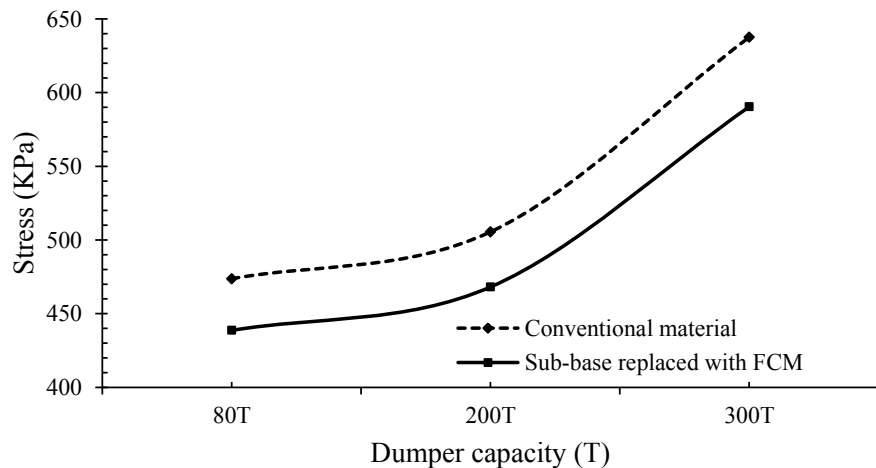


Figure 5.5: Stress behaviour vs. dumper capacity

Analysis was carried out considering the existing dimension with 520 kPa, 555 kPa and 700 kPa load (Figures 5.4 and 5.5 ). It is observed that as the load or dumper capacity increases the maximum strain and stress of haul road pavement increase. The maximum strain values are 7587 micro-strain and 5636 micro-strain for 300T and 80T dumper capacity respectively which is much higher compared to critical strain limit (Appendix, Page-155; Figure 5.3) . When sub-base material was replaced with best obtained FCM the strain value reduced by 40% i.e. to 3360 micro-strain. Maximum

stress reduced by 7% for 80T dumper capacity. Similar values were obtained for 200T and 300T dumper capacity. But the rises in maximum stress and strain values with existing dimension were steeper when dumper capacity increased to 300T. Maximum stress and strain values were 590 kPa and 4524 micro-strain respectively for 300T dumper capacity using FCM in sub-base. The stress and strain values for both cases i.e. with conventional material as well as with replaced fly ash composite in sub-base were above critical strain limit. It increases the probability of failure in haul road pavement.

Hence further analyses were carried out by changing thickness of layers as well as material properties (Table 5.2 ). Material properties have direct effect on stiffness of pavement.

Table 5.2: Young's modulus, E (MPa) and Thickness, t (m) of the pavement layers for proposed dimensions

Case ID	Layer							
	Surface		Base		Sub-base		Sub-grade	
	E	t	E	t	E	t	E	t
C	500	0.15	350	0.2	186	0.35	50	0.5
D	500	0.15	350	0.2	186	0.5	50	1.0
E	500	0.15	350	0.2	186	1.0	50	2.0
F	500	0.3	350	0.4	186	1.0	50	2.0
G	500	0.5	350	1	186	1	50	2.0
H	500	0.5	350	1	186	1.5	50	2.0

Analyses were carried out considering high elastic values (Table 5.3 ) in surface course and base course for 80T, 200T and 300T dumper capacity. The obtained stress and strain values are above critical limit. Hence change in the thickness of pavement layers was made and simulation carried out.

The thickness of haul road pavement was changed. Maximum thickness of pavement considered was 5.0m [191]. Different thicknesses considered were between 1.2 and 5.0m (Table 5.3 ). Analyses were carried out using developed FCMs in sub-base. It was observed that as pavement thickness increased maximum stress and strain values decreased. The maximum strain obtained were more than critical strain limit up to 3.35 thicknesses for each case i.e. for 80T, 200T and 300T dumper capacity. How-

ever as the thickness of pavement increase to 3.7m and above, maximum strain values were less than the critical strain limit for 80T and 200T dumper capacity. For 300T dumper the value was slightly higher i.e. 1570 micro-strain. The strain values were less than the critical strain limit for all considered cases beyond pavement thickness of 4.5m. At a thickness of 5.0m dumper with 300T capacity produced maximum stress and strain values. The detail stress and strain values obtained for different dimensions are given in table 5.2.

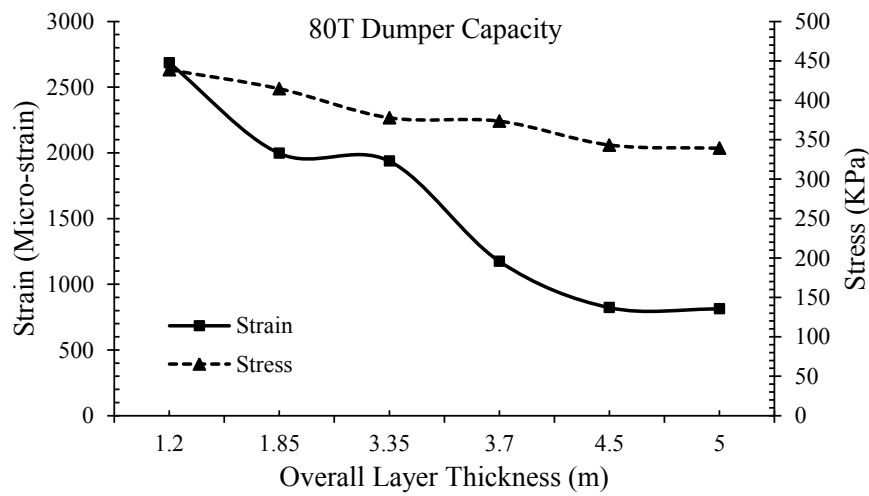


Figure 5.6: Maximum strain and stress values for different pavement thickness for 80T dumper



Table 5.3: Maximum stress and strain values for different dumper capacity and pavement thickness

Pavement Thickness (m)	Dumper Capacity					
	80T		200T		300T	
	Maximum Stress (kPa)	Maximum Strain(micro-strain)	Maximum Stress (kPa)	Maximum Strain(micro-strain)	Maximum Stress (kPa)	Maximum Strain(micro-strain)
1.20	473.7	5636	505.5	6015	637.6	7587
	438.6	3360	468.1	3587	590.4	4524
	484	2685	516.6	2866	651.5	3614
1.85	414.6	1996	442.5	2130	558.2	2687
3.35	377.8	1937	403.2	2067	508.6	2607
3.70	373.5	1174	398.6	1253	502.8	1580
4.50	339.2	822	362	877	456.6	1107
5.00	343.3	812	366.4	867	462.1	1094

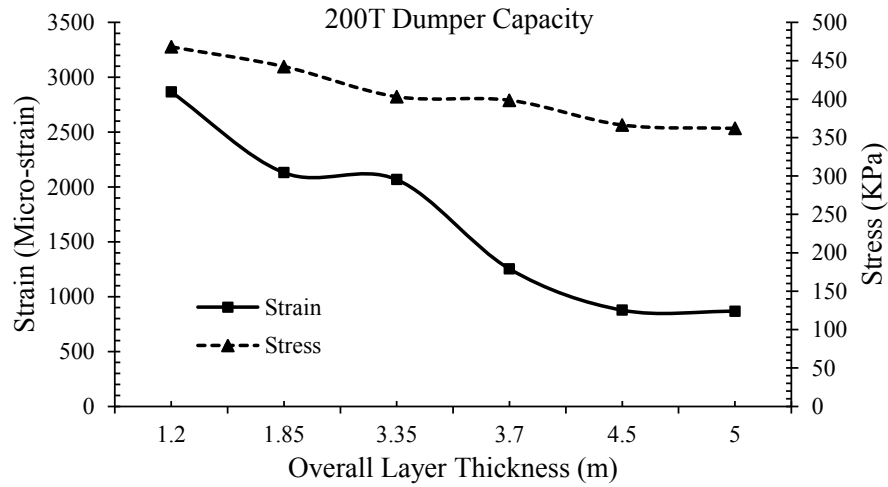


Figure 5.7: Maximum strain and stress values for different pavement thickness for 200T dumper

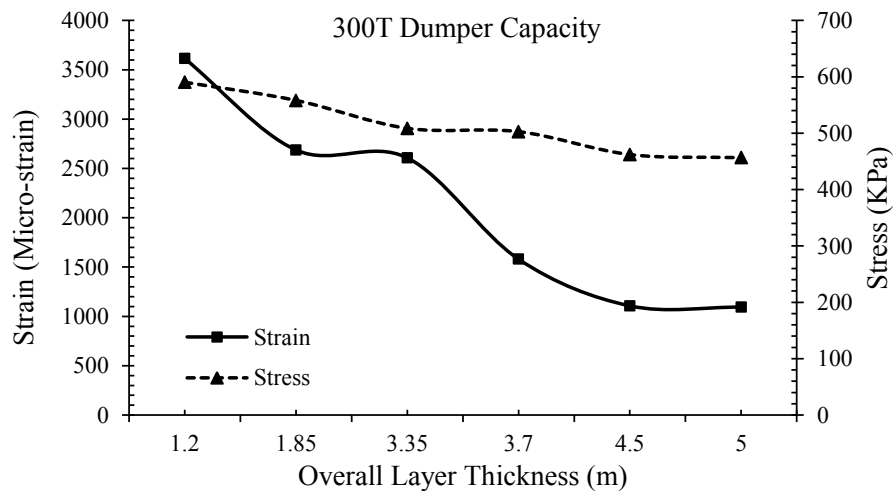


Figure 5.8: Maximum strain and stress values for different pavement thickness for 300T dumper

Further numerical analysis were carried out using the elastic parameters to evaluate the performance of the composite materials cured at 28 days only as those are comparable to 7 days and 14 days cured behaviour of the best developed composite.

The Poisson's ratio and Young's modulus values of the developed composite materials were determined from Ultrasonic pulse velocity test (Table 5.4 ). The static tests involve destructive approaches where load is applied at an incremental step.

Table 5.4: Young's modulus, E (MPa) and Poisson's ratio of different developed composites

Compositions (FA+O/B+CL) *CL= Clinker	Curing period	
	28 Days	
	Young's modulus	Poisson's ratio
88FA+10O/B+2CL	70	0.29
86FA+10O/B+4CL	87	0.28
84FA+10O/B+6CL	106	0.27
82FA+10O/B+8CL	152	0.26
78FA+20O/B+2CL	82	0.28
76FA+20O/B+4CL	100	0.27
74FA+20O/B+6CL	116	0.25
72FA+20O/B+8CL	160	0.24
68FA+30O/B+2CL	104	0.26
66FA+30O/B+4CL	129	0.24
64FA+30O/B+6CL	150	0.23
62FA+30O/B+8CL	186	0.20
58FA+40O/B+2CL	92	0.27
56FA+40O/B+4CL	112	0.25
54FA+40O/B+6CL	135	0.24
52FA+40O/B+8CL	172	0.22

During testing flaws, cracks develop and close till hydrostatic conditions exist beyond which cracks/ flaws keep on extending till failure occurs. These values are less than the values for conventional materials as well as less than the maximum strain limits experienced [194, 191]. It confirms that the developed composite material could be a better alternative to the conventional material.

The stress and strain at different depth vary between 500 to 10 KPa and 1100 to 200 micro-strains respectively for all the composites (Figures 5.11 , 5.12 , 5.13 , 5.14 , 5.15 , 5.16 , 5.17 , 5.18). These values are less than the values for conventional materials as well as less than the maximum strain limits experienced [194, 191].

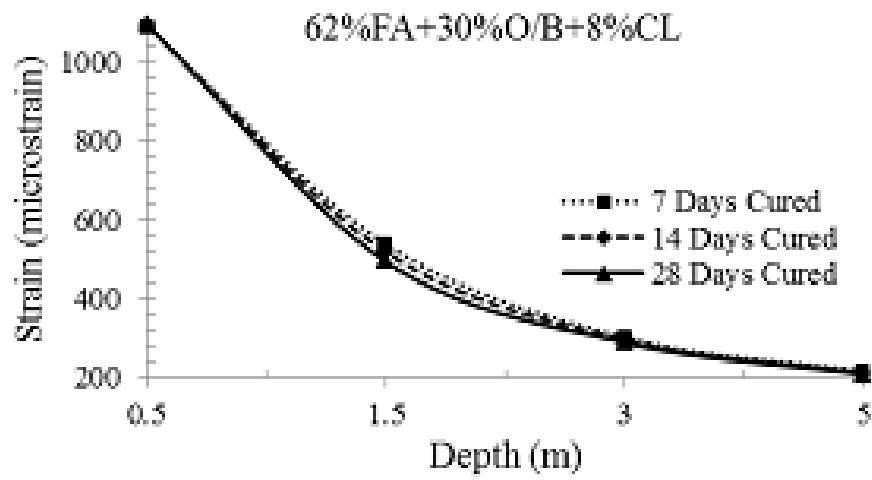


Figure 5.9: Strain values with (62%FA+30%OB+8%CL) composite

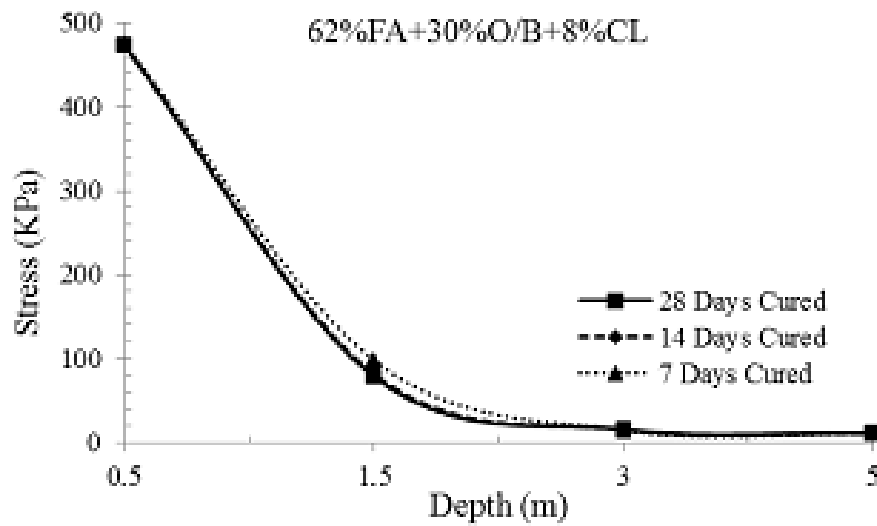


Figure 5.10: Strain values with (62%FA+30%OB+8%CL) composite

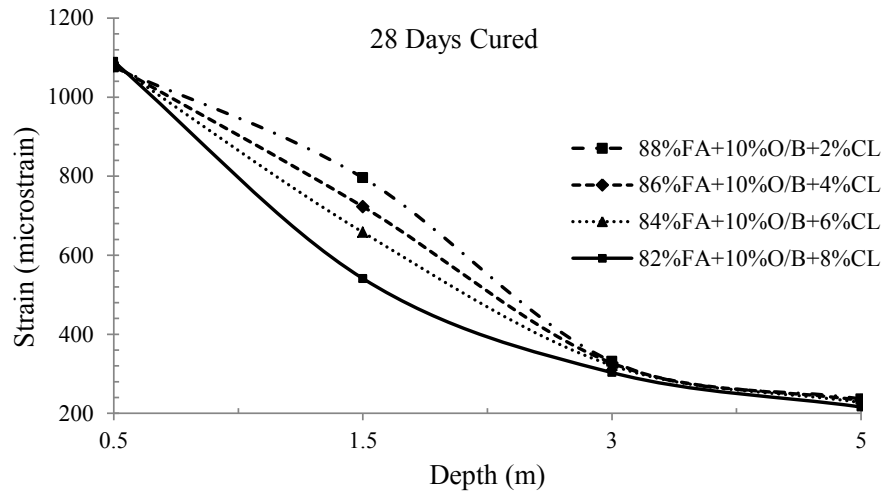


Figure 5.11: Strain values with composites containing 10% mine overburden as sub-base material

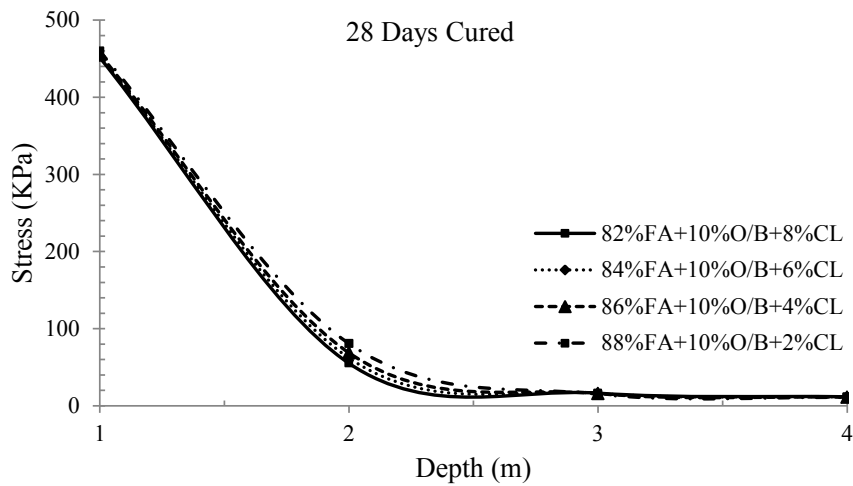


Figure 5.12: Stress values with composites containing 10% mine overburden as sub-base material

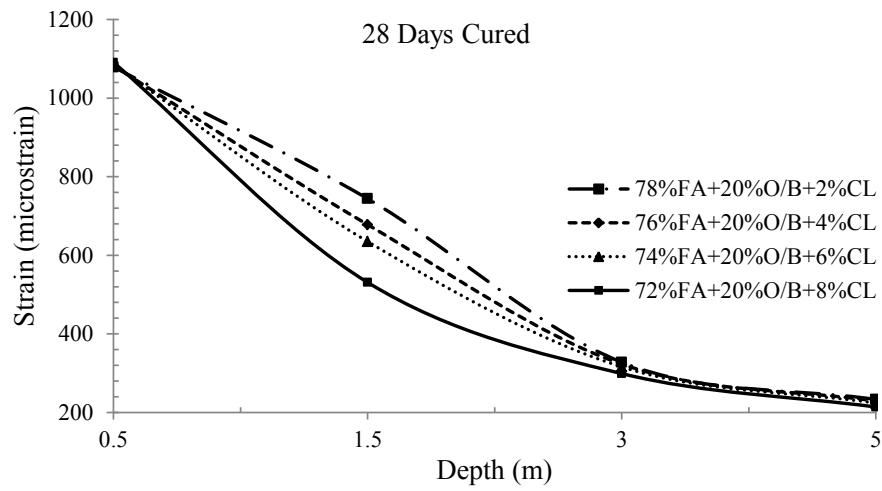


Figure 5.13: Strain values with composites containing 20% mine overburden as sub-base material

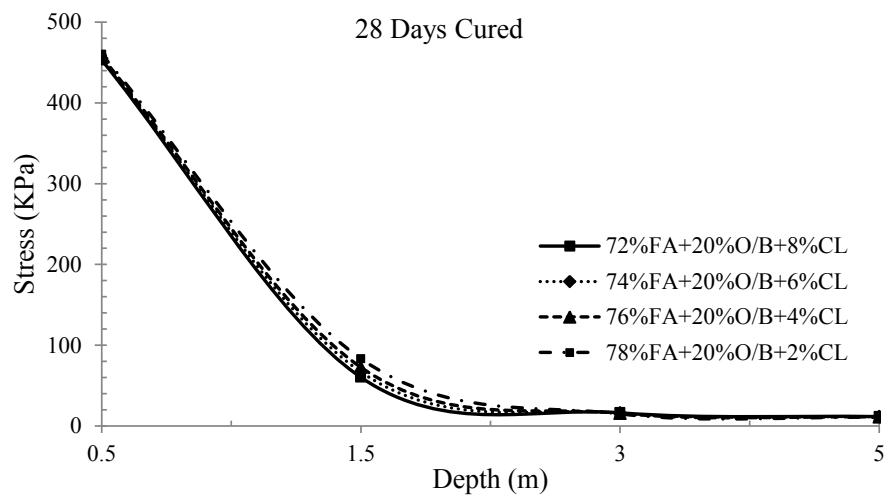


Figure 5.14: Stress values with composites containing 20% mine overburden as sub-base material

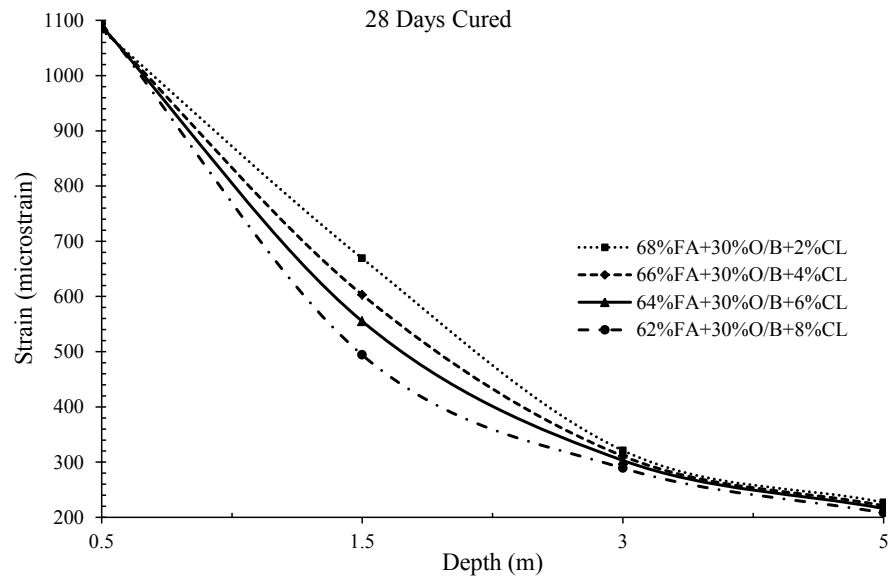


Figure 5.15: Strain values with composites containing 30% mine overburden as sub-base material

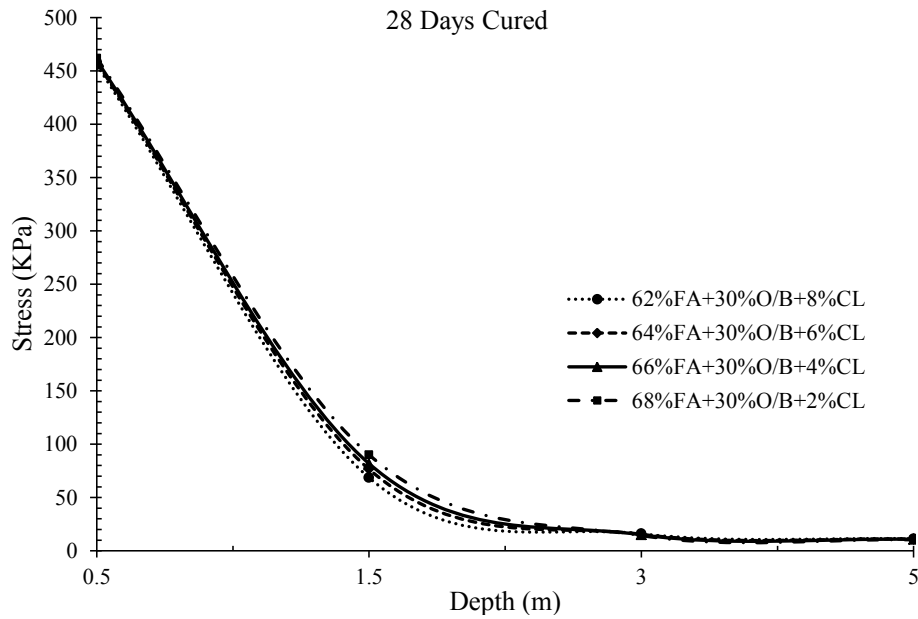


Figure 5.16: Stress values with composites containing 30% mine overburden as sub-base material

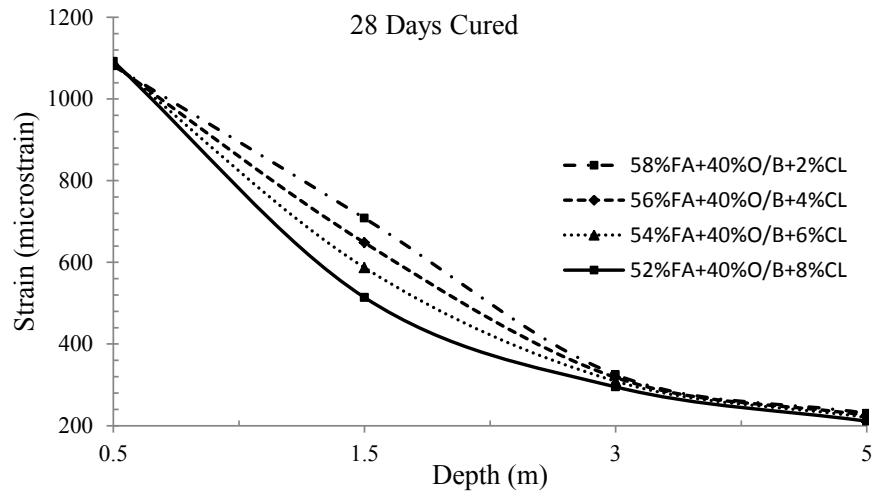


Figure 5.17: Strain values with composites containing 40% mine overburden as sub-base material

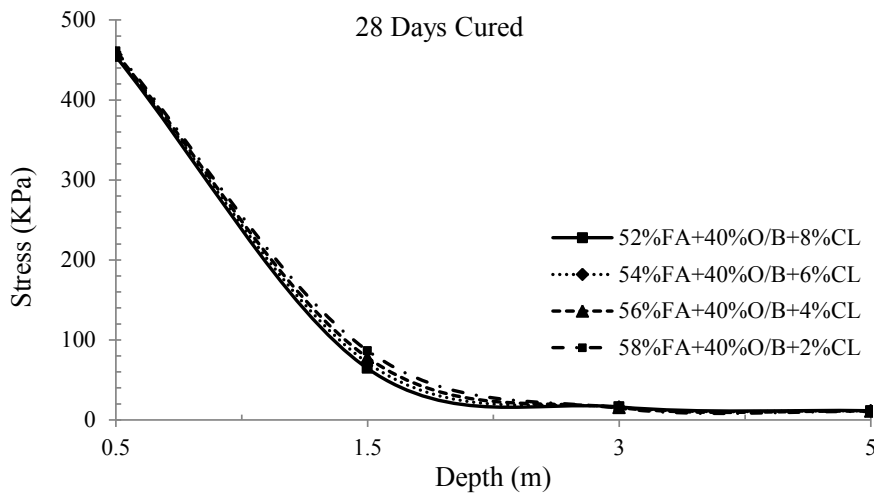


Figure 5.18: Stress values with composites containing 40% mine overburden as sub-base material



# Chapter 6

## Summary and Conclusion

Mine economics depends on the performance of haul road apart from other factors. The behaviour of surface course depends on that of the layers beneath it. Traditionally overburden material is used for haul road construction. Fly ash disposal is a major challenge both to power plant operations as well as to other stake holders. In the current investigation, performance of clinker stabilized fly ash-mine overburden mixes were evaluated for haul road application. Different composite materials were prepared, developed and characterized in addition to characterization of ingredients. Strength characteristics of fly ash composites are studied through different tests as CBR, unconfined compressive strength, Brazilian tensile strength and ultrasonic pulse velocity. Microstructural analyses carried out for better understanding of mechanism of clinker, fly ash and overburden interaction. The change in surface morphology and variation in chemical compositions due to formation of hydration products were analyzed through SEM and EDX. X-ray diffraction analyses were carried out to identify phases of hydration products. The numerical investigation as 2D finite element analyses was carried out to study the effectiveness of the developed composite materials on the stress-strain behaviour of haul road pavement. The conclusions are divided into three different sections as follows:

1. Characterization of ingredients
2. Characterization of developed composites

3. Performance evaluation of developed FCMs through simulation

## 6.1 Untreated Materials

1. Mine overburden has major chemical constituents of silica 48%, alumina 29% and iron oxide 8% and mineral constituents of Kaolinite and Quartz and acidic in nature.
2. Mine overburden material is poorly graded sand-silt mixtures.
3. Mine overburden has high maximum dry density ( $1941 \text{ kg/m}^3$ ) and low optimum moisture content (14.2%) compared to fly ash. It exhibits low CBR value in soaked condition.
4. It is not suitable to be used as road construction material alone. It possesses low compressive strength (343 kPa).
5. The fly ash used for the investigated was class F type. The major chemical constituents of fly ash are silica 53%, alumina 33% and iron oxide 6% with major mineral constituents as Quartz, Sillimanite and Mullite.
6. Fly ash has high optimum moisture content (22.3%) and low maximum dry density ( $1296 \text{ kg/m}^3$ ) due to the fact that particles themselves are hollow or cenospheres and hold a considerable quantity of water internally. It exhibits very low CBR value (0.70%) at soaked condition.
7. The maximum dry density decreased from  $1941 \text{ kg/m}^3$  to  $1296 \text{ kg/m}^3$  and optimum moisture content increased from 14.2% to 22.3% with increase in fly ash content in the untreated composites.
8. The UCS values of fly ash-overburden composites were not significant ( $< 400 \text{ kPa}$ ) even after 28 days curing.
9. The CBR values of untreated fly ash-overburden composite materials were low ( $< 3\%$ ) at soaked condition and hence those are unsuitable for road construction.

10. There was not much strength gain in the untreated composites with varying curing periods e.g. from 7 days to 28 days.

## 6.2 Treated Materials

1. The maximum dry density of all the treated composite materials increased with increase in clinker content as specific gravity of clinker is higher than that of fly ash and overburden.
2. The CBR values increased with increase in clinker content. It increased from 1.09% to 79.94% in soaked condition.
3. The composite with 62%FA, 30% O/B and 8% clinker exhibited maximum compressive strength of 1.4 MPa at 28 days curing as compared to other developed composites.
4. The unconfined compressive strength increased with increase in clinker content and curing period.
5. Similar trend like CBR and unconfined compressive strength was also observed for the Brazilian tensile strength ( 150 kPa with 62%FA, 30% O/B and 8%)
6. Fly ash mixed with 30% mine overburden and 8% clinker produced highest compressive strength (1.4 MPa), tensile strength (150 kPa) and CBR value (140%) as compared to that of other composites (82%FA+10%O/B+8%CL), (72%FA+20%O/B+8%CL), (52%FA+40%O/B+8%CL).
7. The ultrasonic pulse velocities varied in the range of 553 m/s to 1785 m/s for varying curing periods.
8. The composite containing 62% fly ash and 30% mine overburden treated with 8% clinker produced highest ultrasonic velocity (1785 m/s) as compared to that of other composites at 7, 14 and 28 days of curing respectively.

9. The P-wave velocity increased with increase in clinker content from 2% to % although the rate of increase varies.
10. The P-wave velocity changed marginally by varying fly ash percentage. Young's modulus values and Poisson's ratios also followed the same trend as the P-wave velocity.
11. The morphology of all the mixes showed the formation of hydrated gel at 28 days curing. The voids between the particles were filled by growing hydrates with curing time.
12. Microanalysis and compositional analysis confirmed the formation of cementitious compounds such as calcium silicate hydrate (CSH), calcium aluminate hydrate (CAH) and calcium aluminate silicate hydrate (CASH) which leads to increase in strength of the material over time.
13. The major chemical constituents are alumina, silica, iron oxide, calcium oxide in the composites. Very small or negligible percentages of Na, Mg, K, S and Ti, elements are found in the mixes.
14. The CaO content (25.3%), CaO/SiO<sub>2</sub> ratios (0.693) are highest in the composite containing 62% fly ash and 30% mine overburden treated with 8% clinker as compared to other composites which exhibited maximum strength.
15. Clinker content showed a significant effect on the strength development and pozzolanic reaction rate of natural pozzolans.
16. There exists strong relationship between CBR and CaO content, CBR and CaO/SiO<sub>2</sub> with R<sup>2</sup> =0.982 and 0.988 respectively.

### 6.3 Numerical Analysis

1. The strain at the surface course with conventional material is above the critical limit with fixed sub-base thickness (0.35m). Replacement with FCM did not give any significant improvement.

2. The maximum strain reduced drastically from 3614 micro-strain to 1094 micro-strain with 300 T when sub-base thickness changed from 0.35 to 1.5 m. All the composites exhibited less than the critical strain and stress values for 1.5m thick sub-base.
3. About 28 MT of fly ash can be used in 5 km long, 20 m wide and 5 m thick haul road for 200 opencast mines (Appendix, Page-154).
4. The developed FCM (62%FA+30%O/B+8%CL) has strong potential to be used as sub-base material.

## **6.4 Recommendation for future work**

The aim and objectives of the investigation were limited to laboratory investigation. It is recommended to investigate the following for a better understanding of the haul road economics.

1. Long term effects of FCM should be evaluated in actual field condition.
2. Effect of the FCM on ground water quality should be evaluated.

# Bibliography

- [1] Acosta H.A., Edil T.B and Benson C.H., *Soil stabilization and drying using fly ash*, *Geo Engineering Report No. 03-03*, *Geo Engineering Program, University of Wisconsin*, Madison, USA.2003.
- [2] Ahlvin R.G., Ulery H.H., Hutchinson R.L. and Rice J.L.,*Multiple wheel heavy gear load pavement tests*, Vol 1 Basic Report, USA Waterways Exp. Stn. Report, AFWL- TR-70-113, 1971.
- [3] Ahmaruzzaman M., *A review on the utilization of fly ash*, *Journal of Progress in Energy Combust. Sci.*, 36 (2010): pp. 327-363.
- [4] Anon, *Lime Stabilization Construction Manual*, 8th ed., National Lime Association, Arlington, Va, US, 1985.
- [5] Antiohos S. and Tsimas S., *Activation of fly ash cementitious systems in the presence of quick-lime Part I. Compressive strength and pozzolanic reaction rate*, *Journal of Cement and Concrete Research*, 34 (2004): pp. 769-779.
- [6] Arora S. and Aydilek A.H., *Class F fly-ash-amended soils as highway base materials*, *Journal of Materials in Civil Engg.* ASCE 17 (2005):pp. 640-649.
- [7] ASTM, *Specification for coal fly ash and raw or calcined natural pozzolan for use in concrete*. in: *Annual book of ASTM standards, concrete and aggregates*, American Society for Testing Materials, Philadelphia, vol. 04.02. C618-08, 2008.
- [8] Atkinson T., *Design and layout of haul roads*. SME Mining Engineering Handbook, 2nd ed., Society of Mining, Metallurgy, and Exploration, Inc. Littleton, Colorado, 1992.
- [9] Baghdadi Z.A., Fatani M.N. and Sabban N.A., *Soil modification by Cement kiln dust*, *Journal of Materials in Civil Engineering*, 7 (1995): pp. 218-222.
- [10] Baker M.D. and Laguros J.G., *Reaction products in fly ash concrete*, *Fly ash and coal conversion by-products: characterisation, utilisation and disposal*, G.J. MaCarthy, F.P. Glasser and D.M. Roy eds, Materials Research Society, Pittsburgh, 43 (1985): pp. 73-83.
- [11] Bakhoriij A.M.,*Laboratory measurements of static and dynamic elastic properties in carbonate*,*PhD Thesis university of alberta,Canada*,2010.
- [12] Baker W.R and Gonzalez C.R.,*Fundamental of the CBR Equation*,*TransPortation Systems workshop*, 2008, April 21-24, pp 1-12.

- 
- [13] Barstis W.F. and Crawley A.B., *The use of fly ash in highway construction U.S. 84/98 Adams County. FHWA Demonstration Project 59, Report No. 84-DP59-MS-05, Mississippi Department of Transportation Research Division, P O Box 1850, Jackson MS 39215- 1850, 2000.*
- [14] Behera B. and Mishra M.K., Strength behaviour of surface coal mine overburden fly ash mixes stabilised with quick lime, *International journal of surface mining, reclamation and environment*, 2011, pp. 1-17.
- [15] Berry E.E., Fly ash for use in concrete, *The Canadian center for mineral and energy technology, CANMET, 1985.*
- [16] Bowels J., *Engineering Properties of soil and their measurements*, 4th ed., Mc Graw- Hill, Boston, 1992.
- [17] Beeghly J.H., *Recent Experiences with lime fly ash stabilization of pavement subgrade soils, base and recycled asphalt, in: proc. of Int. Ash Utilization Symposium'03, Centre for Applied Energy Research, Univ. of Kentucky, 2003 Paper 46, pp. 1-18.*
- [18] BEML, Construction and mining equipment, Bharat Earth Movers Limited, India, 2011
- [19] Bergeson K.L. and Mahrt D., *Reclaimed fly ash as selected fills under PCC pavement, in: Proc. of Mid-content transportation symposium, Iowa State University , Ames, Iowa, 2000, pp. 147-150.*
- [20] Bottner C. U. The role of the space charge density in particulate processes in the example of the electrostatic precipitator. *Powder Technology*, 2003, pp. 285-294.
- [21] Bowles J.E., *Physical and Geotechnical Properties of Soils, 2nd ed., McGraw-Hill Book Company , New York, USA, 1984.*
- [22] Brennan M.J. and O'Flaherty C.A., *Highways the location, design, construction and maintenance of road pavements, 4th ed., Elsevier publication, 2001.*
- [23] Butalia S.T., *Rehabilitating asphalt highways: coal fly ash used on Ohio full depth reclamation projects, Case Study-18, Coal Combustion Product Partnership, Environmental Protection Agency, USA, 2007, pp. 1-4.*
- [24] Canter, L.W. and Knox, R.C., *Ground water pollution control, Lewis Publishers, Inc., Chelsea, Mich., 1985.*
- [25] Capco, *Pulverized fuel ash as reclamation fill, Report of the China Light and Power Co. Ltd., Hong Kong, 1990, pp.1-34.*
- [26] Caterpillar, *Caterpillar Performance Handbook. 40th ed., Caterpillar Inc., Peoria, Illinois, USA, 2010.*
- [27] Cetin B., Aydilek A.H. and Guney Y., *Stabilization of recycled base materials with high carbon fly ash, Journal of Resources, Conser. Recycl., 54 (2010): pp. 878-892.*

- [28] Chaulya S.K., Singh R.S., Chakraborty M.K. and Tewary B.K., *Bioreclamation of coal mine overburden dumps in India*, *Journal of Land Contamination and Reclamation*, 8 (2000): pp. 189-199.
- [29] Chironis N.P, *How to build better haul roads*, *Journal of Coal Age*, 11 (1978): pp. 122-128.
- [30] Chu T.Y., Davidson D.T., Goecker W.L. and Moh Z.C., *Soil stabilization with lime-fly ash mixtures: preliminary studies with silty and clayey soils*. *Highway Research Board Bulletin* , 108 (1955): pp. 102 - 112.
- [31] Chugh Y.P. and Mohanty S., *A field demonstration of an unstabilised F-Fly ash-based road subbase*, *Proceedings on Fly ash India 2005, Fly ash Utilisation Programme* , TIFAC, DST, New Delhi, 2005,pp. VIII 3.1-3.16.
- [32] Cicek T. and Tanrıverdi M., *Lime based steam autoclaved fly ash bricks*. *Journal of Constr. and Building Mater*, 21(2007): pp. 1295-1300.
- [33] CMPDIL HQ, *Technical manual on Guidelines for planning, design and construction of haul road*, *Central Mine Planning and Design Institute Limited, Ranchi, India*. 2000.
- [34] Collins J.L., Fytas K. and Singhal R., *Design, construction and maintenance of surface mine haul roads*, in: *Proc. of the Symposium on Geotechnical stability in Surface Mines, Calgary, Canada*, 1986, pp. 39-49.
- [35] Consoli N.C., Prietto P.D.M., Carraro J.A.H. and Heineck K.S., *Behavior of compacted soil-fly ash-carbide lime mixtures*, *Journal of Geotechnical and Geoenvironmental Engineering*, 127, (2001): pp. 774-782.
- [36] Croft J.B., *The pozzolanic reactivities of some New South Wales fly ashes and their application to soil stabilization*. *Australian Road Research Board, Vermont South* , Victoria, 2 (1964): pp. 1144-1168.
- [37] Das B., *Principles of Geotechnical Engineering, 3rd ed.*, PWS- Kent Publishing Company, Boston, 1994.
- [38] Das S.C. and Prakash S., *Behaviour of lime stabilized Titagarh PFA through laboratory tests*, *IE (I). Journal of civil*, 70 (1990): pp. 181-186.
- [39] Das S.K. and Yudhbir, *Geotechnical properties of low calcium and high calcium fly ash*, *Journal of Geotechnical and Geological Engineering*, 24 (2006): pp. 249-263.
- [40] Davis R.E., *A review of pozzolanic materials and their use in cement concrete*, *Special Technical Publication*, ASTM, 99 (1949): pp. 3-15.
- [41] Dermatas D. and Meng X., *Utilization of fly ash for stabilization/solidification of heavy metal contaminated soils*, *Journal of Engineering Geology*, 70 (2003): pp. 377-394.



- [42] De Santayana F.P. and Mazo C.O., *Behaviour of fly ash in experimental embankments*, in: *Proc. of Thirteenth Int. Conference on Soil Mechanics and Foundation Engineering, New Delhi*, 1994, pp. 1603-1606.
- [43] Desai C.S. and Abel J.F., *Introduction to the Finite Element Method, A numerical method for Engineering Analysis, 1st India ed., S.K. Jain for CBS publisher*, 1987.
- [44] DiGioia A.M., McLaren R.J., Burns D.L. and Miller D.E., *Fly ash design manual for road and site application*, vol. 1: Dry or conditioned placement, Manual prepared for EPRI, CS-4419, Research project 2422-2, Interim report, Electric Power Research Institute, Palo Alto, California, 1986.
- [45] Dimter S., Rukavina T. And Barisic I., *Application of the ultrasonic method in evaluation of properties of stabilized mixes*, *The Baltic Journal of Road and Bridge Engg.*, 6(2011): pp. 177-184.
- [46] Duncan J.M., Monismith C.L. and Wilson E.C., *Finite element analysis of pavements*, *Highway Research Board, Highway Research Record 228* (1968): pp. 18-33.
- [47] Edil T.B., Benson C.H., Bin-Shafique Md S., Tanyu B.F., Kim W.H. and Senol A., *Field evaluation of construction alternatives for roadway over soft subgrade*, *Transportation Research Board, 81th Annual Meeting, Washington, D.C.*, 02-3808, 2002.
- [48] Edil, T.B., Sandstrom L. K. and Berthouex, P.M., (1990). *Interaction of inorganic leachate with compacted pozzolanic fly ash*, *Journal of Geotechnical Engg.*, ASCE, 118(1992):pp.1410-1430.
- [49] Erol M., Genc A., Ovecoglu M.L., Yucelen E., Kucukbayrak S. and Taptik Y., *Characterization of a glass-ceramic produced from thermal power plant fly ashes*, *Journal of European Ceramic Society*, 20 (2000): pp. 2209- 2214.
- [50] Faluyi S.O. and Amu O.O., *Effects of Lime Stabilization on the pH Values of Lateritic Soils in Ado-Ekiti, Nigeria*, *Journal of Applied Sci.*, 5 (2005): pp. 192-194.
- [51] Foster C.R. and Ahlvin R.G., *Stress and deflections induced by a uniform non-circular load*, in: *Proc. of Highway Research Board*, Vol 33, Washington, DC, USA, 1954.
- [52] Fung R., *Surface mine haul road design. Surface mine engineering technology; engineering and environment aspects*, *Noyes Data corp.*, USA, 1981.
- [53] Galaa A.M., Thompson B.D., Grabinsky M.W. and Bawden W.F., *Characterizing stiffness development in hydrating mine backfill using ultrasonic wave measurements*, *Canadian geotechnical journal*, 2011.
- [54] Galdwin M.T., *Ultrasonic stress monitoring in underground mining*, *International Journal of rock mechanics and mining sciences*, 1982, Vol.19, pp. 221-228
- [55] Gatti G. and Tripiciano L., *Mechanical behaviour of coal fly ashes*, in: *Proc. of 10th International conference on Soil mechanics and foundation engineering, Stockholm*, 2 (1981): pp. 317-322.

- 
- [56] Ghosh A. and Dey U., *Bearing ratio of reinforced fly ash overlying soft soil and deformation modulus of fly ash*, *Journal of Geotextiles and Geomembranes*, 27 (2009): pp. 313-320.
- [57] Ghosh A. and Subbarao C., *Tensile Strength Bearing Ratio and Slake Durability of Class F Fly Ash Stabilized with Lime and Gypsum*, *Journal of Materials in Civil Engg.*, 18 (2006): pp. 18-27.
- [58] Ghosh A. and Subbarao C., *Hydraulic conductivity and leachate characteristics of stabilized fly ash*, *Journal of Environmental Engg.*, ASCE, 124(1998): pp. 812-820.
- [59] Ghosh A. and Subbarao C., *Microstructural development in fly ash modified with lime and gypsum*, *Journal of Mater, in Civil Eng*, 13 (2001): pp. 65-70.
- [60] Ghosh A., *Environmental and engineering characteristics of stabilized low lime fly ash*, Ph.D thesis, Indian Institute of Technology, Kharagpur, India, 1996.
- [61] Gidley J.S. and Sack W.A., *Environmental aspects of waste utilization in construction*, *Journal of Environmental Engg.*, ASCE, 110 (1984): pp. 1117-1133.
- [62] Goh A.T.C. and Tay J. H., *Municipal solid-waste incinerator fly ash for geotechnical applications*, *Journal of Geotechnical Engg.*, ASCE, 199 (1993): pp.811-825
- [63] Good Year, Good Year (PTY) Ltd., *Kriel Colliery tyre load analysis*, *Kriel Colliery internal report*, Kriel, USA, 1990.
- [64] Goswami R.K. and Mahanta C., *Leaching characteristics of residual lateritic soils stabilised with fly ash and lime for geotechnical applications*, *Journal of Waste Management*, 27 (2007): pp. 466-481.
- [65] Gray D.H. and Lin Y.K., *Engineering properties of compacted fly ash*, *Journal of Soil Mech. Foundation Engng .*, ASCE, 98 (1972): pp. 361-380.
- [66] Green R.E., *Introduction to ultrasonic testing*. *American society of non-destructive testing*, 1991, pp.1-21.
- [67] Hanne O., Timo N., Hannu K. *Increase the utilisation of fly ash with electrostatic precipitation*, *Minerals Engineering*, 19, 2006, pp. 1596-1602.
- [68] Heath W. and Robinson R., *Review of published research into the formation of corrugations on unpaved roads*. Transport and road research laboratory (TRRL) Supp report 620, Department of the Environment, Dept of Transport, Crowthorne, UK, 1980.
- [69] Hobeda P., *Use of Waste Material from Coal Combustion in Road Construction*, NTIS, 1984, Temimi M., Camps J.P. and Laquerbe M., *Valorization of fly ash in the cold stabilization of clay materials*, *Journal of Resources, Conservation and Recycling*, 15 (1995): pp. 219-234.
- [70] Hopkins T.C., Beckham T.L., Sun C. and Ni B., *Resilient Modulus of Kentucky Soils. Research Report*, *Kentucky Transportation Centre, University of Kentucky*, 2001.

- 
- [71] Huang, W.H. and Lovell C.W., *Bottom ash as embankment material, Geotechnics of waste fills - theory and practice*, ASTM STP1070, A. Landva and G. D. Knowles, eds. American Society for Testing and Materials, Philadelphia, pp. 71 - 85.
- [72] Husrulid W. and Kuchta M., *Openpit mine planning and design: Vol-I Fundamentals*, 2nd ed., Taylor and Francis Plc., London, UK, 2006.
- [73] Indraratna B., Nutalaya P., Koo K.S. and Kuganenthira N., *Engineering behaviour of a low carbon, pozzolanic fly ash and its potential as a construction fill*, Can. Geotech. Journal of, 28 (1991): pp. 542-555.
- [74] Ismaiel H.A.H., *Treatment and improvement of the geotechnical properties of different soft fine-grained soils using chemical stabilization*, Ph.D thesis, Martin Luther University Halle, Wittenberg, 2006.
- [75] Jackson N.M. Schultz S. Sander P. and Schopp L., *Beneficial use of CFB ash in pavement construction applications*, Journal of Fuel 88 (2009): pp. 1210-1215.
- [76] Jadhao P.D. and Nagarnaik P.B., *Strength Characteristics of Soil Fly Ash Mixtures Reinforced with Randomly Oriented Polypropylene Fibers*, in: *proc. of First International Conference on Emerging Trends in Engineering and Technology*, IEEE, DOI 10.1109/ICETET.2008.208, 2008 pp. 1044-1049.
- [77] Jha N.C., *Mining Industry and the people around*, *Transactions of the mining geological and metallurgical institute of India*, ISSN: 0371-9538, 107 (2011): pp. 1-11.
- [78] Jones R., *The Nondestructive Testing of Concrete*, *Magazine of Concrete Research* 1(2), 1949.
- [79] Joshi R.C., Duncan D.M. and Master Mc H.M., *New and conventional engineering uses of fly ash*, *Journal of Transportation Engg.*, ASCE, 101 (1975): pp. 791-806.
- [80] Kaliske M., Freitag S. and Oeser M., *Tire-Pavement Contact Modeling*, in: *Proc. of the Symposium of Advances in Contact Mechanics (Prof. J.J. Kalker)*, Delft, Netherlands, 2008: pp. 22-24.
- [81] Kaniraj S.R. and Havanagi V.G., *Compressive strength of cement stabilized fly ash-soil mixtures*, *Journal of Cement and Concrete Composites*, 29 (1999): pp. 673-677.
- [82] Karpuz C. and Pasamehmetoglu A.G., *Field Characterization of weathered ankara andesites*, *Engineering geology*, 1997, Vol.46, No.1, pp. 1-17.
- [83] Kasaibati K., Burczyk J.M. and Whelan M.N., *Effects of selecting subgrade resilient modulus on asphalt overlay design thicknesses*, *Transportation Research Record TRB No. 1473*, Transportation Research Board National Research Council, Washington D.C., 1995.
- [84] Knapton J., *The Structural design of heavy duty pavements for ports and other industries*, *British ports federation, london, England*, 1988.

- 
- [85] Kaufman W.W. and Ault J.C., *Design of surface mine haulage roads - A manual*. Information circular 8758, U.S. Department of Interior, Bureau of Mines, 1977.
- [86] Kettil P., Lenhof B., Runesson K. and Wiberg N.E., *Simulation of inelastic deformation in road structures due to cyclic mechanical and thermal loads*, *Journal of Computers and Structures*, 85 (2007): pp. 59-70.
- [87] Kewalramani M.A. and Gupta R., *Concrete compressive strength prediction using ultrasonic pulse velocity through artificial neural networks*, *Journal of Automation in Construction*, 15 (2006): pp. 374-379.
- [88] Khanna K. and Justo C.E.G., *Highway Engineering*, 8th ed., Khanna Publishers, Roorkee, 2001.
- [89] Kim S. H., Lee K. W. Experimental study of electrostatic precipitator performance and comparison with existing theoretical prediction models, *Journal of Electrostatics* 48, 1999, pp.3-25.
- [90] Koukouzas N. Mineralogical and elemental composition of fly ash from pilot scale fluidised bed combustion of lignite, bituminous coal, wood chips and their blends, *Fuel* 86 ,2007, pp. 2186-2193
- [91] Krishna K.C., *CBR behaviour of fly ash-soil-cement mixes*, *Ph.D thesis, Indian Institute of Science*, Bangalore, India, 2001.
- [92] Kumar M.A. and Raju G.V.R.P., *Use of lime cement stabilized pavement construction*, *Indian Journal of Eng. and Materials Sc.*, 16 (2009): pp. 269-276.
- [93] Kumar S. and Patil C.B., *Estimation of resource savings due to fly ash utilization in road construction*, *Journal of Resources, Conservation and Recycling*, 48 (2006): pp. 125-140.
- [94] Kumar V., *Design and construction of haul roads using fly ash*, *M.S thesis, University of Alberta*, Canada, 2000.
- [95] Kumar V., *A comprehensive model for fly ash handling and transportation for mining sector*, in: *Proc. of Fly ash an opportunity for Mining Sector*, New Delhi, India, 2010.
- [96] Laguros J.G. and Zenieris P., *Feasibility of using Fly ash as a binder in coarse and fine aggregate for bases*. *University of Oklahoma, Norman, Oklahoma*. Report No. ORA, 1987, pp. 155- 404.
- [97] Lav A.H. and Lav M.A., *Microstructural development of stabilized fly ash pavement base material*. *Journal of Mater. in Civil Eng*, 12 (2000): pp. 157-163.
- [98] Lav A.H., Lav M.A. and Goktpe A.B., *Analysis and design of a stabilized fly ash as pavement base material*, *Journal of Fuel*, 85 (2006): pp. 2359-2370.
- [99] Leonards G.A. and Bailey B., *Pulverized coal ash as structural fill*, *Journal of Geotech. Engg Div.*, ASCE, 108 (1982): pp. 517-531.
- [100] Leslie R. and Cheesmam W., *An Ultrasonic Method of studying Deterioration and Cracking in Concrete Structures*, *Journal of American Concrete Institute* (1949).

- [101] Liu G., Petrological and mineralogical characterizations and chemical composition of coal ashes from power plants in Yanzhou mining district, china, *Fuel processing Technology* 85,2004, pp. 1635-1646.
- [102] Lockner D., The role of acoustic emission in the study of rock fracture, *international journal of rock mechanics, mining science and geomechanics*,1993,Vol.30, No.7, pp. 873-899.
- [103] Ma J., Chugh Y.P. and Deb D., Finite element analysis of the effect of sandstone channel in the roof on the stability of a longwall face, *SME annual meeting USA*, 2001.
- [104] Mackos R., Butalia T., Wolfe W. and Walker H.W., *Use of lime-activated class F fly ash in the full depth reclamation of asphalt pavements: environmental aspects*, in: Proc. of World of Coal Ash Conference '09, Lexington, Kentucky, USA, paper no 121.
- [105] Madenga V., Zou D.H. and Zhang C., Effects of curing time and frequency on ultrasonic wave velocity in grouted rock bolts, *Ultrasonics* ,Vol.49, Issue:2.2009. pp.162-171.
- [106] Malhotra V.M., *Fly ash in concrete. 2nd ed., Ottawa, Canada, CANMET Publication on Concrete*, 1994.
- [107] Malhotra V., *Testing Hardened Concrete: Nondestructive Methods, 1st ed., Iowa State University Press*, 1976 .
- [108] Malhotra V.M. and Carino N.J., *CRC Handbook on non-destructive testing of concrete*, CRC press, 1991, *Florida USA* .
- [109] Marshek D.B., *The selection of gravels for use on unsealed access roads*, in: *Proc. of Australian IMM conference on off- highway truck haulage, Mt Newman, Australia*, 1982: pp. 23-31.
- [110] Mc Carthy D.F., *Essentials of soil mechanics and foundations-Basic geotechnics*, 2007, pp. 315.
- [111] McLaren R.J. and DiGioia A.M., *The typical engineering properties of fly ash*, in: *Proc. of conf. on geotechnical practice for waste disposal: Geotechnical special publication No. 13, ASCE, Wood. R.D. (ed.), New York, 1978, pp. 683-697.*
- [112] Metcalfe R.D., Connor J.N., Druskovich D., Blackford M.G. and Short K., The influence of fly ash morphology and phase distribution on collection in an electrostatic precipitator *Australian institute of physics 17th National Congress* 2006, December 3-8, pp no. WC0083.
- [113] Meyers J.F., Pichumani R. and Kapples B.S., *Fly ash as a construction material for Highways*, Report No. FHWA-FP-76-16, US Department of Transportation, Washington D.C. USA, 1976.
- [114] Michelin, *Michelin Truck Tire Service Manual*, Michelin North America, Inc., Greenville, South Carolina, USA, 2005.
- [115] Mingkai Z., Weiguo S., Shaopeng W. and Qinglin Z., *Study on phosphogypsum fly ash lime solidified material*, *Journal of advances in building technology*, 1 (2002): pp. 929-934.

- 
- [116] Mining officials, *Personal Communication, Bharatpur opencast project, Mahanadi Coalfields Limited*, 2008.
- [117] Ministry of Coal, *The Export Committee Report part II on Road Map for Coal Sector Reforms, Govt. of India*, New Delhi, 2007.
- [118] Minnick L.J., *Fundamental characteristics of pulverized coal fly ashes*, in: Proc. of ASTM, 59 (1959): pp. 1155-1177.
- [119] Mishra M.K., *Experimental and Numerical analysis of behaviour of model pillars trapped with reinforced fly ash composites*, Ph.D thesis, Indian Institute of Technology, Kharagpur, India, 2003.
- [120] Mishra S.R., Kumar S., Park A., Rho J., Losby J. and Hoffmeister B.K., *Ultrasonic characterization of the curing process of PCC fly ash*, *Journal of Materials Characterization*, 50 (2003): pp. 317-323.
- [121] Mishra M.K. and Rao K.U.M., *Geotechnical Characterisation of Fly ash Composites for Back-filling Mine Voids*. *Journal of Geotech and Geol Eng*, 24 (2006): pp. 1749-1765.
- [122] Misra A., *Cold-in-place recycling of asphalt pavements using self-cementing fly ash: analysis of pavement performance and structure number*, Final Report for Combustion By-products recycling Consortium, West Virginia University, Virginia, 2008.
- [123] MOEF, Gazette notification for Ministry of Environment and Forests. no. 563, Ministry of Environment and Forests, New Delhi, India 1999.
- [124] Mohammad L.N., Titi H.H. and Herath A., *Intrusion technology: An innovative approach to evaluate resilient modulus of subgrade soils Application of Geotechnical Principles in Pavement engineering*, American Society of Civil Engineers, Geotechnical Special Publication Number, 85 (1998): pp. 39-58.
- [125] Mohanty S. and Chugh Y.P., *Structural Performance Monitoring of an unstabilised Fly ash based road subbase*, *Journal of Transportation Engineering*, 132 (2006): pp. 964-969.
- [126] Morgan J.R., Tucker J.S. and McInnes D.B., *A mechanistic design approach for unsealed mine haul roads*, *Pavement Design and Performance in Road Construction 1412* (1994): pp. 69-81.
- [127] Moulder E., *A mixture of fly ashes as road base construction material*, *Journal of Waste Management*, 16 (1996): pp. 15-20.
- [128] Moulton K.L., *Technology and utilization of power plant ash in structural fills and embankments*, *West Virginia University*, Morgantown W.V., 1978.
- [129] Mukharjee A.K. Green col from opencast col mine-A Concept *Indian Mineral industry journal*, 2012, May 11, pp.91-96.
- [130] Murthy V.N.S., *Soil mechanics and foundation engineering*, 2009, Chapter 10, pp. 244.

- 
- [131] Nahi M.H., Ismail A. and Ariffin A.K., *Analysis of Asphalt Pavement under nonuniform Tire-pavement Contact Stress using Finite Element Method*, *Journal of Applied Sciences*, 11 (2011): pp. 2562-2569.
- [132] Naik T.R. and Singh S.S., Fly ash generation and utilization-an overview, *Recent trends in fly ash utilization, society of forest and environmental managers India*, 1993, March, pp.1-25.
- [133] Navarrete B., Canadas L., Cortes V., Salvador L., Galindo J. Influence of plate spacing and ash resistivity on the efficiency of electrostatic precipitators. *Journal of Electrostatics*, 39,1997. 65-81.
- [134] Nicholson P., Kashyap V. and Fugli C., *Lime and fly ash admixture improvement of tropical Hawaiian soils*, *Transportation Research Record*, Washington, DC, Report No 1440, 1994.
- [135] O'flaherty C.A., *Highways The location, design, constructin and maintenance of pavements*, Chapter 9, pp.239.
- [136] Openshaw S.C., Utilization of coal fly ash, *Florida center for solid and hazardous waste managment,SUS*, Florida, 1992.
- [137] Ottosen N.S., Evaluation of concrete cylinder tests using finite element,*Journal of engineering mechanics ASCE*,1984, Vol. 110, No.3, pp. 465-481.
- [138] Pandian N. S., Rajasekhar C. and Sridharan A.,(1995). *Fly ash-lime systems for the retention of lead ions*, in: *Proc. of Indian Geotechnical conference, Bangalore*, 1 (1995): pp.219-222.
- [139] Pandian N.S., *Fly ash characterization with reference to geotechnical applications*, *Journal of Indian Inst. of Sc.*, 84 (2004): pp. 189-216.
- [140] Pandian N.S. and Balasubramonian S., *Leaching studies on ASTM type F fly ashes by an accelerated process method*, *Journal of Testing Evaluation*, ASTM, 28 (2000): pp. 44-51.
- [141] Pandian N.S., Rajasekhar C. and Sridharan A., *Studies on the specific gravity of some Indian coal ashes*, *Journal of Testing and Evaluation*, ASTM, 26 (1998): pp. 177-186.
- [142] Pandian N.S., Sridharan A. and Srinivas S.,*Angle of internal friction for pond ashes*, *Journal of Testing and Evaluation*, ASTM, 28 (2000): pp. 443-454.
- [143] Parker K. R. *Applied electrostatic precipitation*. Blackie Academic and Professional, London, (UK),1997.
- [144] Pati M. Mahadevan M.R. and Bera J., Fly ash a case study of solid waste management,*Environmental issues and waste management in mining and allied industries*,2001, Feb 23-24, pp. 90-95.
- [145] Ping V.W., *Implementation of the Resilient Modulus in the State of Florida Flexible Pavement Design Procedure*, 2001.

- 
- [146] Poran C. J. and Ahtchi-Ali, F. *Properties of solid waste incineration fly ash*, *Journal of Geotech. Engg.*, ASCE, 115 (1998): pp. 1119-1133.
- [147] Porter O.J., *The preparation of sub-grades. in: Proc. of the Highway Research Board, Washington*, 18 (1938): pp. 324-33 1.
- [148] Porter O.J. *Development of the original method for highway design, in: Proc. of the American Society of Civil Engineers*, 75 (1949): pp. 11-17.
- [149] Prabakar J., Dendorkar N. and Morchhale R.K., *Influence of fly ash on strength behavior of typical soils*, *Journal of Construction and Building Materials*, 18 (2004): pp.263-267.
- [150] Queralt I., Querol X., Lopez-Soler A. and Plana F., *Use of coal fly ash for ceramics: a case study for a large Spanish power station*, *Journal of Fuel*, 76 (1997): pp. 787-791.
- [151] Rahim A.M. and George K.P., *Automated Dynamic Cone Penetrometer for Subgrade Resilient Modulus Characterization. Transportation Research Record No 1806, Transportation Research Board, National Research Council*, 2002, pp. 70-77.
- [152] Rai A.K., Paul B. and Singh G., *A study on physico chemical properties of overburden dump materials from selected coal mining areas of Jharia coalfields, Jharkhand, India, Int. Journal of Environmental Sc.*, 1 (2011): pp. 1350-1360.
- [153] Ravina D. Mechanical properties of structural concrete incorporating a high volume of class F fly ash as partial fine sand replacement, *Materials and structures*,1998, Vol.31, pp. 84-90.
- [154] Reddy B.V.V, and Gourav K., Strength of lime-fly ash compacts using different curing techniques and gypsum additive,*journal of materials and structures*,2011, pp.1793-1808.
- [155] Rehsi S.S. and Garg S.K., *Characteristics of Indian fly ashes, in: Proc. of National workshop on utilization of fly ash, Roorkee*, 1988: pp. 131-135.
- [156] Roode M.V., *X-ray diffraction measurement of glass content in fly ashes and slag*, *Journal of Concr. Res.*, 17 (1987): pp. 183-197.
- [157] Rotaru A. and Boboc V. Physical properties of pozzolana fly ash from thermal power plant of Iasi, Romania, *International conference on Risk management, assessment and mitigation*, pp. 187-192
- [158] Sahay A.N., *R and D initiatives in utilization of fly ash in coal sector, in: Proc. of Fly ash an opportunity for Mining Sector, New Delhi, India*, 2010.
- [159] Sahoo J.P. and Pradhan P.K., Effect of lime stabilized soil cushion on strength behaviour of expansive soil,*international journal of geotechnicl and geological engineering*,2010, pp. 889-897
- [160] Sahu B.K., *Improvement in California Bearing Ratio of Various Soils in Botswana by Fly Ash, in: Proc. of Int. Ash Utilization Symposium, Centre for Applied Energy Research, University of Kentucky*, Paper No. 90, 2001.



- [161] Sahu B.K, *Use of fly ash for stabilizing sub-standard road construction materials in Botswana*, in: *Proc. of Fly ash India 2005, Fly ash Utilisation Programme, TIFAC, DST, New Delhi*, 2005, pp. VIII 10.1-10.9.
- [162] Sarkar A.,Rano R., Udaybhanu G. and Basu A.K., A Comprehensive characterization of fly ash from a thermal power plant in Eastern India,*Fuel processing technology*, 2006, vol.87 issue:3, pp 259-277.
- [163] Sen Gupta J., *Characterization of Indian coal ash and its utilization as building material*, in: *Proc. Int. Conf. on Environmental Impact of Coal Utilization from Raw Materials to Waste Resources (K. C. Sahu, ed.)*, Indian Institute of Technology, Bombay, 1991: pp.165-184.
- [164] Senapati M., R., *Fly ash from thermal power plants - waste management and overview*, Current Science,2011, June 25, Vol. 100, No. 12,.
- [165] Senol A., Edil T.B, Bin-Shafique M.S., Acosta H.A and Benson C.H., *Soft Subgrades' stabilization by using various fly ashes*, *Journal of Resources, Conservation and Recycling*, 46 (2006): pp. 365-376.
- [166] Manjrekar V.D., Choudhary V.N. and Gautam K.V.V.S., Geology and mineral resources of orissa, *Society of geoscientists and allied technologists*, 2009, pp.210.
- [167] Shanthakumar S.,Singh D. N., Phadke R.C., Characterization of Fly Ash from Various Locations of Electrostatic Precipitator,*The 12th International Conference of International Association for Computer Methods and Advances in Geomechanics(IACMAG)*,2008, October 1-6, pp. 2261-2268
- [168] Shen W., Zhou M. and Zhao Q., *Study on lime-fly ash-phosphogypsum binder*, *Journal of Construction and Building Materials*, 21 (2007): pp. 1480-1485.
- [169] Shen W., Zhou M., Ma W., Hu J. and Cai Zhi., *Investigation on the application of steel slag-fly ash-phosphogypsum solidified material as road base material*, *Journal of Hazardous Materials*, 164 (2009): pp. 99-104.
- [170] Shenbaga R.K. and Gayathri V., *Permeability and consolidation characteristics of compacted fly ash*, *Journal of Energy Engineering*, 130 (2004): pp. 18-43.
- [171] Sherwood P.T. and Ryley M.D., *Use of stabilized pulverized fuel ash in road construction*, *Road Research Laboratory Report, Ministry of Transport*, UK, 49 (1966): pp. 1-44.
- [172] Siddharthan R., Norris G.M. and Epps J.A.,*Use of FWD data for pavement material characterization and performance*, *Journal of Transport Engg.*, ASCE, 117 (1991): pp.660-678.
- [173] Siddique R. Coal fly ash in waste materials and by-products in concrete,*Springer Berline*,2007, Chapter 6, pp. 177-234
- [174] Singh D.N., *Influence of chemical constituents of fly ash characteristics*, in: *Proc. of Indian Geotechnical Conference, Madras*, 1996, pp. 227-230.

- 
- [175] Singh R.N. and Ghosh A.K., *Engineering Rock Structure in Mining and Civil Construction*, ISBN 0415 400139, Taylor and Francis Group Plc., London, UK, 2006.
- [176] Singh D.N. and Kolay P.K., *Simulation of ash-water interaction and its influence on ash characteristics*, *Progress in Energy and Combustion Science*, 28 (2002): pp. 267-299.
- [177] Singh S.P and Kumar P., *Utilisation of fibre reinforced fly ash in road sub-bases*, in: *Proc. on Fly ash India 2005, Fly ash Utilisation Programme*, TIFAC, DST, New Delhi, 2005, pp. VIII 17.1-17.8.
- [178] Siswosoebrotho B.I., Younger J.S. and Erwanto T., *Compaction and CBR strength characteristics of Karimun Island granite mixed with Suralaya pulverized fuel ash*, in: *Proc. of the Eastern Asia Society for Transportation Studies*, 4 (2003): pp. 302-312.
- [179] Sivapullaiah P.V., Prashanth J.P. and Sridharan A., *Optimization of lime content for fly ash*, *Journal of Testing and Evalu.*, 23 (1995): pp. 222-227.
- [180] Sobhan K. and Mashnad M., *Tensile Strength and Toughness of Soil-Cement-Fly-Ash Composite Reinforced with Recycled High-Density Polyethylene Strips*, *Journal of Materials in Civil Engineering*, ASCE, 14 (2002): pp. 177-184.
- [181] Soliman N.N., *Laboratory testing of lime fixed fly ash and FGD sludge. Geotechnics of Waste Fills - Theory and Practices*, ASTM STP 1070, Philadelphia, American Society for Testing and Materials, 1990.
- [182] Solis-Carcano R. and Moreno E. I., *Evaluation of concrete made with crushed limestone Aggregate Based on Ultrasonic Velocity*, *Journal of Construction and Building Materials* 22 (2008): pp. 1225-1231.
- [183] Sridharan A. and Prakash K., *Geotechnical Engineering Characterization of Coal Ashes*, 1st ed., S.K. Jain for CBS Publishers, New Delhi, 2007.
- [184] Sridharan A., Pandian N.S. and Chitti Babu G., *Strength behaviour of Indian coal ashes, Technical report of task force on Characterisation of fly ash submitted to Technology Mission-Fly ash disposal and utilization, Dept. of Science and Technology, Govt. of India*, vol. 4, 2001a.
- [185] Sridharan A., Pandian N.S. and Srinivas S., *Compaction behaviour of Indian coal ashes, Technical report of task force on Characterisation of fly ash submitted to Technology Mission-Fly ash disposal and utilization, Dept. of Science and Technology, Govt. of India*, vol.3, 2001b.
- [186] Sridharan A., Pandian N.S. and Srinivas S., *CBR behaviour of Indian coal ashes, Technical report of task force on Characterisation of fly ash submitted to Technology Mission-Fly ash disposal and utilization, Dept. of Science and Technology, Govt. of India*, Vol. 5, 2001c.
- [187] Sridharan A., Pandian N.S. and Srinivas S., *Compaction behaviour of Indian coal ashes, Ground Improvement, London*, 4 (2000): pp. 1-10.
- [188] Sridharan A., Rajasekhar C. and Pandian N.S., *Fly ash as pre-filter material for zinc ions*, in: *Proc. of Indian Geotechnical conference, Warangal 1994*, pp.79- 82.

- 
- [189] Sridharan A., Pandian N.S. and Prasad P.S., *Liquid Limit Determination of Class F Coal Ash*, *Journal of Testing and Evaluation*, ASTM, 28 (2000): pp. 455-461.
- [190] Stankus J.C. and Gou S., *Computer Automated Finite Element Analysis - A powerful tool for Fast Mine Design and Ground Control Problem Diagnosis and Solving*, www.jenmar.com, 2001, pp.1-12
- [191] Tannant D.D. and Regensburg B., *Guidelines for mine haul road design. 1st ed.*, University of Alberta, Canada, 2001.
- [192] Tannant D.D. and Kumar V., *Properties of fly ash stabilized haul road construction Materials*, *Int. Journal of Surface. Mining, Reclamation Environ.*, 14 (2000): pp. 121-135.
- [193] Temimi M., Rahal M.A., Yahiaoui M. and Jauberthie R., *Recycling of fly ash in the consolidation of clay soils*, *Journal of Resources, Conservation and Recycling*, 24 (1998): pp. 1-6.
- [194] Thompson R.J. and Visser A.T., *Mine haul road maintenance management systems*, *Journal of The South African Institute of Mining and Metallurgy*, ISSN 0038-223X/3.00 + 0.00, 2003, pp. 303-312.
- [195] Thompson R.J. and Visser A.T., *An overview of the structural design of mine haul roads*, *Journal of the South African Institute of Mining and Metallurgy*, SA ISSN 0038-223X/3.00+0.00, 1996, pp. 29-37.
- [196] Thompson R.J., *The Design and Management of Surface Mine Haul Roads*, *Ph.D. thesis*, Faculty of Engineering, University of Pretoria, 1996.
- [197] Thompson R.J. and Visser A.T., *A mechanistic structural design procedure for surface mine haul roads*. *International Journal of Surface Mining, Reclamation and Environment* 11 (1997): pp.121-128.
- [198] Throne D.J. and Watt J.D., *Composition and pozzolanic properties of pulverized fuel ashes*, II. Pozzolanic properties of fly ashes as determined by crushing strength tests on lime mortars, *Journal of Appl. Chem.*, 15 (1965): pp. 595-604.
- [199] Tishmack J.K., *Bulk chemical and mineral characteristics of coal combustion by-products, coal combustion by-products*, SIUC, Carbondale, 1996, October 29-31.
- [200] Toth P.S., Chan H.T. and Cragg C.B., *Coal ash as structural fill with special reference to Ontario experience*, *Can. Geotech. Journal*, 25 (1988): pp. 694-704
- [201] Trivedi A. and Sud V.K. Collapse behaviour of coal ash *Journal of geotechnical and environmental engineering ASCE*, 2004, Vol.130, No.4, pp.403-415.
- [202] Turgut P., *Masonry composite material made of limestone powder and fly ash*, *Journal of Powder Technology*, 204 (2010): pp. 42-47.
- [203] Turnbull W.J. and Ahlvin R.G., *Mathematical expression of the CBR relationships*, in: Proc. of 4th Int. Conf. on Soil Mech. and Foundation Engg., London, UK, 2 (1957): pp. 178.

- [204] Ulusay R., Arlkan F., Yoleri M.F. and Caglan D., *Engineering geological characterization of coal mine waste material and an evaluation in the context of back-analysis of spoil pile instabilities in a strip mine*, SW Turkey, *Journal of Engineering Geology*, 40 (1995): pp. 77-101.
- [205] Vary A., Material property characterization, *American society of non-destructive testing*, 1991, pp. 383-431
- [206] US EPA, *Solid Waste Leaching Procedure Manual*. Cincinnati, OH. SW-924, US Environmental Protection Agency, 1985.
- [207] Vasconles G., Lourenco P.B., Alves C.A.S. and Pamplona J., Ultrasonic evaluation of physical and mechanical properties of granites *Ultrasonics Vol.48 no.5*, 2008, pp. 453-466.
- [208] Vassilev S. V., Vassileva C. G. 2007. A new approach for the classification of coal fly ashes based on their origin, composition, properties and behavior. *Fuel*, 86, 1490-1512.
- [209] Vasquez E. and Alonso E.E., *Fly ash stabilization of decomposed granite*, *X ICSMFE*. 2 (1981): pp. 391-395.
- [210] Vesperman K.D., Edil T.B. and Berthouex P.M., *Permeability of Fly Ash and Fly Ash-Sand Mixtures, Hydraulic Barriers in Soil and Rock*, ASTM STP 874, American Society for Testing and Materials, Philadelphia, 1985, pp. 289-298.
- [211] Vishwanathan R., Saylak D. and Estakhri C., *Stabilization of subgrade soils using fly ash*, in: *Proc. of the Int. Ash Utilization Symposium, Lexington, Kentucky*, 1997, pp. 204-211.
- [212] Vittal U.K.G. and Mathur S. *Enhancement of haul road serviceability by using fly ash*, in: *Proc. of the Fly ash an opportunity for Mining Sector, New Delhi, India*, 2010.
- [213] Vittal U.K.G. and Mathur S., *Construction of rural roads using fly ash-some case studies*, in: *Proc. of the Fly ash India 2005*, Fly ash Utilisation Programme, TIFAC, DST, New Delhi, 2005, pp. VIII 2.1-2.8.
- [214] Wade N.H., *Design Manual for Surface Mine Haul Roads*, Monenco Consultant Limited, Calgary, Alberta, 1989.
- [215] Wang Y., Ren D. and Zhao F., *Comparative leaching experiments for trace elements in raw coal, laboratory ash, fly ash and bottom ash*, *International Journal of Coal Geology*, 40 (1999): pp. 103-108.
- [216] Yamatami J. and Kotake Y., Pillar control and effects of backfilling support at Osaka mine, *International journal of rock mechanics, mining science and geomechanics*, 1986, Vol. 23, No.2, pp. 44-53
- [217] Yesiller N., Hanson J.L. and Usmen M.A., *Ultrasonic Assessment of Stabilized Soils*, in: *Proc. Of the ASCE Geotechnical Institute Soft Ground Technology (GSP 112)*: pp. 170-181.
- [218] Yoder E.J. and Witczak M.W., *Principles of Pavement Design*, 2nd ed., Wiley, New York, 1975.

- [219] Yudhbir and Honjo Y., *Applications of geotechnical engineering to environmental control*, in: Proc. of 9th Asian Reg. Conf. on S. M. and F. E., Bangkok, Thailand, 2 (1991): pp.431-469.
- [220] Zou D.H.S., Cheng J., Yue R. and Sun X., Grout quality and its impact on guided ultrasonic waves in grouted rock bolts, *International journal of rock mechanics and mining sciences and geomechanics*, 2010, Vol.19 ,Issue:5, pp. 221-228.

# Publications

1. Behera B., Mishra M.K., **Mallick S.R.**, California Bearing ratio behavior of mine overburden stabilized fly ash, *The Indian Mineral industry Journal*, GEOMINTECH publ., 2010, May 11-12, pp. 133- 135.
2. **Mallick S.R.**, Mishra M.K., A review on Status of Coal ash in India- Present scenario and future prospects, in Proceedings, *International Conference on Technological Challenges and Management issues of Sustainability of Mining Industries*, NIT Rourkela, 2011 Aug 4 -6, pp. 321-329.
3. **Mallick S.R.**, Mishra M.K., Parida K.T., Fly Ash- An Alternative Mine Haul Road Construction Material, *The Indian Mining and Engineering Journal*, MINETECH publ., 2011, Nov 18-19, pp. 125-128.
4. **Mallick S.R.**, Mishra M.K., Bearing Capacity and Modulus behaviour of Clinker Stabilized Fly ash-Mine Overburden Mixes for Haul Road Application in proceedings, *National Conference on Development of Coal and Mineral Resources- Economic, Technological and Environmental Issues*, *The Institution of Engineers (India)*, West Bengal State Centre, 2012, Feb 23-24, pp. 40-45.
5. **Mallick S.R.**, Mishra M.K., Replacement of conventional material with FCMs in sub-base of opencast mine haul road to reduce strain-An investigation, *The Indian Mineral industry Journal*, GEOMINTECH publ., 2010, May 11-12, pp. 125-128.
6. **Mallick S.R.**, Mishra M.K., California Bearing Ratio and Young's Modulus behaviour of Clinker Stabilized Fly ash-Mine Overburden Mixes, *Journal of Recent Trends in Civil Engineering and Technology* (Under Review).
7. **Mallick S.R.**, Mishra M.K., Strength Evaluation of Clinker Stabilized Fly ash-Mine Overburden Composites as an Alternative Haul Road Construction Material, *Journal of Emerging Materials Research* (Under Review).
8. **Mallick S.R.**, Mishra M.K., Geotechnical Characterization of Clinker Stabilized Fly ash-Coal Mine Overburden Mixes for Sub-base of Mine Haul Road, *Journal of Coal Combustion and Gasification Products* (Under Review).

# BIO-DATA

## Soumya Ranjan Mallick

Date of Birth: 06 March, 1985

### **Permanent Address:**

S/O: Parameswar Mallick

AT- Lahunipada

PO- Lahunipada

Lahunipada - 770040

Sundargarh, Odisha.

Phone(1): (+91) 9437545820

Phone(2): (+91) 9437647168

e-mail: mallicksoumyaranjan@gmail.com

e-mail: Soumya\_mining2008@rediffmail.com

### **Qualification**

- B. Tech.(Mining Engineering), 2008  
Orissa School of Mining Engineering, Keonjhar
- 10+2 level (Science), 2002  
Govt. Junior College, Rourkela
- 10th level, 2000  
Saradhapur High School, Saradhapur

### **Experience:**

- Lecturer, Department of Mining Engineering, Orissa School of Mining Engineering, Keonjhar, September-2008 to September-2009
- Senior Research Fellow, CSIR Project, Department of Mining Engineering, NIT, Rourkela, Since September-2010

# Appendix

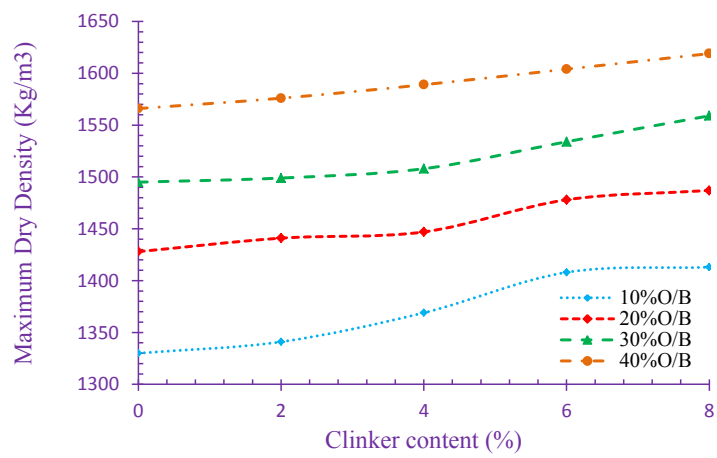


Figure 1: Variation of Maximum dry density with clinker content

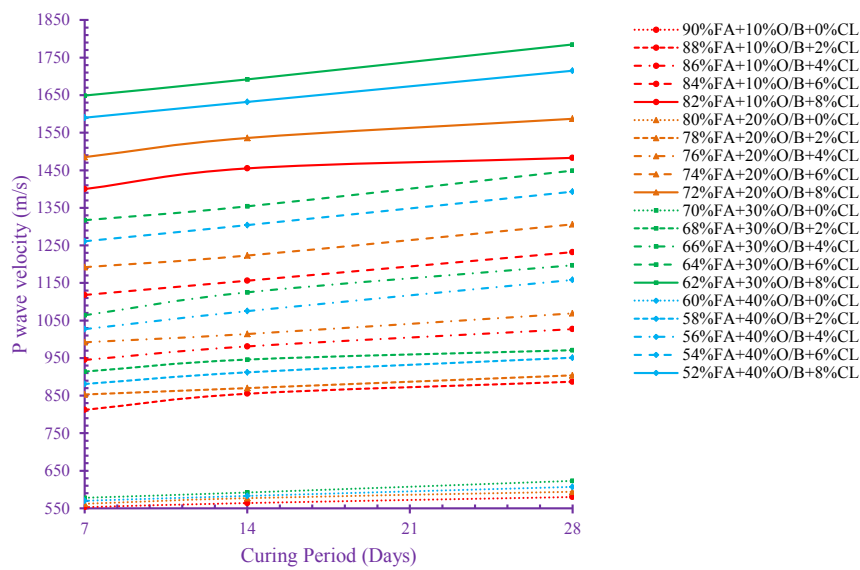


Figure 2: Effect of curing period on P-wave velocity of developed composites



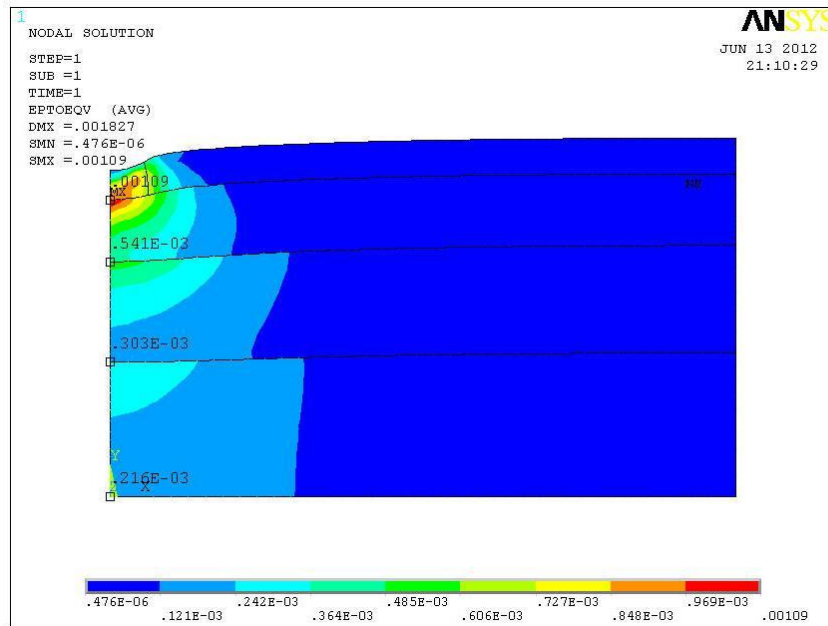


Figure 3: Strain at various layers of haul road pavement with (82FA+10O/B+8CL) composite

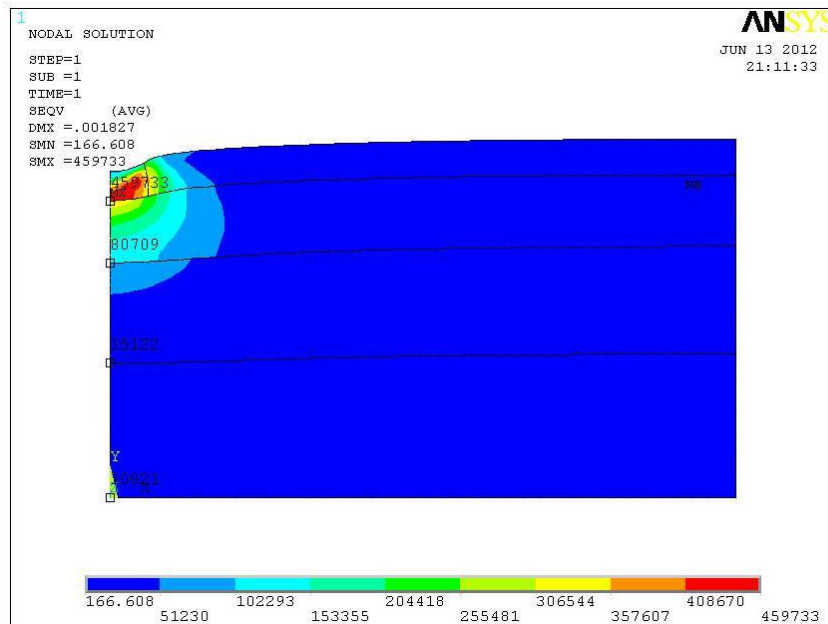


Figure 4: Stress at various layers of haul road pavement with (82FA+10O/B+8CL) composite

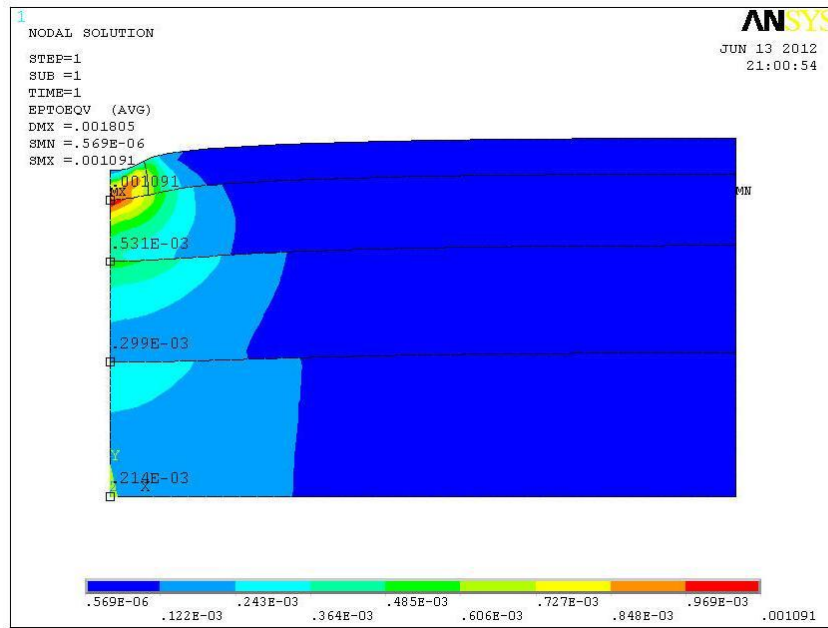


Figure 5: Strain at various layers of haul road pavement with (72FA+20O/B+8CL) composite

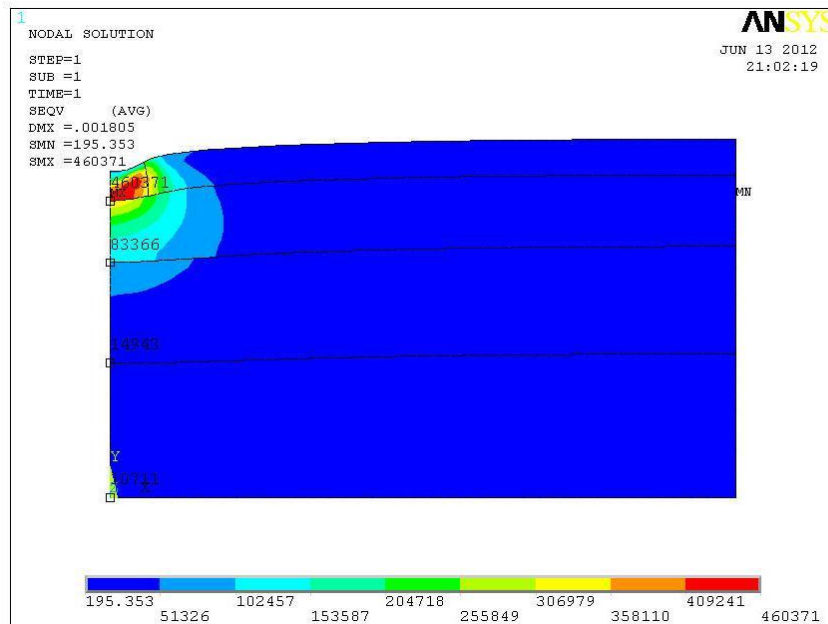


Figure 6: Stress at various layers of haul road pavement with (72FA+20O/B+8CL) composite

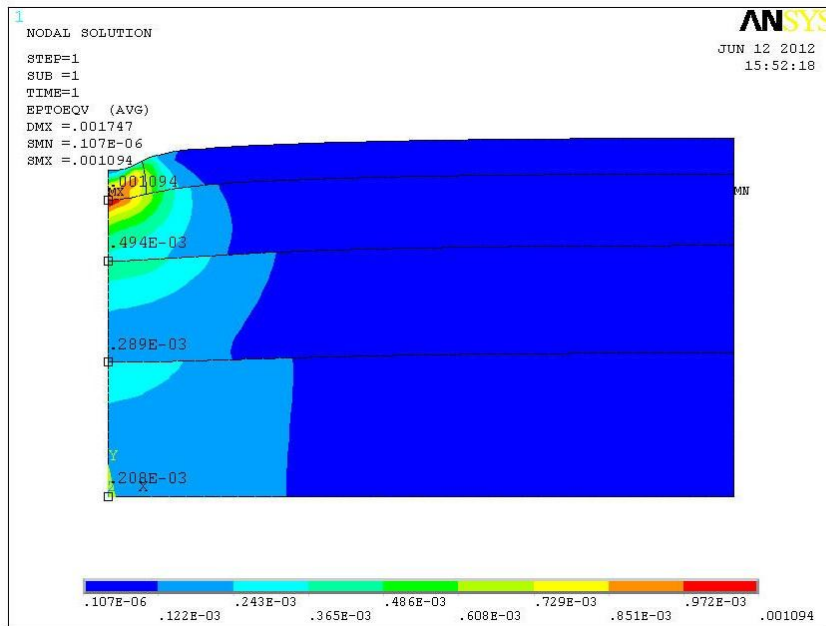


Figure 7: Strain at various layers of haul road pavement with (62FA+30O/B+8CL) composite

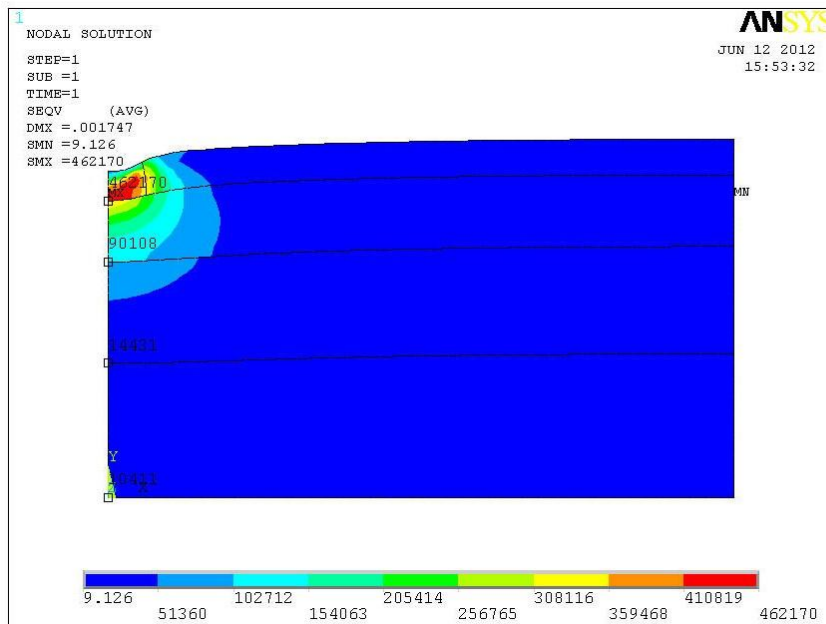


Figure 8: Stress at various layers of haul road pavement with (62FA+30O/B+8CL) composite

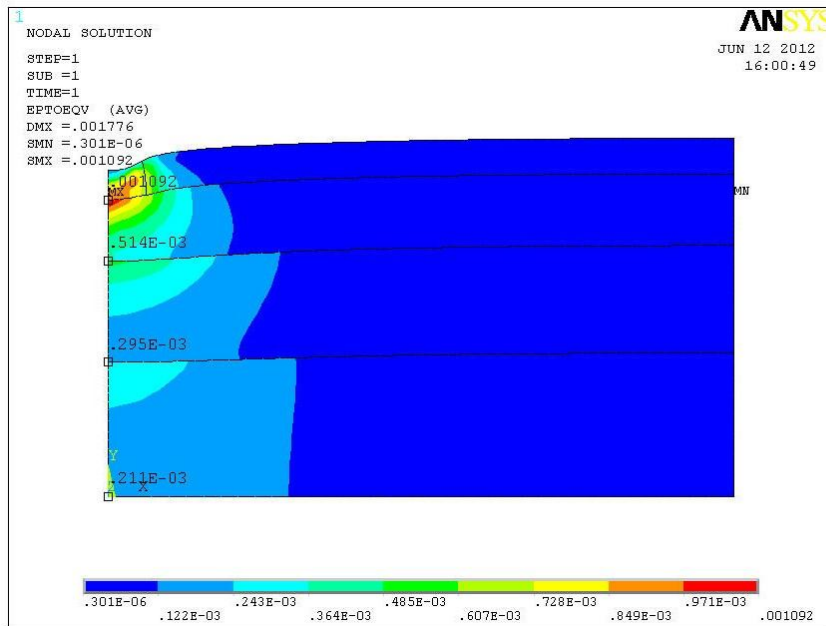


Figure 9: Strain at various layers of haul road pavement with (52FA+40O/B+8CL) composite

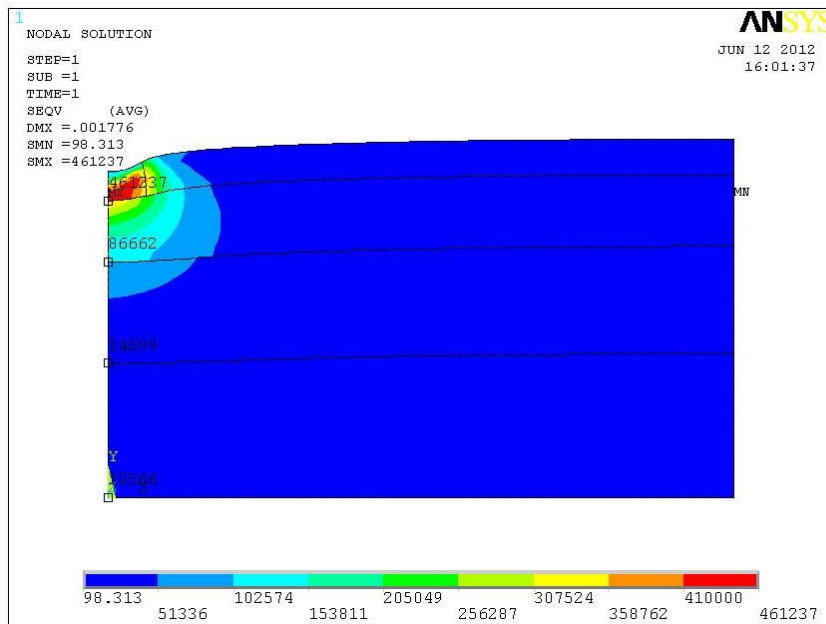


Figure 10: Stress at various layers of haul road pavement with (52FA+40O/B+8CL) composite

### **Possibilities of fly ash usage**

Any permanent haul road length = 5km

Haul road width = 20m

Sub-base thickness = 1.5m

No. of surface coal mine = 200

Volume of the road pavement = 5km×20m×1.5m

$$= 5000 \times 20 \times 1.5 \text{ m}^3$$

$$= 150000 \text{ m}^3$$

Density of the fly ash composite material = 1559 kg/ m<sup>3</sup>

Quantity of material used = 1559 kg/m<sup>3</sup>×150000 m<sup>3</sup>

$$= 233850000 \text{ kg}$$

$$= 0.233 \text{ MT}$$

Material used for 200 opencast mines = 0.233×200 = 46.6 MT

Fly ash usage @ 30% of the material = 60%×46.6 MT = 27.96 MT

## Determination of Critical Strain Limit

$$E = 80,000 / N^{0.27} \text{ [191]}$$

Where,

E = allowable strain limit (micro-strain);

N = number of load repetitions

Tonnage on Haul road of Basundhara opencast coal mine/year = 7 MT.

Dumper capacity used = 80 T

The gross vehicular weight = 160 T (BEML/Caterpillar website)

Operating Life of mine = 20 years (assumed) and typical major road maintenance program = once in 5 years.

Total load carried by the road before major repair and maintenance =  
7,000.000/yr x 5yr = 35 MT

Number of loaded trucks over road = 35,000,000/80 = 4, 37,500

The number of load cycles (two axles) = 437500 \* 2 = 8, 75,000 (ignoring empty trucks)

The critical strain limit =  $E = 80,000 / (8, 75,000)^{0.27} = 1989 \simeq 2000$  micro-strain

**1. How r is replaced by P and p?**

$$\text{Pressure} = \frac{\text{Load}}{\text{Area}}$$

$$p = \frac{P}{A} = \frac{P}{f r^2}$$

$$\Rightarrow r^2 = \frac{P}{f \cdot p}$$

$$\Rightarrow r = \sqrt{\frac{P}{f \cdot p}}$$

**2. How the series of equations 2.4 to 2.8 derived?**

$$\frac{t^2}{P} + \frac{1}{pf} = D \dots\dots\dots 2.4$$

$$t = K\sqrt{P} \dots\dots\dots 2.1$$

$$\Rightarrow t^2 = K^2 P$$

$$\Rightarrow \frac{t^2}{P} = K^2$$

$$\text{So } K^2 + \frac{1}{pf} = D \dots\dots\dots 2.5$$

$$\text{We can write } t = \sqrt{P \left[ D - \frac{1}{pf} \right]} \dots\dots\dots 2.4$$

$$D = \frac{1}{8.1.CBR} \frac{in^2}{lb} \dots\dots\dots 2.6$$

$$t = \sqrt{P \left[ \frac{1}{8.1.CBR} - \frac{1}{pf} \right]} \dots\dots\dots 2.7$$

$$\text{We know } r^2 = \frac{P}{f \cdot p}$$

$$\Rightarrow f r^2 = \frac{P}{p}$$

$$\Rightarrow A = \frac{P}{p}$$

So Equation 2.7 can be written as  $t = \sqrt{\frac{P}{8.1.CBR} - \frac{A}{f}}$ .....2.8

**3. How equation 2.14 obtained from equation 2.13?**

$$\dagger_t = \dagger_0 \left[ \frac{1}{1 + K^2 \cdot p \cdot f} \right] \dots\dots\dots 2.13$$

$$\Rightarrow \dagger_t = \dagger_0 \left[ \frac{1}{f \left( \frac{1}{f} + K^2 \cdot p \right)} \right]$$

$$\Rightarrow \dagger_t = \dagger_0 \left[ \frac{1}{p \cdot f \left( \frac{1}{p \cdot f} + K^2 \right)} \right]$$

$$\Rightarrow \dagger_t = \left[ \frac{1}{f \left( \frac{1}{p \cdot f} + K^2 \right)} \right] \dots\dots\dots 2.14$$